ANALYSIS OF GLUCOCORTICOID ACTION IN NEURAL STEM CELLS

by

Melanie Elizabeth Peffer

Bachelor of Science, University of Pittsburgh, 2009

Submitted to the Graduate Faculty of

The School of Medicine in partial fulfillment

of the requirements for the degree of

Doctor of Philosophy

University of Pittsburgh

2014

UNIVERSITY OF PITTSBURGH

SCHOOL OF MEDICINE

This dissertation was presented

by

Melanie Elizabeth Peffer

It was defended on

April 21, 2014

and approved by

Committee Chair: Deborah L. Chapman, Ph.D., Associate Professor, Department of Biological Sciences

Thomas E. Smithgall, Ph.D., Professor, Department of Microbiology and Molecular Genetics

Alan Wells, D.M.Sc., M.D., Professor, Department of Pathology

Steffi Oesterreich, Ph.D., Professor, Department of Pharmacology and Chemical Biology

Dissertation Advisors: Donald B. DeFranco, Ph.D., Professor, Department of Pharmacology and Chemical Biology

A. Paula Monaghan-Nichols, Ph.D., Associate Professor, Department of Neurobiology

Copyright © by Melanie Elizabeth Peffer

2014

ANALYSIS OF GLUCOCORTICOID ACTION IN NEURAL STEM CELLS

Melanie Elizabeth Peffer, Ph.D.

University of Pittsburgh, 2014

Approximately one-eighth of women in the United States go into pre-term labor and are prescribed synthetic glucocorticoids (GCs) to minimize complications of prematurity and increase the likelihood of fetal survival. Despite these beneficial effects, GCs have permanent negative consequences on brain development, which may lead to neuropsychiatric disorders such as post-traumatic stress disorder, depression and anxiety later in life. The mechanistic bases for these GC induced neurodevelopmental changes are unknown. Therefore, we used neural progenitor/stem cells isolated from the cerebral cortex (CC-NPSCs) or hypothalamus (HT-NPSCs), to identify novel mechanisms for how GCs could impact the developing brain.

In CC-NPSCs, we identified a role for Caveolin-1 (Cav-1) in mediating crosstalk between the rapid and genomic actions of the glucocorticoid receptor (GR). Using Cav-1 KO mice, we identified approximately 100 genes that are differentially responsive to GC treatment in the Cav-1 KO CC-NPSCs. Therefore, we established a role for Cav-1 in regulating the genomic action of GR. Phosphorylation of the GR impacts its genomic action, and GC-induced phosphorylation of GR at Serine 211, but not Serine 226 was altered in the Cav-1 KO. Using chromatin immunoprecipitation experiments, we determined that pSer211-GR recruitment to certain target genes was altered in Cav-1 KO CC-NPSCs. Therefore, we propose that Cav-1 dependent GC action impacts hormone regulated transcription through its influence on site-specific phosphorylation of GR.

RNA-Seq analysis of male/female HT-NPSCs treated with Dexamethasone (Dex, a synthetic GC) identified sexually dimorphic GR regulated genes. Using candidates from the RNA-Seq analysis, we identified GC mediated programming effects on *Fkbp5* and *H19.* In response to a previous exposure to Dex, female, but not male, HT-NPSCs re-treated with Dex have attenuated induction of the *Fkbp-5* gene. *H19* was similarly GC-regulated in both male and female, but previous treatment with Dex resulted in GC-mediated repression instead of activation. Since *H19* harbors a miRNA implicated in regulation of stem cell proliferation, changes in its regulation may be a contributing factor in the altered proliferative response to Dex seen in pre-treated HT-NPSCs. Therefore, HT-NPSCs exposed to Dex exhibit sexually dimorphic and long lasting changes in gene expression and NPSC function.

TABLE OF CONTENTS

LIST OF TABLES

LIST OF FIGURES

PREFACE

First and foremost, I would like to thank Don and Paula, not only for their support and mentoring in the lab, but also for the flexibility and kindness shown as my personal life has thrown several curve balls my way over the last four years. I would also like to thank them for their encouragement in reaching my own career goals instead of trying to make my career a carbon copy of their own. I am also grateful to everyone who has helped with my project—Janie Zhang, Teresa Liu, and Uma Chandran, Soumya Luthra and Anish Chakka for help with the bioinformatic analysis.

To my musician friends at Ingomar United Methodist and Pine Creek Community Band—Thank you for keeping me sane. Playing with you is always a joy and has often given me a much-needed rest.

I would also like to acknowledge my parents—my Mom for raising me to be a strong woman and my Dad for instilling a love and appreciate for the science around us everyday.

Finally, I must thank everyone who has helped me bring my crazy idea called “Choose Your Own Science Adventure” to life (and give another thank you to Don for teaching me the value of “crazy ideas!”) Matthew Beckler, Joan Lakoski, Chris Schunn, Jackie Newman, Judy Cameron and my colleagues at the Pittsburgh Zoo and PPG Aquarium, Mandy Revak, Grace Fields, and Margie Marks.

This thesis is dedicated to my best friend and husband, Kevin, who has been with me from AP Biology to today providing unwavering love and support.

This thesis is also dedicated to my students—from the elementary school science fair participants to the Zoo U. students. No matter what, my students always put things into perspective for me of why I chose this career path and gave me the biggest push of all to persevere.

1.0 INTRODUCTION

1.1 GLUCOCORTICOIDS AND THE GLUCOCORTICOID RECEPTOR

Glucocorticoids (GCs) are steroid hormones that serve a variety of roles to regulate homeostasis. For example, GCs serve a critical role in the body's stress response and also in regulating circadian rhythms. GCs bind to two different nuclear receptors, the glucocorticoid receptor (GR) and the mineralocorticoid receptor (MR). GR is widely expressed throughout the body whereas MR expression, although expressed in the brain, is generally limited to organs or tissues that are aldosterone sensitive such as the kidney, colon, and salivary glands (1).

Within the brain, GR is expressed in all regions whereas MR expression is limited to the hippocampus and limbic regions (2). Although the MR is activated by the mineralocorticoid aldosterone to aid in salt and water balance, the majority of receptors are bound to physiological GCs—cortisol in humans, corticosterone in rodents (3). Interestingly, only the GR binds to synthetic GCs such as Dexamethasone (Dex) and Betamethasone (Beta) (4), but the MR binds cortisol with much higher affinity than the GR, Kd: 0.5 nM versus 5.0nM respectively (5). Since MR has a higher affinity for cortisol, under resting conditions in the brain the MR and not GR is primarily occupied by cortisol. However, under stressful conditions when plasma cortisol levels rise, the occupation of GR increases (6). This interaction between MR/GR and is thought to help regulate the stress response with MR controlling early arousal and reaction and GR to resolve the

stress response and aid in processing and storage of memories related to the situation (5). Some have suggested that the balanced activation of MR and GR is critical for maintenance of mental health. For example, in response to early life stress, epigenetic modifications of the GR can occur leading to changes in its expression and consequent alterations in stress response and cognitive performance later in life (5).

GR action is essential for a variety of physiological processes including development, metabolism, central nervous system function, hypothalamic pituitary adrenal (HPA) axis regulation (see §3.1.1), and immune response (7, 8). For example, in the cardiovascular system GCs regulate blood pressure homeostasis by inhibiting the production of vasodilators like nitric oxide (9). GCs also regulate energy homeostasis through the regulation of processes such as gluconeogenesis in the liver to increase glucose levels in response to exercise or stress (9). GR is also implicated in proper embryonic development. For example, GR null mice have abnormal lung development and die shortly after birth from respiratory failure (9). GCs are also implicated in proper development of the brain through processes such as enhancing the maturation of neurons (2), although at high doses they can have negative consequences (see §1.3).

The GR belongs to the Type 1 group of nuclear receptors (NRs) along with the mineralocorticoid, androgen, estrogen and progesterone receptors (10). NRs are a large family of ligand activated transcription factors that regulate a variety of cellular processes through various mechanisms. These mechanism include post-translational modification of the NRs, ligand dependent/independent actions, and genomic and/or rapid signaling (11). The GR can signal through both genomic (discussed below) and rapid signaling pathways (discussed in §2.1.2). In genomic signaling, the inactive GR resides within the cytoplasm of the cell bound to heat shock proteins (hsp90, hsp70, and p23) as well as to the immunophilins FKBP51 and FKBP52 (12).

GCs passively diffuse through the cell membrane and bind to the cytoplasmically localized GR to cause a conformational change and consequent activation of the receptor. During the conformational change, the GR dissociates from the chaperone proteins and two nuclear localization sequences are revealed. The GR homodimerizes and then translocates to the nucleus where it binds to DNA at GR specific hormone response elements. Each NR binds to its own specific DNA sequence called a hormone response element. In the case of the GR, these hormone response elements are called GC response elements or GREs. GREs are imperfect palindromes that contain two 6 base pair half sites. The homodimer of GR binds in such a manner that each half site is bound by one GR (12). Interestingly, these GREs vary between different cell types. These different GREs are thought to serve as allosteric regulators of the GR, and cause distinct structural changes depending on the cell type, thereby resulting in a discrete function (13). In addition, receptor binding is also influenced by baseline (pre-treatment) chromatin accessibility. Namely, the majority of GR binding sites are found in pre-existing regions of open chromatin (14). Furthermore, the vast majority (~90%) of GREs are found further than 5 kilobases away from the transcriptional start site, and approximately 16% can be found either 50 kilobases upstream of the transcriptional start site, or 50 kilobases downstream of the stop codon (15). Once the receptor is bound to DNA it undergoes additional conformational changes to recruit other transcriptional regulators to affect gene transcription. For example, to exert repressive effects on transcription, after binding of the GR to DNA co-repressors such as nuclear receptor co-repressor (NCoR) and the silencing mediator of retinoic acid and thyroid hormone receptor (SMRT) may be recruited. The presence of these co-regulators then triggers the recruitment histone deacetylases to trigger changes in chromatin and consequent gene repression (9). There are also examples where GR may interact with other transcription factors to

regulate gene transcription without direct DNA binding. Within the liver, these transcription factors include AP-1, nuclear factor-κB, signal transducers and activators of transcription (STAT) family members and CCAAT-enhancer-binding proteins (C/EBP) family members. In fact, transcriptional activation of the Haptoglobin gene is mediated by GR interacting directly with STAT3 and C/EBPβ (16).

The GR shares several similar structural features with other NR as shown in Figure 1. The amino-terminal domain (NTD) is not highly conserved, but contains the activation function-1 (AF-1) domain. The AF-1 domain is critical for transcriptional activation. In fact, when separated from the rest of the receptor, the AF-1 domain is capable in activating transcription in a ligand independent manner (11). The AF-1 region is a critical site for post-translational modifications including phosphorylation, sumoylation, and ubiquitination that control receptor transcriptional activity and stability. The DNA binding domain or DBD is the most highly conserved domain. The DBD facilitates DNA binding to specific sequences through two zinc finger motifs. Notably, a single amino acid change within certain regions of the DBD can alter the receptor's ability to bind to GREs versus estrogen receptor response elements (11). The hinge (H) region is poorly conserved between receptors but its flexibility allows for the receptor to adopt different conformations. The hinge region also contains a nuclear localization sequence that aids in receptor shuttling from the cytoplasm to the nucleus. The ligand-binding domain (LBD) is a multifunctional region and has three distinct roles—ligand binding, receptor dimerization and supports transcriptional activation via the AF-2 domain. GCs bind the GR within a hydrophobic pocket in the LBD. The LBD also contains the AF-2 region which aids in ligand mediated activation of the receptor. In addition, the LBD serves as a docking point for the formation of GR homodimers. For other non-steroid hormone members of the NR superfamily,

the LBD can facilitate the formation of heterodimers with the retinoid X receptor. The LBD also serves as a point of interaction with transcriptional corepressors. Finally, the LBD allows GR and other Type I NRs to interact with heat-shock proteins in the cytoplasm (11).

The GR can have various post-translational modifications such as phosphorylation or sumolyation that impact its transcriptional activity (8). In fact, different phosphorylation patterns within the AF-1 region can dictate which target genes will be bound by GR (17). For example, in cells containing a GR that is unable to be phosphorylated at S404, microarray studies indicate major alterations in global transcriptional responses to hormone ultimately resulting in activation of different signaling pathways and changes in GC dependent cell death (18). A variety of kinases can phosphorylate the GR at different serine residues including cyclin-dependent kinases, mitogen-activated protein kinases, and glycogen synthase kinase (GSK) 3β (8, 18). Phosphorylation of the GR is implicated in a variety of human diseases and also in an individual's response to treatment. For example, in asthma patients increased phosphorylation of the GR at S134 was associated with a decreased anti-inflammatory benefit of inhaled GCs (12). GR phosphorylation at S211 is associated with activation of gene expression whereas pSer226-GR is associated with transcriptional repression. Therefore, a ratio between the two GR phosphoisoforms can be used as a readout of transcriptional activity. In fact, alterations of this ratio in the brain are associated with depression. Furthermore, in women who report heightened levels of depression, anxiety and stress tend to have increased levels of nuclear pSer226-GR (19).

Within the AF-1 region of the GR, there are three major phosphorylation sites, S203, S211, and S226 (Figure 2). The GR can be phosphorylated at these sites under both basal conditions (S203 and S226) and in the presence of agonists (S211) (17). Furthermore, different

phospho-isoforms of the GR are localized to different regions of the cell. For, example, pSer211-GR and pSer226-GR are found in the nucleus of the cell whereas the pSer203-GR form is found predominantly in the cytoplasm (17). Different phospho-isoforms of the receptor also have differences in the kinetics of recruitment to the regulatory regions of different target genes. For example, as shown by chromatin immunoprecipitation experiments, maximal recruitment of pSer226-GR occurs within 15 minutes whereas maximal pSer211-GR does not occur until 45 minutes after initial treatment (17).

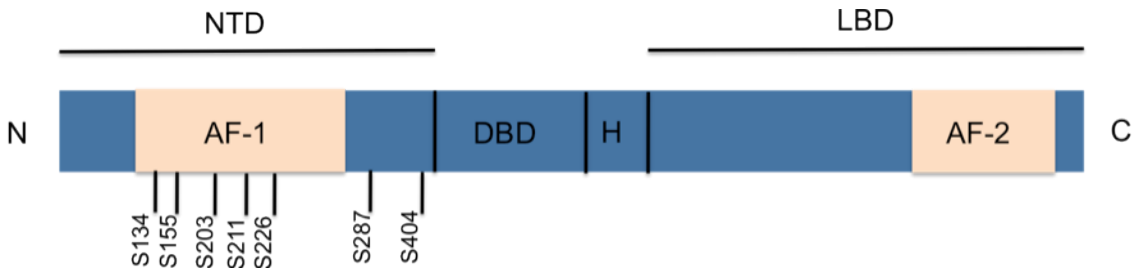

Figure 1. Schematic of the GR highlighting major sites of phosphorylation.

Disruptions in phosphorylation of the receptor can result in altered transcriptional responses leading to changes in cell function (17, 18). For example, phosphorylation of the GR at S404 by GSK3β results in diminished GR function and increased degradation of the receptor. In cells containing a GR unable to be phosphorylated at S404, there are global alterations in transcriptional response resulting in overall changes in GC induced apoptosis (18). In addition, treatment with growth factors such as brain derived neurotrophic factor (BDNF) concurrent with GC treatment results in distinct patterns of phosphorylation and gene transcription. For example, treatment with BDNF causes phosphorylation of the GR at S155 and S287 and results in the regulation of a distinct subset of genes (20).

1.2 CLINICAL USAGE OF GLUCOCORTICOIDS

GCs are commonly used as treatment for a multitude of illnesses such as asthma, allergies, rheumatoid arthritis, multiple sclerosis, and type 1 diabetes mellitus (8). Given the potent anti-inflammatory actions of GCs, they are commonly used to treat a wide variety of inflammatory diseases including conjunctivitis, asthma, eczema, and rheumatoid arthritis (9). GCs also have a wide variety of immunosuppressive effects. For example, GCs suppress both dendritic cell maturation and migration of neutrophils. Consequently, GCs are widely used for immunosuppression in organ transplant patients (9). Given their anti-proliferative and anti-angiogenic properties, GCs may also be used to treat some forms of cancer (9).

Importantly, synthetic GCs are prescribed to women in or at risk for pre-term labor to decrease the complications of prematurity, particularly to prevent respiratory distress syndrome and intraventircular hemorrhage in the fetus (21). The lungs are one of the last major organ systems to develop and treatment with GCs speeds up lung maturation by increasing the production of surfactant therefore, decreasing the risk for respiratory distress syndrome. GR can also mediate maturation and differentiation within the developing lung, particularly within the mesenchyme derived cells (22). Treatment with GCs also decreases the risk for intraventricular hemorrhage by stabilizing the germinal matrix, an area of the brain that is heavily vascularized and vulnerable to injury (21). GCs can also be used during the fetal period to prevent virilization of female infants with congenital adrenal hyperplasia and to prevent inflammation during surgery to correct congenital cardiac defects (23, 24).

Clinically, there are two classes of synthetic GCs that are used during the fetal period, Dex and Beta. Although Dex and Beta are very similar structurally, varying only in the position of a methyl group, they have different dosing schedules and varying potencies. For example, 6

mg Dex are given four times with 12 hour in between in each dosing whereas 12mg of Beta are given twice 24 hours apart (25). Dex and Beta also have similar potencies for activating genomic GR, although Dex has a 5-fold greater potency for activating the rapid action of GR (26). Head to head comparisons of the two GCs in developing mice indicated that overall Beta produced a greater pulmonary benefit without retarding growth (27).

1.3 IMPLICAITONS FOR USE OF GLUCOCORTICOIDS DURING BRAIN DEVELOPMENT

Unlike naturally secreted GCs, clinically relevant synthetic GCs are not inactivated by enzymes found in the placenta (28). Furthermore, GCs easily cross the blood brain barrier via simple diffusion (4). Since GCs are used during the fetal period ***while the brain is still developing***, it is therefore not surprising that data from both human and animal models indicates that GC treatment results in long lasting alterations in the central nervous system.

In mouse models, treatment with GCs results in decreased proliferation in the hippocampus and cerebral cortex and impaired cognitive function (4, 29). Studies in rats indicate that prenatal treatment with Dex, results in impaired radial migration in the cerebral cortex (30). Sheep born at term but treated prenatally with GCs have deficits in myelination and smaller brain size that persists into adulthood (4). Furthermore, studies in non-human primates indicate that term born animals treated prenatally with GCs have smaller hippocampi and impaired differentiation of neurons (reviewed in (4)). In the adult rat hippocampus, stress or exogenous treatment with the GC corticosterone results in diminished neurogenesis and enhanced

differentiation of oligodendrocytes (31). Therefore, studies in a variety of model systems have underscored the negative effects of GCs on the central nervous system.

In humans, prenatal usage of GCs is associated with decreased cerebral cortex surface area, attention deficits, decreased cognitive performance, and increased aggressive and destructive behaviors (reviewed in (4)). A recent study in term born infants indicated that children exposed prenatally to synthetic GCs grow up to have significant thinning of the cerebral cortex, particularly in the rostral anterior cingulate cortex. Furthermore, thinner cortices in the left rostral anterior cingulate cortex were associated with increased affective behaviors (32). Children, particularly females, treated prenatally and born at term also have altered stress reactivity and may therefore be more vulnerable to stress related neuropsychiatric disorders (33). Studies in children treated postnatally with GCs give conflicting results regarding changes in overall brain structure. Cheong et al report that adolescents treated postnatally with Dex, had smaller brains overall, particularly in the white matter, thalami, and basal ganglia and no changes in gray matter (34). In contrast, a smaller study reported a 35% reduction in total gray matter and no difference in white matter (35). The aforementioned studies took place over a decade apart in two different countries, so variability between the two may be related to differences in cohort and advances in medical technology. Regardless, postnatal and prenatal treatment with Dex clearly results in overall changes in brain structure.

While the mechanism(s) responsible for these alterations are not well established, they may involve changes in neural progenitor/stem cell proliferation and/or differentiation thereby disrupting the development of neuronal circuits essential for higher order cognitive or behavioral function.

1.4 STUDYING THE IMPACT OF GLUCOCORTICOIDS ON BRAIN DEVELOPMENT USING A NEUROSPHERE MODEL

Studies examining GC effects on neural progenitor-stem cell (NPSC) function in a variety of experimental systems uncovered a number of affected pathways and signaling molecules. For example, in rat embryonic neural stem cells, GCs decreased proliferation by enhanced degradation of the cell cycle regulator, Cyclin-D1 (36). In the mouse cerebellum, neonatal treatment with Dex increased apoptosis of the neural progenitor cells within the extra granule cell layer and decreased overall numbers of internal granule layer neurons (37). GC effects on the differentiation of NPSCs are varied and conflicting; reduced differentiation of glial cells by GCs was reported in mesencephalic NPSCs and adult rat hippocampal progenitor cells while GCs increased differentiation of glia in human NPSC cultures (38-40).

In these studies, NPSCs were cultured as 3-dimensional neurospheres (Figure 3). NPSCs were isolated from E14.5 mouse cerebral cortex (§2) or hypothalamus (§3). We chose to use E14.5 as there are detectable levels of GR expression (41), but the embryo is still in a hormone-naïve state. In addition, there is significant expansion of NPSCs at E14.5 therefore increasing the number of cells available to harvest. To maintain their undifferentiated state, neurospheres are cultured in the presence of epidermal growth factor (EGF) and/or fibroblast growth factor-1 (FGF-1) (Figure 3). Cells are broken up and replated or passaged (P) once per week and the number of passages denoted by a number i.e. P1 or P3. EGF and FGF are crucial for promoting renewal and expansion of the NPSC, and it is important to note that cells responsive to these growth factors maintain the ability to differentiate into neurons, astrocytes and oligodendrocytes (42, 43). The advantage of this model lies in the ability of neurospheres to properly recapitulate the *in vivo* differentiation order of neurons and glia under *in vitro* conditions (44, 45) (Figure 3).

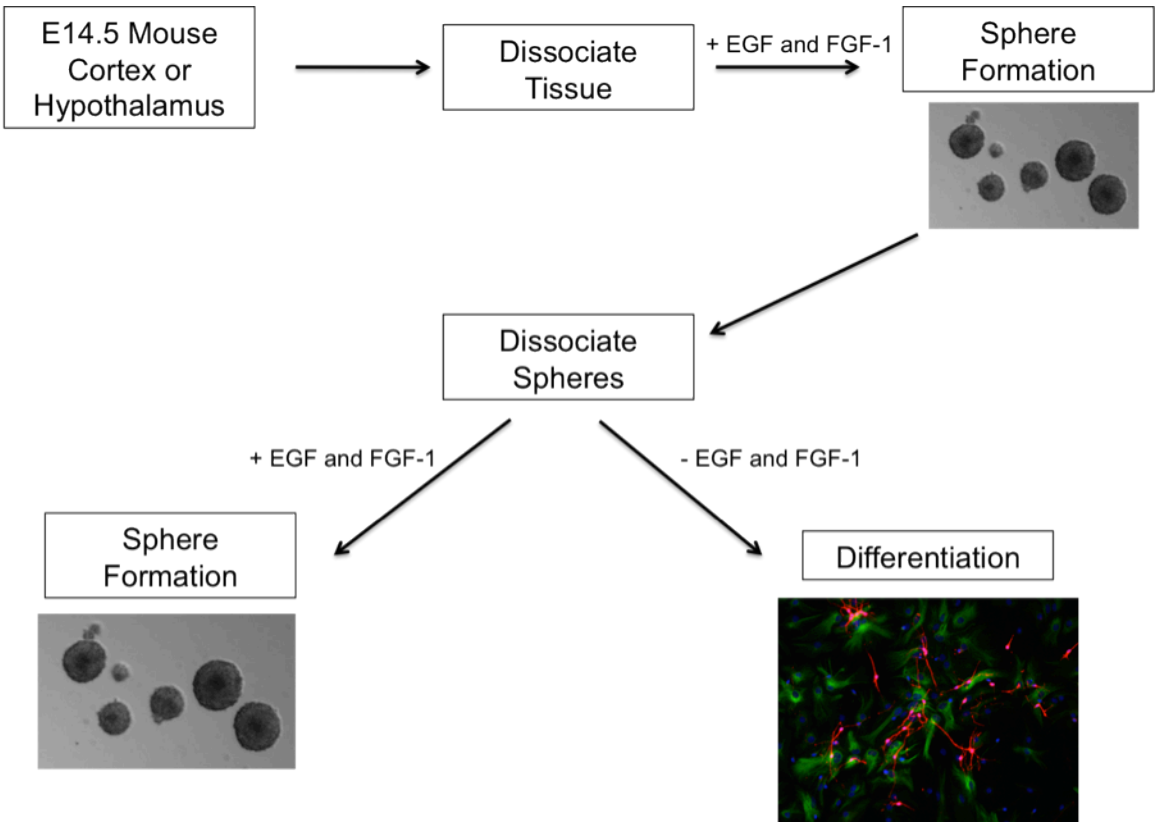

Figure 2. Schematic of neural progenitor/stem cell culture.

Cells cultured in the presence of EGF and FGF-1 form 3D balls of cells called neurospheres. Cells cultured under adherent conditions on Poly-D-Lysine and laminin treated glass coverslips without EGF and FGF-1 differentiate in neurons, astrocytes, and oligodendrocytes. Neurospheres can be passaged weekly at least five times.

1.5 GOALS OF DISSERTATION

The beneficial nature of GCs in decreasing the negative consequences of prematurity (i.e. respiratory distress syndrome, intraventricular hemorrhage) is undisputed. However, in multiple studies including *in vitro* analysis of NPSCs, animal models, and human studies all indicate permanent negative consequences on the biology of NPSCs (36-40), gross anatomy of different structures of the brain (cerebral cortex, hippocampus) (4), and changes in behavior and stress reactivity (32, 33). Although we currently do not have a clear mechanism for the nature of these deficits, one potential way to abrogate these negative consequences while maintaining the beneficial nature of glucocorticoids is to develop a better understanding of the molecular changes occurring at the level of NPSCs. Therefore, this study takes a genome-wide approach to analyze the impact of the synthetic and clinically relevant GC, Dex, on gene expression and biology of NPSCs from the cerebral cortex and the hypothalamus.

In Chapter 2, using NPSCs isolated from E14.5 mouse cerebral cortex, we identified a new role for Caveolin-1 (Cav-1) in mediating cross talk between the genomic and rapid actions of the GR. Loss of Cav-1 resulted in altered regulation of a select group of target genes (~100 genes/14,000 analyzed), many of which are implicated in a variety of processes related to NPSC biology (i.e. proliferation and migration). These changes in gene expression may be the result of changes in phosphorylation of the GR at Serine 211 and altered recruitment of the GR to the regulatory regions of target genes. Better understanding of the impact of genomic, rapid, and the cross talk between the two may indicate which GR pathways are the underlying causes of altered neural development, possibly leading to more directed therapies.

In Chapter 3, we utilized NPSCs isolated from the hypothalami of male or female E14.5 mice. Using RNA-Seq analysis, we uncovered sexually dimorphic patterns of Dex-regulated gene expression. Furthermore, deeper analysis of select target genes uncovered by RNA-Seq demonstrated that certain target genes have long lasting, sexually dimorphic changes in transcriptional responses if previously treated with Dex. *Fkbp-5* was found to be less induced in specifically female cells previously treated with Dex. In contrast, the large intergenic non-coding RNA, *H19*, did not have long lasting sexually dimorphic changes in transcriptional response, but did demonstrate an reversal of GC regulated gene expression. In both male and female cells, a previous treatment with Dex resulted in a future repression of *H19* gene expression instead of the expected gene activation. *H19* also harbors a micro-RNA implicated in proliferation of stem cells (46), and changes in *H19* regulation may underlie the altered proliferative response seen in HT-NPSCs previously exposed to Dex. Therefore, Dex treatment can cause sexually dimorphic, long lasting changes in gene expression. Improved understanding of which genes have long term alterations and their role in neural development and physiology, as well as differences between the sexes may lead to more directed, or potentially sex-specific therapies.

2.0 CAVEOLIN-1 REGULATES THE GENOMIC ACTION OF THE GLUCOCORTICOID RECEPTOR IN NEURAL STEM CELLS

2.1 INTRODUCTION

2.1.1 Development of the Cerebral Cortex

In early development, the neuroepithelium (NE) derives from the ectoderm and gives rise to neurons and glia (47). Prior to the onset of neurogenesis at E12 in the mouse, the cells of the NE divide symmetrically to increase their total numbers (44, 48). At the onset of neurogenesis, NE cells begin to acquire gliogenic features and express astrocytic markers such as astrocyte-specific glutamate transporter (GLAST), glial fibrillary acidic protein (GFAP) and intermediate filament proteins such as nestin and vimentin, and are considered to be radial glia (47).

During the development of the cerebral cortex (CC), the radial glial (RG) cells initially undergo asymmetric divisions, which result in more RG as well as neurons or intermediate progenitor cells (47). RG extend from the ventricular to pial surface and serve as “tracks” for neurons to “follow” to their final destination in the CC (49). RG are also capable of generating neurons, neuronal precursors, and two types of glia, astrocytes, and oligodendrocytes. Consequently, RG are considered to be (at least in rodents) the main source of these cell types in the cortex (49). Right before birth, a competency change occurs in the radial glial allowing differentiation of astrocytes, then oligodendrocytes (47). Astrocytes are the most numerous type

of glial cell and perform a variety of functions including control of blood flow, movement of nutrients, formation of proper synapses and removal of excess neurotransmitters (50, 51). Oligodendrocytes produce myelin, which wraps around the neuronal axons and is essential for the rapid conduction of an action potential (50).

The CC is the largest region of the human brain and regulates higher order abilities, cognition, and emotion (52). Given the complexity and importance of the CC it is not surprising that alterations in its development can contribute to neurodevelopmental diseases such as autism spectrum disorders, schizophrenia, and major depressive disorder (52, 53). In fact, high levels of GC hormones during the fetal period are also linked to the acquisition of neurodevelopmental disorders. For example, maternal stress resulting in elevated levels of GCs during pregnancy is implicated in the child's future development of schizophrenia, anxiety, depression, autism spectrum disorders, and attention deficit hyperactivity disorder (reviewed in: (54)). Furthermore, treatment with synthetic GCs to reduce complications of prematurity is also associated with increased affective behaviors and predisposition to development of neuropsychiatric disorders (see §1.3). Therefore, exposure of the developing CC to high doses of GC may contribute to the development of future disease.

2.1.2 GR Signaling in CC-NPSCs

In CC-NPSCs, GC can act through two signaling pathways via the GR, a member of the nuclear receptor superfamily of transcription factors (5, 7). In classical or genomic signaling, binding of ligand results in GR translocation to the nucleus where it can either activate or repress transcription of target genes (Figure 3, §1.1) (55).

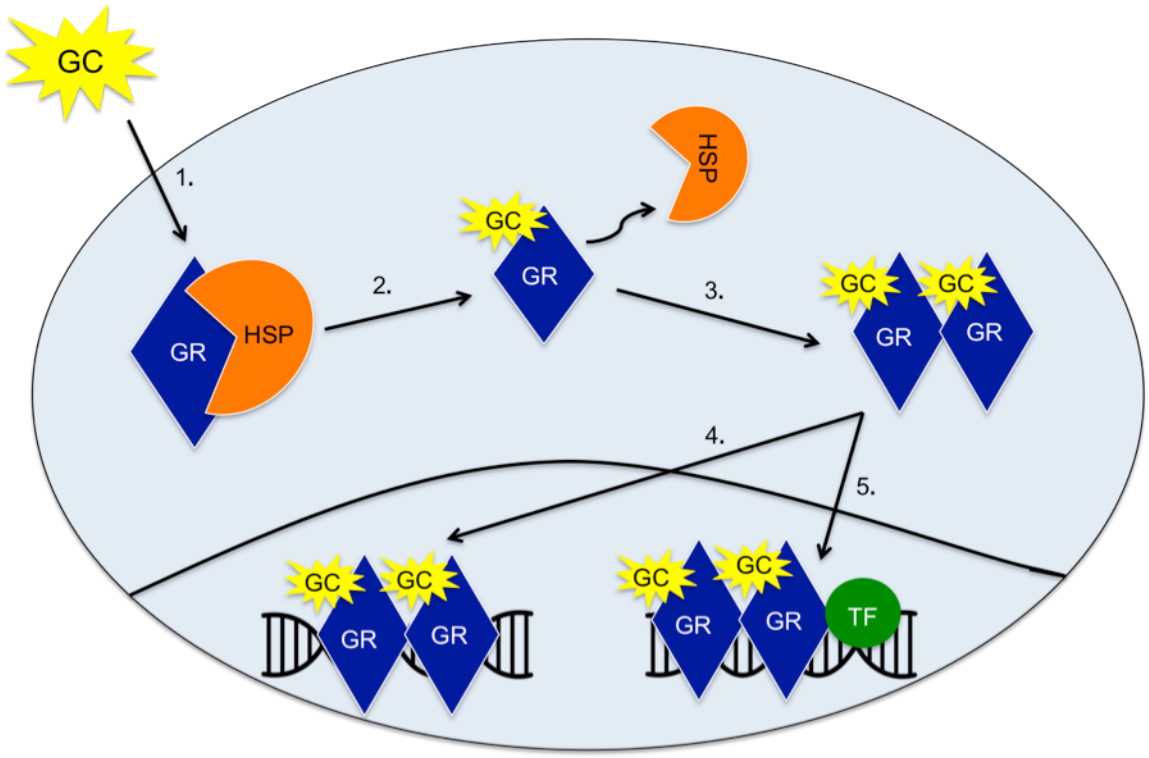

Figure 3. Schematic of genomic GR signaling.

1. GCs passively diffuse through the cell membrane and bind to the GR. 2. Binding of GC to the GR results in its activation and dissociation from associated heat shock proteins (HSP). 3. The activated GR monomer dimerizes and translocates to the nucleus where it regulates gene transcription either by direct binding to DNA (4.) or by interacting with other transcription factors (5.)

In contrast, rapid or non-classical signaling involves a plasma membrane associated GR that is capable of activating kinases, such as mitogen activated protein kinase (MAPK) (Figure 4). These kinases can then influence GR transcriptional response through direct modification of the receptor or its associated transcriptional coregulators (56). Although both rapid and genomic GR signaling operates in NPSCs (29), the degree of interaction between the two pathways, and the how they intersect to influence GC effects on NPSC biology, are unknown.

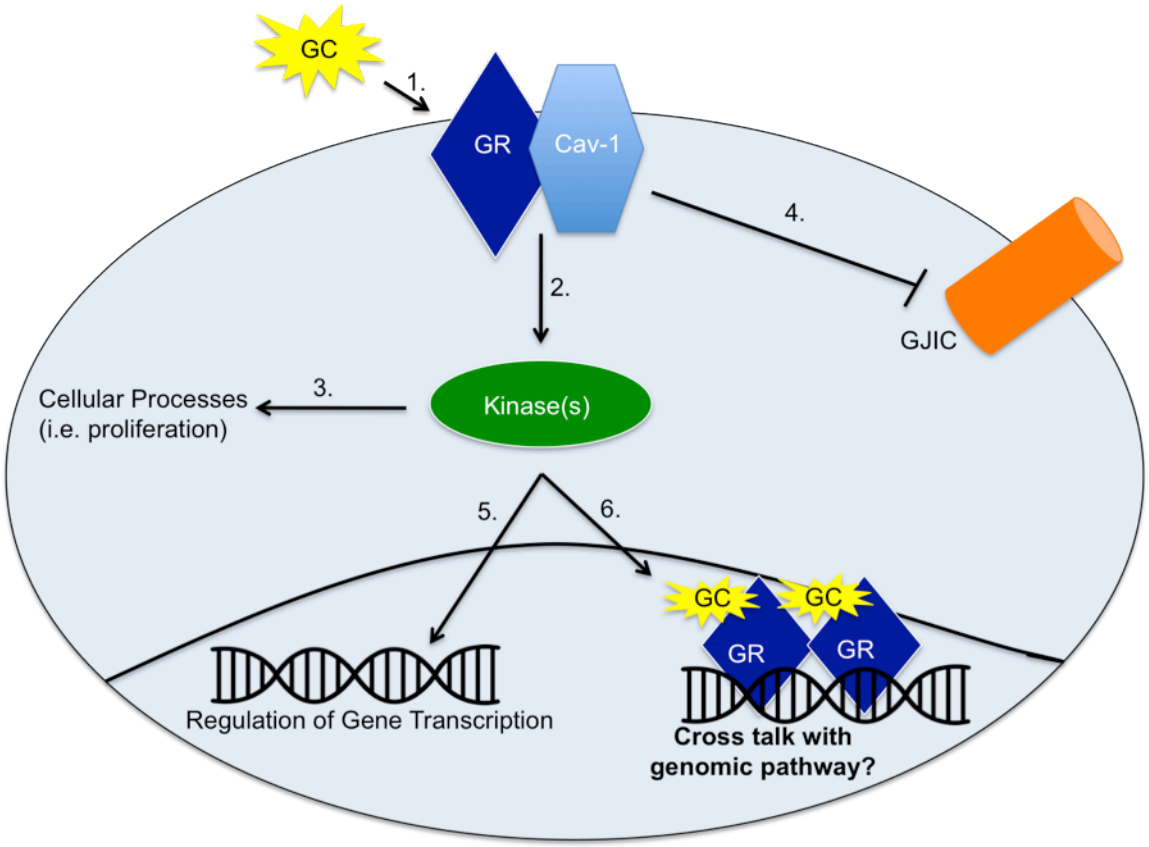

Figure 4. Schematic of rapid GR signaling.

1. GCs activate a membrane localized GR interacting with Caveolin-1 (Cav-1). 2. Upon ligand binding, downstream kinases are rapidly activated to impact a variety of cellular responses (3) and regulate gene transcription (5). 4. Activation of membrane bound GR is also known to inhibit gap junction intercellular communication (GJIC). 6. We hypothesize that the rapid action of the GR can impact its genomic action.

Studies with other steroid hormone receptors such as the androgen and estrogen receptor have revealed mechanisms of cross talk between genomic and rapid actions of the receptors (reviewed in (57)). For example, studies using a mutant mouse where the estrogen receptor (ER) cannot bind to DNA, stimulation with estrogen and activation of a membrane localized ER results in a genomic action, namely by the binding of the NeuroD1 transcription factor to the insulin promoter (58). In prostate cancer cells, paxillin is implicated as a liaison between the rapid and genomic action of the androgen receptor (59).

2.1.3 Caveolin-1 Mediates a Wide Variety of Cellular Processes

Rapid GC signaling in NPSCs that triggers MAPK activation and consequent inhibition of gap junction intercellular communication was previously shown by our laboratory to rely on an interaction between a plasma membrane bound GR and Cav-1 (29). Cav-1 is the major protein subunit of specialized regions of the plasma membrane known as caveolae (60). Cav-1 is implicated in a variety of cellular processes including proliferation, differentiation, and cell migration. In mouse embryonic stem cells, Cav-1 is implicated as a mediator of cell proliferation and loss of Cav-1 via siRNA resulted in lack of a proliferative response when cells were stimulated with EGF (61). In contrast, in the adult mouse loss of Cav-1 results in an increase in proliferation within the subventricular zone (62). Studies in lung epithelial cells reveal a role for Cav-1 in regulating the anti-proliferative action of GCs via its interaction with GR (56). Interestingly, Cav-1 is implicated to have both tumor suppressive and tumor supportive roles depending on the type of cancer (63). Therefore, the role of Cav-1 in regulating proliferation of is very diverse and likely involves many cell specific mechanisms. Cav-1 is also implicated in differentiation of NPSCs as Cav-1 Knock-Out (KO) mice have attenuated astroglial

differentiation (64) and increased neurogenesis (65). Finally, in mouse embryonic stem cells that lack Cav-1, EGF induced cell migration was also significantly decreased, indicating a role for Cav-1 in migration of these cells (61). In adult Cav-1 KO animals, the brain tends to be smaller, and the mice have alterations in overall activity, impaired motor activity, alterations in gait, spatial memory impairment, and increased anxiety (66, 67). Taken together, loss of Cav-1 results in wide changes in cellular biology that may lead to abnormalities in the entire animal.

2.1.4 Rationale and Summary

Given the role of Cav-1 in mediating the rapid response of GR (29, 56), we set out to examine whether Cav-1 could also participate in classical genomic GR signaling and impact the anti-proliferative response of NPSCs to Dex (Figure 4). Here we show that loss of the Dex-mediated anti-proliferative response in NPSCs derived from Cav-1 KO mice is associated with the alterations in Dex-induced gene expression of an established negative regulator of the cell cycle in NPSCs, serum and glucocorticoid-induced kinase-1, *Sgk-1* (68). We also revealed more global effects of Cav-1 deletion on the GR transcriptome and uncovered a mechanism for Cav-1 mediated crosstalk between rapid and genomic GR signaling that impacts site-specific GR phosphorylation and chromatin recruitment of GR.

2.2 MATERIALS AND METHODS

Mouse CC-NPSC cultures: NPSCs were derived from embryonic day 14.5 (E14.5) cerebral cortex of wild-type C57Bl/6 (C57) or Cav-1 KO mice and grown as three-dimensional neurosphere cultures (29). Cells were passaged every seven days and experiments were performed at P3 unless indicated otherwise.

CC-NPSC BrdU Assays: P1 neurospheres were cultured for 3 days after passaging before replenishment with fresh EGF and FGF-1 (Invitrogen). Approximately 6 h later, cells were treated with 100nM Dex (Sigma Chemicals, St. Louis, MO) or vehicle (Ethanol, EtOH). 10uM Bromodeoxyuridine (BrdU) (Sigma Chemicals, B-9285) was added for 1 h after 23 h of Dex treatment. Neurospheres were then dissociated into single cells and attached to poly-D-lysine (PDL) treated coverslips prior to fixation with 4% paraformaldehyde. Fixed cells were processed for immunocytochemistry using standard methods. A rat anti-BrdU antibody (Abcam, ab6326) was used at 1:500 and Anti-Rat Alexa Flour 488 (Invitrogen, A21208) at 1:1000. Images were captured using a Nikon Eclipse E400 Microscope and Photometrics Cool Snap E52 camera. For SGK-1 inhibitor experiments, GSK650394 (Tocris Bioscience) was used at a concentration of 50nM and added coincident with Dex.

Radial Migration Assay: P3 neurospheres were plated on PDL treated 6-well dishes in the presence of 100 nM Dex or vehicle 2 days after replenishment with EGF and FGF-1. Approximately 10 spheres per well (3 wells per treatment) were imaged at 4, 8, and 24 hours after plating/Dex treatment. Images were captured using an Olympus IX71 inverted microscope. Following imaging, distance migrated was determined using ImageJ. The distance migrated for a

sphere was defined as the distance between the leading edge of the sphere and the furthest migrated point, and this measurement was taken at three different locations per sphere, and averaged together to determine the distance migrated for an individual sphere.

Differentiation Assay: P1 or P3 neurospheres were treated for 24 hours with 100nM Dex or vehicle 2 days after replenishment without EGF and FGF. Following treatment, cells were washed once with NeuroCult™ media with differentiation supplement (StemCell Technologies) and no growth factors, dissociated, viable cells counted using Trypan Blue staining, and plated at a density of 90,000 viable cells/well on coverslips treated with 100ug/mL Poly-D-Lysine and 15ug/mL laminin. After 1 day of differentiation (1DD) cells were fixed in 4% paraformaldehyde. Fixed cells were processed for immunocytochemistry using standard methods. A rabbit anti-olig2 antibody (Abcam, ab81093) was used at 1:1000 and Anti-rabbit Cy3 at 1:400. A chicken anti-nestin antibody (Aves Lab, NES) was used at 1:500 and Anti-chicken Alexa Fluor 488 at 1:000. Images were captured using a Nikon Eclipse E400 Microscope and Photometrics Cool Snap E52 camera.

Microarrays: Total RNA was extracted using Qiagen RNeasy Kit (Qiagen, 74104) from cell pellets comprising biologically distinct neurosphere cultures from C57 or Cav-1 KO embryos treated with 100 nM Dex or vehicle for 4 h (n=5/treatment condition). Total RNA was further processed to determine quality. The 260/280 ratios for all samples was determine to be greater than or equal to 1.8 using a NanoDrop 1000 (NanoDrop, Wilmington, GE) and a RIN value of greater than or equal to 8.0 as determined using a Bioanalyzer 2100 (Agilent Technologies, Santa Clara, CA). Using 500 ng of starting material, samples were then *in vitro* transcribed using the

Ambion MessageAmp Premier Enhanced assay protocol (Ambion Inc, Austin, TX). To confirm cRNA diversity, the Bioanalyzer 2100 was used to generate an eletrophoretogram for each reaction giving information regarding sample yield, integrity, and size diversity against a Universal Human Reference RNA (Stratagene, La Jolla, CA). Fifteen micrograms of purified, amplified, biotin labeled cRNA was fragmented and hybridized on to Affymetrix Mouse Genome 430A 2.0 arrays (13,687 genes, 22,690 probes; Affymetrix Corp. Santa Clara, CA) for 18 h. Washing, staining and scanning of arrays was performed on the Affymetrix Fluidics Station 450 and Scanner 3000 immediately after completion of hybridization. The CEL files were submitted to GEO (accession # GSE49804). Microarrays were performed by University of Pittsburgh genomics core.

Bioinformatic Analysis: Microarray data was first normalized and summarized using the Robust Multichip Average (RMA) method (69). Genes represented on the array with multiple probe sets were assessed and the probe set with the highest inter-quartile ratio was selected for analysis. Genes that were undetectable in all 20 samples analyzed were also removed from the dataset leaving 9916 genes for statistical analysis. Using BRB-Array Tools (70), a student's t-test was used to assess differences between Cav-1 KO Dex vs. EtOH, C57 Dex vs. EtOH and Cav-1 KO vs. C57 EtOH. A one-way ANOVA (False Discovery Rate, FDR 10%) was performed to ascertain genes differentially regulated by Dex treatment in Cav-1 KO versus C57. From this dataset networks and biological functions were assed using the Ingenuity Pathway Analysis (IPA) software (Ingenuity Systems, Redwood City, CA, USA). Hierarchical clustering figures and Venn diagrams are produced in R- Bioconductor.

Using the NextBio Research (Cupertino, CA, USA) data-search and analysis engine, a meta-analysis was performed to compare genes regulated by GC in our studies to 12 other similar publically available datasets (Table 1). Within each dataset, a list of differentially expressed genes was combined to create a master list. From this master list, we refined the data set to identify genes unique to each study.

Collaborators in the University of Pittsburgh Department of Biomedical Informatics performed Bioinformatic analysis.

Table 1. Data sets used for NextBio analysis.

Set ID Number	Cell Type	Hormone	Concentration	Duration of Treatment	Citation
1	E14.5 cerebral cortex from Cav-1 KO Mice	Dexamethasone	0.1μM	4 hours	This Study
2	E14.5 cerebral cortex from C57 (Wild Type) mice	Dexamethasone	0.1μM	4 hours	This Study
3	AtT-20 mouse pituitary	Dexamethasone	0.1μM	4 hours	(71)
4	Multipotent human fetal hippocampal progenitor cell line (HPC03A/07)	Cortisol	0.1μM	12 hours	(72)
5	3134 mouse mammary adenocarcinoma	Dexamethasone	0.1μM	4 hours	(71)
6	C2C12 mouse myotubes	Dexamethasone	1μM	24 hours	(73)
7	C2C12 mouse myotubes	Dexamethasone	1μM	6 hours	(73)
8	Multipotent human fetal hippocampal progenitor cell line (HPC03A/07)	Cortisol	100μM	12 hours	(72)
9	E14.5 cerebral cortex from rat	Corticosterone	1μM	28 hours	(30)
10	Mouse oligodendrocyte precursor cell line (Oli-Neu)	Dexamethasone	1μM	10 hours	(74)
11	Mouse oligodendrocyte precursor cell line (Oli-Neu)	Dexamethasone	1μM	24 hours	(74)
12	Mouse 3T3-L1 preadipocytes	Dexamethasone	1μM	2 hours	(75)
13	Mouse 3T3-L1 preadipocytes	Dexamethasone	1μM	36 hours	(75)
14	Mouse C3H10T1/2 pluripotent stem cell line	Dexamethasone	1μM	1.5 hours	(76)

Quantitative Real Time-PCR (qRT-PCR): For microarray validations, cells isolated from biologically independent samples of each genotype were treated with Dex or ethanol for 4 h and RNA processed using Machery-Nagel Nucelospin RNA II Kit. cDNA synthesis was performed using iScript Select cDNA Synthesis Kit (Bio Rad #170-8897). qRT-PCR reactions were performed on a Stratagene Mx3000P and used iTaq Universal SYBR Green Supermix (Bio Rad #172-5121) and primers with efficiencies calculated to be greater than 80%.

Phospho-GR Westerns: Neurospheres from C57 or Cav-1 KO mice were treated with 100nM Dex for 1 h. Following treatment, cells were lysed in RIPA buffer (10mM Tris-Cl pH 8.0, 1 mM EDTA, 0.5 mM EGTA, 140 mM NaCl, 1% Triton-X, 0.1% Sodium Deoxycholate, 0.1% SDS) supplemented with 1:1000 HALT Protease and Phosphatase Inhibitors (Thermo #1861281). Lysate was subjected to immunoprecipitation using the BuGR2 mouse monoclonal antibody or incubated with non-immune IgG using standard laboratory conditions. Immunoprecipitated material was run on 7.5% SDS-PAGE gel and transferred to a PVDF membrane (Millipore Immobilon-P #IPVH00010). Western blot analysis was performed using the p211-GR antibody (17) and an anti-rabbit horseradish peroxidase secondary antibody (BioRad #170-6515) with a chemiluminescense detection system (Advansta Western Bright ECL #K-12045-D50).

Nuclear Fractionation: Subcellular fractionation was performed according to guidelines provided in the NE-PER kit (Thermo #78833) with lysates from C57 or Cav-1 KO neurospheres treated with Dex or Ethanol for 4 h. Fractions were then separated on 10% SDS-PAGE gels and Western blots performed to detect total GR using the M20 rabbit polyclonal antibody (Santa Cruz, sc-1004) and Cav-1 (BD Biosciences #610059). The purity of fractions was assessed using GAPDH as a marker for cytoplasmic (Santa Cruz, sc-32233) and Lamin-B1 for nuclear proteins (Abcam, ab16048).

Chromatin Immunoprecipitation (ChIP): NPSCs isolated from C57 or Cav-1 KO mice were grown as described above and treated with Dex or vehicle for 1.5 h. Cells were then fixed in 1% formaldehyde for 10 minutes at room temperature. Following fixation, 0.125 M glycine was added for 5 minutes to quench the cross-linking reaction. Cells were washed with PBS twice and frozen at -80 until immunoprecipitation. Prior to sonication, cell pellets were thawed on ice and lysed in ChIP Lysis Buffer (50mM HEPES, 1 mM EDTA, 140 mM NaCl, 10% Glycerol, 0.5% NP-40, 0.25% Triton X-100) with freshly added HALT Protease and Phosphatase Inhibitor Cocktail (Thermo-Fisher). Cell lysate was centrifuges at 5,000 RPM for 5 minutes at 4°C and crude nuclear pellets collected and washed once with ChIP Wash Buffer (10 mM Tris-Cl, 1 mM EDTA, 200 mM NaCl) with freshly added HALT Protease and Phosphatase Inhibitor Cocktail. The pellet was then resuspended in ChIP Sonication Buffer (10 mM Tris-Cl, 1 mM EDTA, 0.5 mM EGTA, 0.5% N-lauroyl-sarcosine) with freshly added HALT Protease and Phosphatase Inhibitor Cocktail and chromatin sonicated using a Bioruptor into fragments of approximately 500-1000 base pairs. Immunoprecipitation of GR was performed with 8 ug of a GR antibody

cocktail (2 ug each of M20 [Santa-Cruz], P20 [Santa-Cruz], H300 [Santa-Cruz] and BuGR2), 8 ug phospho-serine 211 (ab55189), or normal Rabbit IgG (Santa-Cruz, sc-2027) overnight at 4°C. A 1:1 mix of anti-rabbit and anti-mouse Dynabeads (Life Technologies) were used according to manufacturer's instructions. After incubation, beads were washed with low salt immune complex buffer (0.1% SDS, 1% Triton-X 100, 2 mM EDTA, 20 mM Tris-Cl pH 8.1, 150 mM NaCl), high salt immune complex buffer (0.1% SDS, 1% Triton-X 100, 2mM EDTA, 20mM Tris-Cl pH 8.1, 500 mM NaCl), LiCl immune complex buffer (0.25 M LiCl, 1% NP-40, 1% deoxycholate, 1mM EDTA, 10mM Tris-Cl pH 8.1) and finally in 1x TE. Crosslinks were then removed via an overnight proteinase-K digestion (Ambion #AM2546) and DNA purified using a standard phenol-chloroform extraction protocol. Purified DNA was then analyzed using quantitative real-time PCR. Primers were designed based on GR ChIP-Seq data published by (14, 15, 77, 78) and coordinates used are shown in Table 2.

Table 2. Coordinates used to generate primers for ChIP analysis

Gene Name	Coordinates
Fkbp-5	Chr17: 28556870-28557847
RhoJ	Chr12: 76404969-76405723
Sgk-1	Chr10: 21683041-21683190

2.3 RESULTS

2.3.1 Differences in the biology of Caveolin-1 Knock-Out and C57 Wild-Type CC-NPSCs.

2.3.1.1 The Anti-Proliferative effects of Dex in CC-NPSCs Requires Cav-1

The contribution of rapid GR signaling to the anti-proliferative effects of GCs exerted on a variety of tissue and cell types remains unresolved (36, 38, 56). Since rapid signaling effects of GCs on MAPK activation and GJIC are lost upon Cav-1 deletion in embryonic CC-NPSCs (29), we tested whether the anti-proliferative effects of GCs were altered in Cav-1 KO CC-NPSCs. As shown in Figure 5, Dex did not significantly impact proliferation of CC-NPSCs in Cav-1 KO neurospheres, which contrasts with C57 CC-NPSCs where proliferation was reduced by 10%. Furthermore, basal proliferation of embryonic CC-NPSCs was not affected by Cav-1 deletion (Figure 5A, 5B). Therefore, in embryonic CC-NPSC cultures, Cav-1 was an essential component of a GR signaling pathway that operates to limit proliferation.

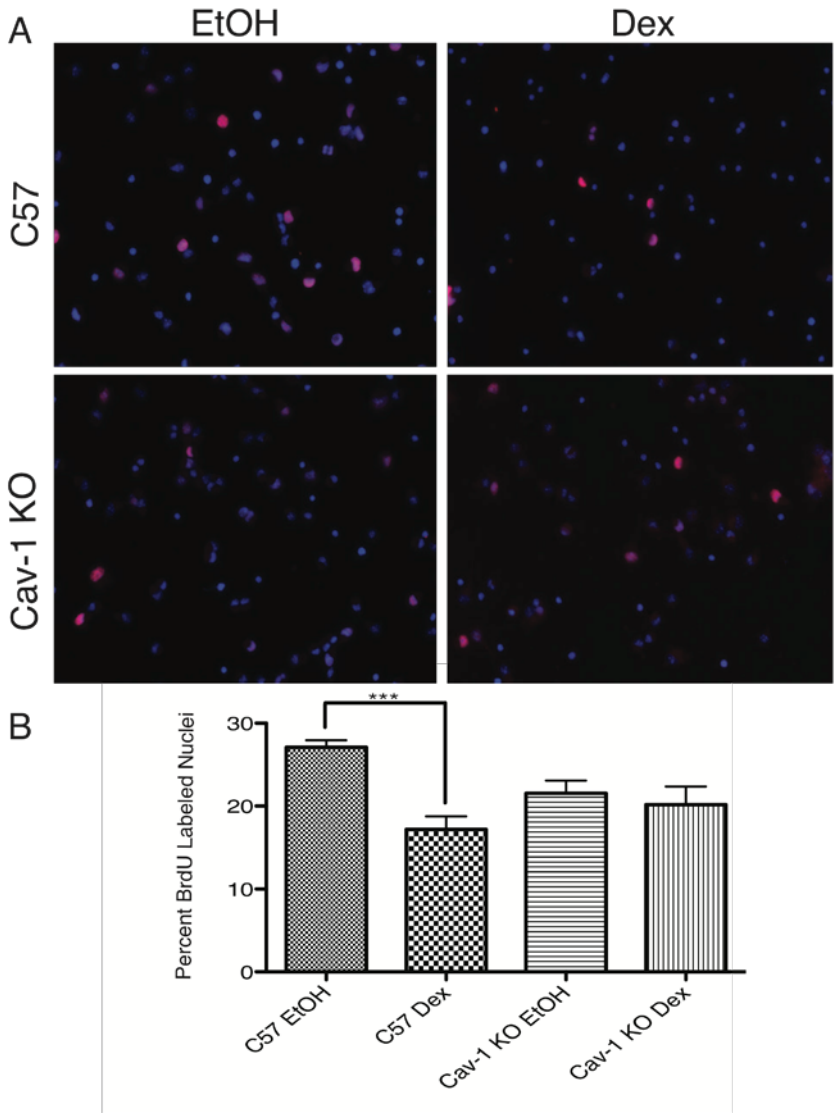

Figure 5. Anti-proliferative effects of Dex in CC-NPSCs requires Cav-1

A. C57 or Cav-1 KO CC-NPSCs were treated with Dex or vehicle (Ethanol; EtOH) for 24 h and pulsed with BrdU during the last hour of treatment. Immunocytochemistry was performed to detect BrdU positive nuclei (pink). Nuclei were visualized by DAPI staining (blue). B. Three independent coverslips per biological replicate were counted to ascertain the percentage of cells that passed through S-phase (i.e. BrdU positive nuclei). Error bars represent SEM, n=3 biological replicates. One-way ANOVA with Tukey's post test, $p<0.001$.

2.3.1.2 Cav-1 Deletion Abolished GR induction of Sgk-1, a Gene Required for the Anti-Proliferative Effect of Dex in CC-NPSCs.

We previously established that inhibition of GJIC by the rapid action of GR was associated with an inhibition of S-phase progression in cultured CC-NPSCs (29). Our observation that transient pharmacologic inhibition of GJIC is also sufficient to reduce CC-NPSC proliferation (29) was recently confirmed in cultured embryonic stem cell- derived neural progenitors and in embryonic neural progenitors isolated from the CC (79). Recent studies in human hippocampal neural progenitor cells indicate that the antiproliferative properties of GCs are dependent upon at least one genomic GR target gene, *Sgk-1* (68). Consistent with these findings, *Sgk-1* is also required for the anti-proliferative effect of GCs in our CC-NPSC cultures, since treatment with an SGK-1 inhibitor (GSK650394) blunts the growth inhibitory affect of Dex (Figs. 6A, 6B). *Sgk-1* was a GR target gene in C57 but not in Cav-1 KO CC-NPSCs as revealed by qRT-PCR analysis following a 4 hr Dex treatment (Fig. 6C). Thus, the role of Cav-1 in GC mediated effects on the cell cycle may extend beyond its impact on rapid GR signaling and influence genomic action of the receptor.

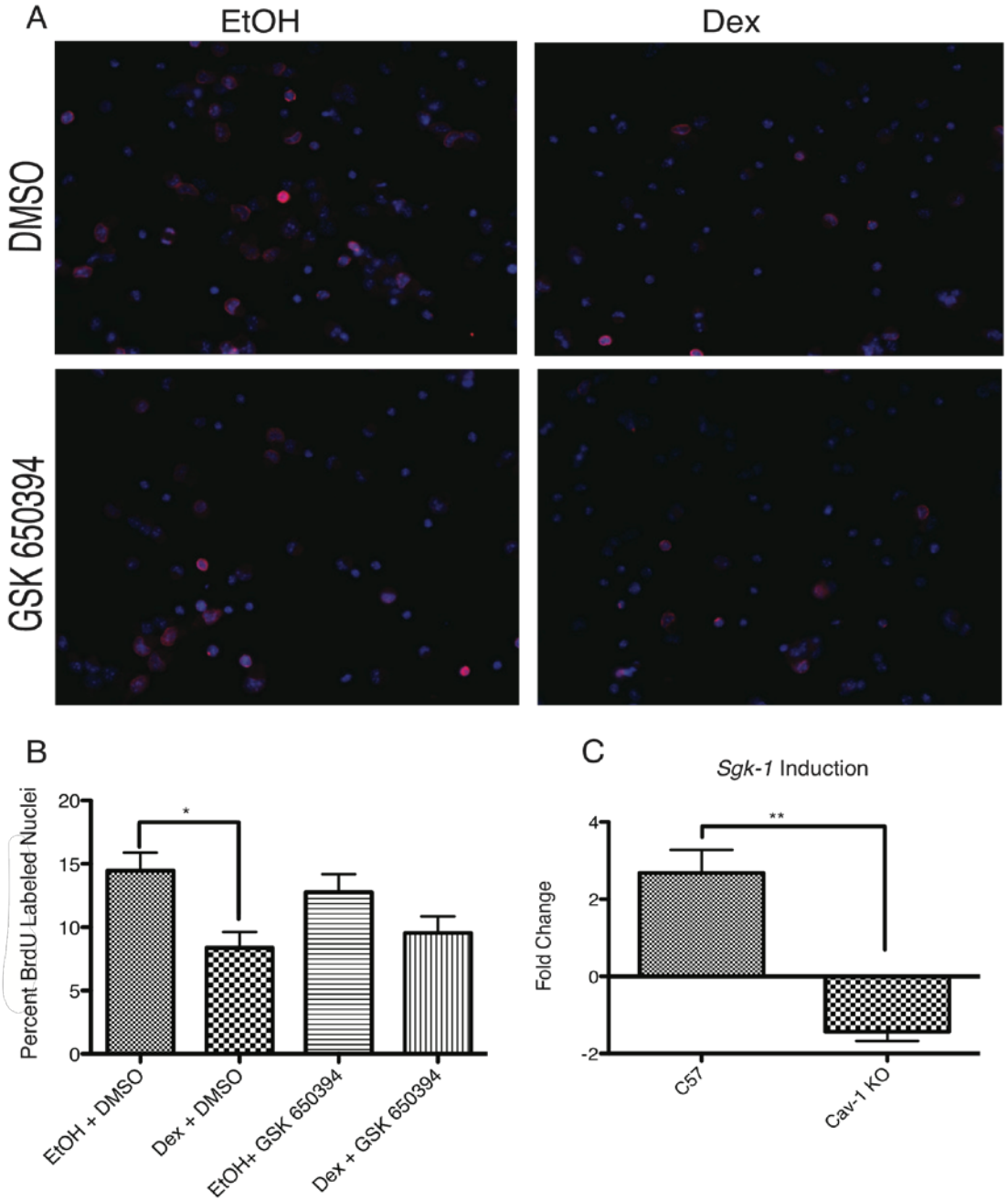

Figure 6. Anti-proliferative effects of Dex in CC-NPSCs requires SGK-1

A. C57 or Cav-1 KO cells were treated with Dex and/or the SGK-1 inhibitor, GSK650394 and the appropriate vehicle (EtOH or DMSO) for 24 h and pulsed with BrdU during the last hour of treatment. Immunocytochemistry was performed to detect BrdU positive nuclei (pink). Nuclei were visualized by DAPI staining (blue). B. Three independent coverslips per biological

replicate were counted to ascertain the percentage of cells that passed through S-phase (i.e. BrdU positive nuclei). Error bars represent SEM, n=3 biological replicates. One-way ANOVA with Tukey's post-test, $p<0.05$. C. qRT-PCR analysis of *Sgk-1* mRNA indicates that significant induction of *Sgk-1* occurs after a 4 h Dex treatment in C57 but not Cav-1 KO CC-NPSCs (Student's t-test, $p<0.01$).

2.3.2 Cav-1 Deletion Results in Enhanced CC-NPSC Radial Migration

Since both Cav-1 (61) and GC treatment (30) are implicated in altering cell migration, we next determined if loss of Cav-1 resulted in alterations in CC-NPSC migration. In the vehicle treated groups, loss of Cav-1 resulted in a significant increase in the total distance migrated (139.09 uM in C57 and 182.15 uM in Cav-1 KO) from the leading edge of the cell after 24 hours (Figure 7). Furthermore, in the Cav-1 KO cells, but not C57, Dex treatment resulted in significantly enhanced migration (Figure 7) (154.3 uM C57+ Dex and 139.09 uM C57 + EtOH versus 207.29 uM Cav-1 KO + Dex and 182.16 uM Cav-1 KO +EtOH). Therefore, loss of Cav-1 results in enhancement of CC-NPSC radial migration.

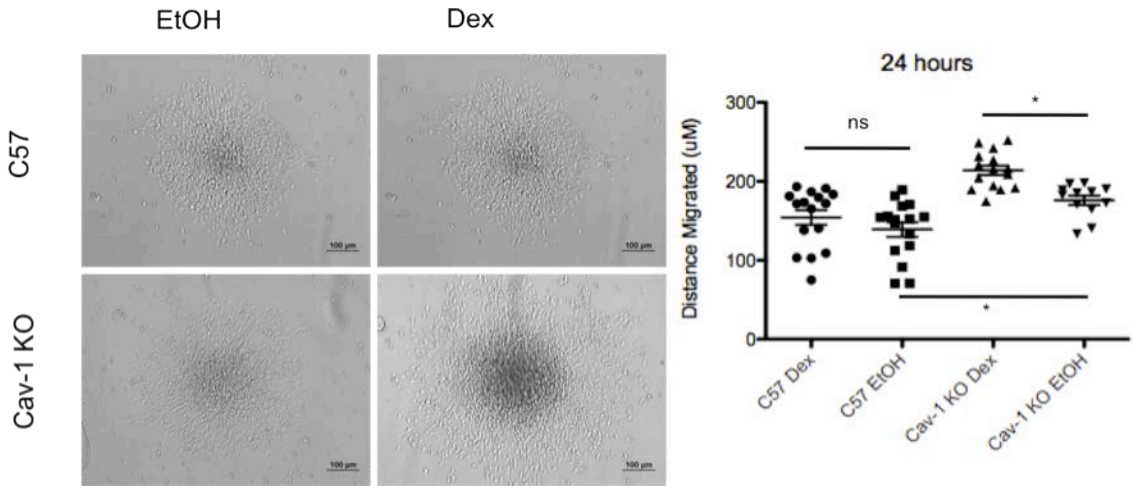

Figure 7. Loss of Cav-1 results in Enhanced CC-NPSC migration.

Neurospheres were allowed to adhere to PDL treated tissue 6-well tissue culture dishes and migrate in the presence of Dex or EtOH over a period of 24 hours. Approximately 30 spheres per condition per replicate were analyzed using ImageJ to ascertain the total distance migrated. Under basal conditions, Cav-1 KO CC-NPSCs migrate further than corresponding C57 CC-NPSCs. Cav-1 KO, but not C57 CC-NPSCs also have a pro-migratory response to Dex treatment. n=4 C57 and n=4 Cav-1 KO, One-way ANOVA with Tukey's post test, * indicates $p<0.05$.

2.3.3 Cav-1 Deletion Alters GC-Induced Differentiation of Oligodendrocytes

Previous studies revealed a role for Cav-1 in regulating astroglial and neuronal differentiation (64, 65). Recent work in the adult rat hippocampus revealed that stress or exogenous treatment with GCs results in decreased neurogenesis and enhanced oligodendrogenesis (31). Therefore, we used an *in vitro* differentiation assay to determine if loss of Cav-1 or treatment with Dex resulted in changes in the abundance of oligodendrocyte progenitors. Preliminary data indicates that at P1 and P3, in both C57 and Cav-1 KO cells, treatment with Dex results in an increase in the abundance of olig2 positive cells. Olig2 is a marker for oligodendrocyte progenitors therefore this data suggests that the differentiation of oligodendrocytes is enhanced in response to Dex treatment (Figure 8, Table 3). Interestingly, in P1 Cav-1 KO CC-NPSCs there appears to be a stronger Dex effect at P1 that is lost by P3, whereas in C57 CC-NPSCs, the greatest Dex response is observed at P3 (Table 3) indicating that sensitive periods where oligodendrocyte differentiation can be influenced by Dex varies in response to loss of Cav-1.

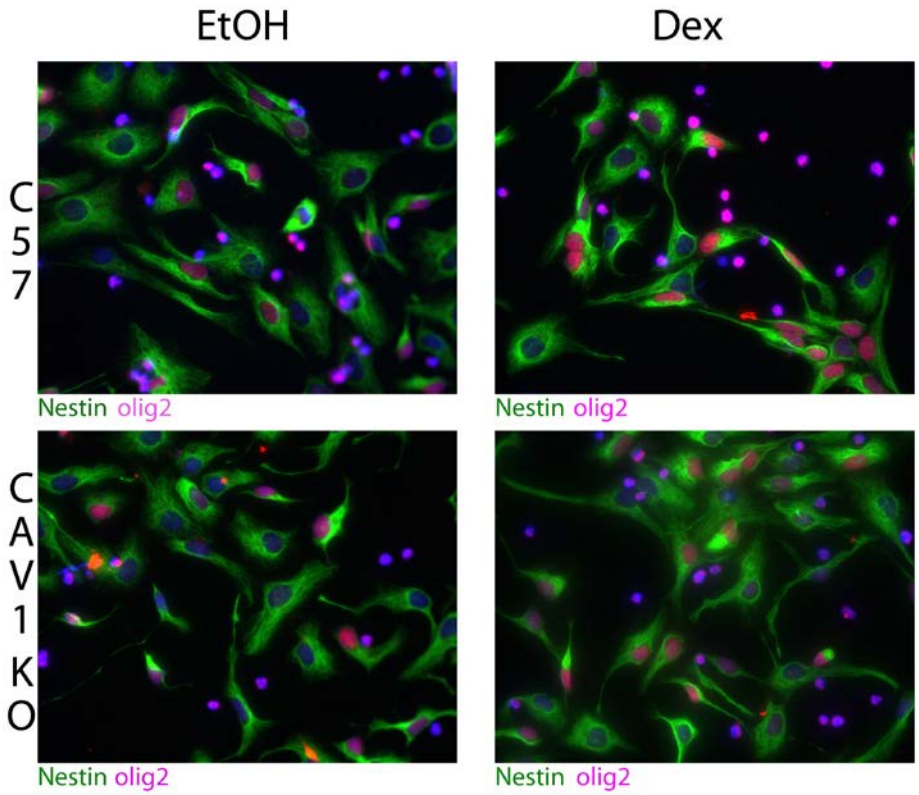

Figure 8. Preliminary data indicates that loss of Cav-1 results in altered GC-induced differentiation of oligodendrocytes.

P3 neurospheres from C57 or Cav-1 KO animals were treated for 24 hours with Dex or EtOH, dissociated, and plated on PDL and laminin treated coverslips in the presence of differentiation media and no growth factors. Cells were allowed to differentiate for a period of 24 hours prior to fixation and processing for immunocytochemistry. The number of olig2 (pink) positive cells was ascertained on independent coverslips to obtain the average percentages shown in Table 1. n=1 C57 and n=1 Cav-1 KO. Nestin, a marker of neural stem cells is shown in green.

Table 3. Percentage of olig2 labeled cells in P1 and P3 CC-NPSCs at 1DD.

Olig2 Positive Cells	P1	P3
C57 + EtOH	56.7%	49.08%
C57 + Dex	62.7%	73.8%
Cav-1 KO + EtOH	60.8%	61.6%
Cav-1 KO + Dex	79.75%	72.4%

2.4 ALTERATIONS IN GR MEDIATED GENE EXPRESSION BETWEEN CAV-1 KO AND C57 CC-NPSCS

2.4.1 Analysis of Cav-1 loss on GR Transcriptome in CC-NPSCs.

To examine Cav-1 regulation of genome-wide GR transcriptional responses, C57 and Cav-1 KO CC-NPSCs were subjected to microarray expression analysis. When compared to C57 CC-NPSCs, Cav-1 KO cells demonstrate differential basal expression of 186 genes (FDR < 0.1) with 44 genes exhibiting higher expression in Cav-1 KO cells and 20 genes lower expression by at least 1.5 fold. The transcripts with lowest expression in the Cav-1 KO versus C57 cells were Cav-1, as expected, and the ribosomal protein S9 (Rps9) gene, whose expression had previously been shown to be highly dependent upon Cav-1 (80). When Dex treated Cav-1 KO and C57 CC-NPSCs were compared for gene expression, 568 genes (excluding Cav-1 and Rps9) were differentially Dex responsive (FDR < 0.1). In general, Dex responsive genes were regulated in the same direction in both C57 and Cav-1 KO CC-NPSCs as shown in a heat map (Figure 9). However, individual genes do exhibit differences in Dex responsiveness between the two genotypes.

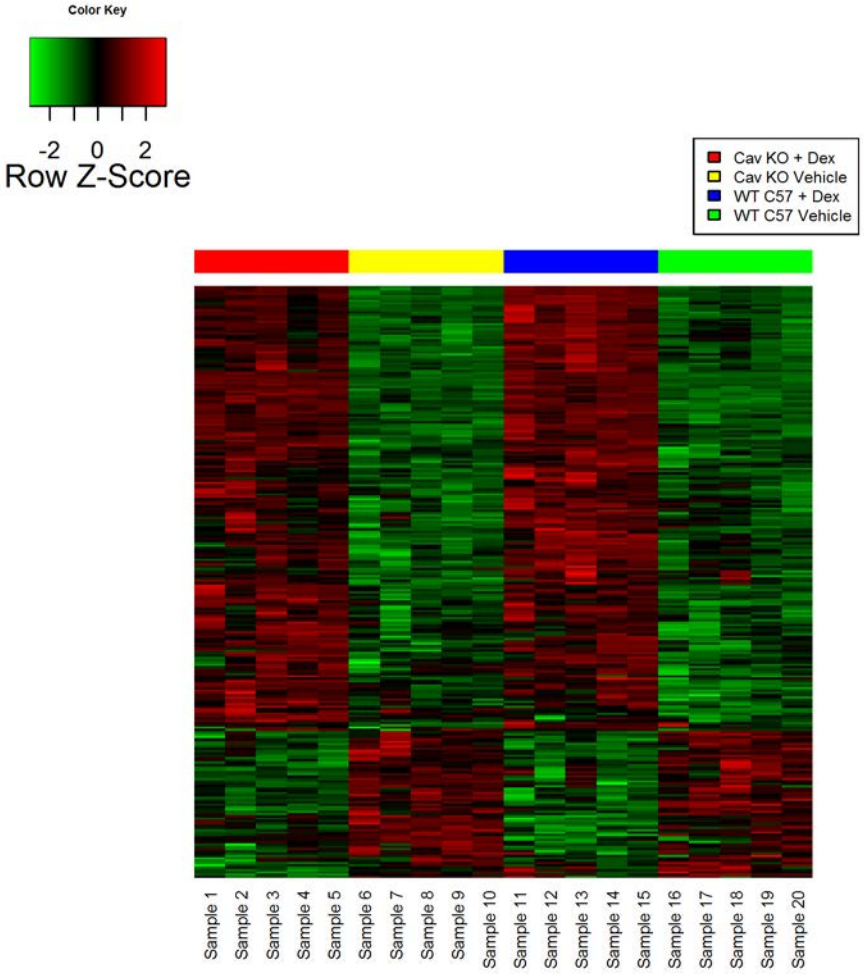

Figure 9. Loss of Cav-1 results in differential regulation of a subset of GR target genes.

Dex responsive genes between C57 and Cav-1 KO CC-NPSCs were clustered using Pearson's dissimilarity as distance measure and Average Linkage method for linkage analysis. The data are represented using a z-score normalized before plotting the heatmap. For each gene (row), the Z-score is calculated by subtracting the expression value by mean expression across all samples (centering) and dividing by standard deviation (scaling).

A number of genes that were induced by Dex at least 2.5 fold and exhibited robust differences in Dex regulated expression between C57 and Cav-1 KO CC-NPSCs were validated by qRT-PCR using independent NPSC cultures (Figure 10). For this analysis, we examined both well-established GR target genes (e.g. *Fkbp-5*) and genes with limited reports of GC responsiveness (e.g. *Gcnt2).* Specifically, Dex induction of *Fkbp-5*, *Gcnt2*, *RhoJ*, *Pcolce2*, *Mal*, *Adm* and *Arl4d* mRNA expression was significantly reduced in Cav-1 KO versus C57 CC-NPSCs (Figure 10). We also observed that *Cxcr4* did not attain similar levels of repression in response to Dex treatment in Cav-1 KO CC-NPSCs (Figure 10). Therefore, Cav-1 effects on GR action are not limited to rapid signaling (29) but also extend globally to genomic responses.

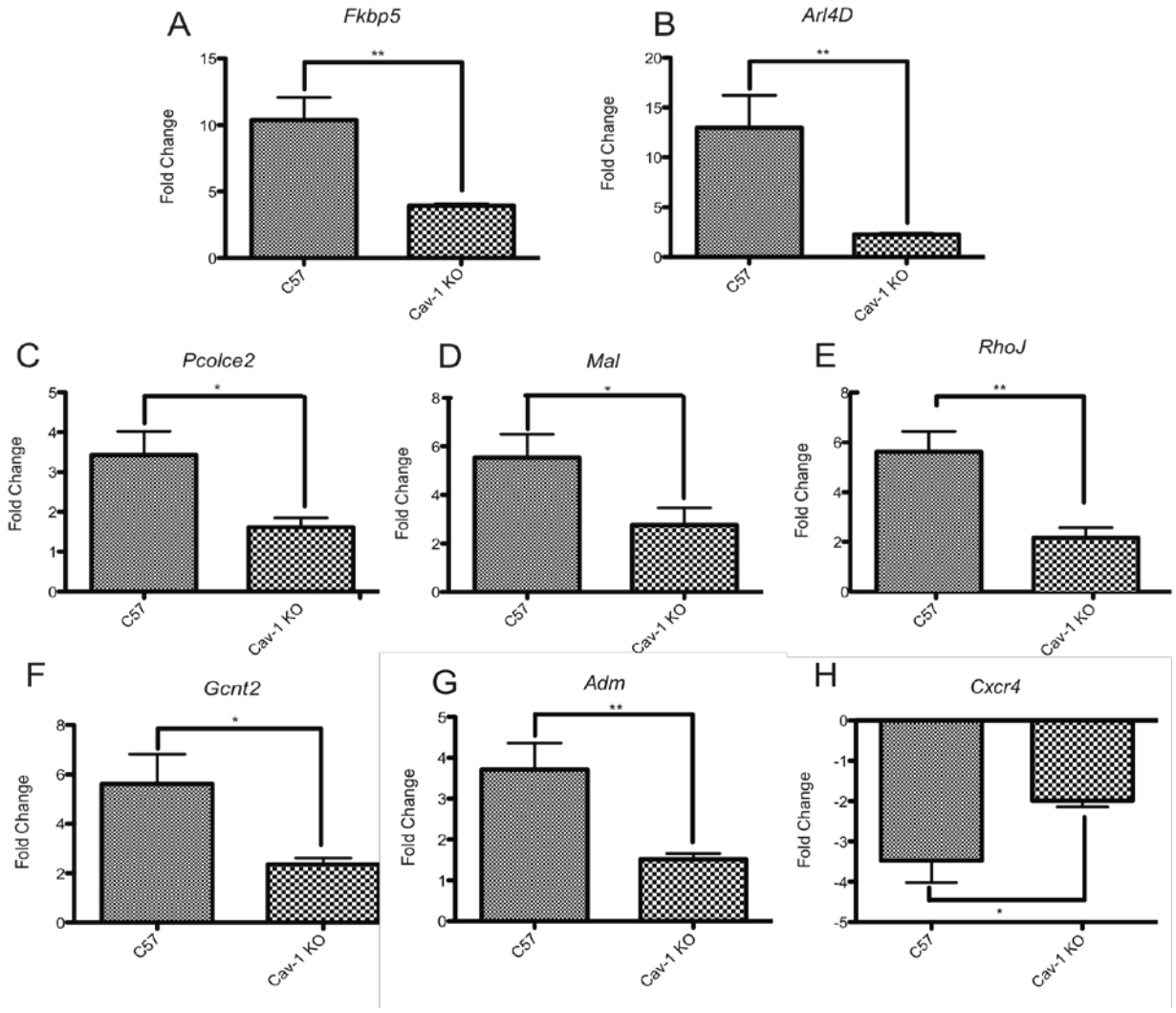

Figure 10. A subset of genes is differentially regulated by GR in C57 versus Cav-1 KO CC-NPSCs.

C57 or Cav-1 KO NPSCs from tissues independent of those used for microarray analysis were treated for 4 h with 100 nM Dex and mRNA expression of indicated genes analyzed using qRT-PCR. Although all genes shown are significantly induced in response to Dex, activation is attenuated in the Cav-1 KO cells. Error bars represent SEM, n=6. Student's t-test, * represents $p<0.05$, ** represents $p<0.01$.

Ingenuity® pathway analysis (IPA) was used to examine components of molecular networks and pathways defined by Dex regulated genes in C57 and Cav-1 KO CC-NPSCs. As shown in Figure 11C and 11D, the most significant functional networks defined by Dex responsive genes in C57 CC-NPSCs were distinct from networks formed in Cav-1 KO CC-NPSCs. For example, in C57 CC-NPSCs, cell cycle genes comprise the top two highly rated networks; 9 of the next 10 highly rated gene networks included molecules involved in development, particularly in the nervous system (Fig. 11C). Figure 4A shows the most highly rated cell cycle network in Dex treated C57 NPSCs. Included in this network are genes such as *Pcolce2* (Fig. 10C) and *Zbtb16* (data not shown), which were validated as GR targets by qRT-PCR of independent samples. In addition, top canonical pathways within this cell cycle network include a number of nuclear receptors; retinoid acid receptor, GR, peroxisome proliferation activating receptor alpha (PPARa)/retinoid X receptor alpha (RXRa), estrogen receptor and thyroid hormone receptor/RXRa.

A

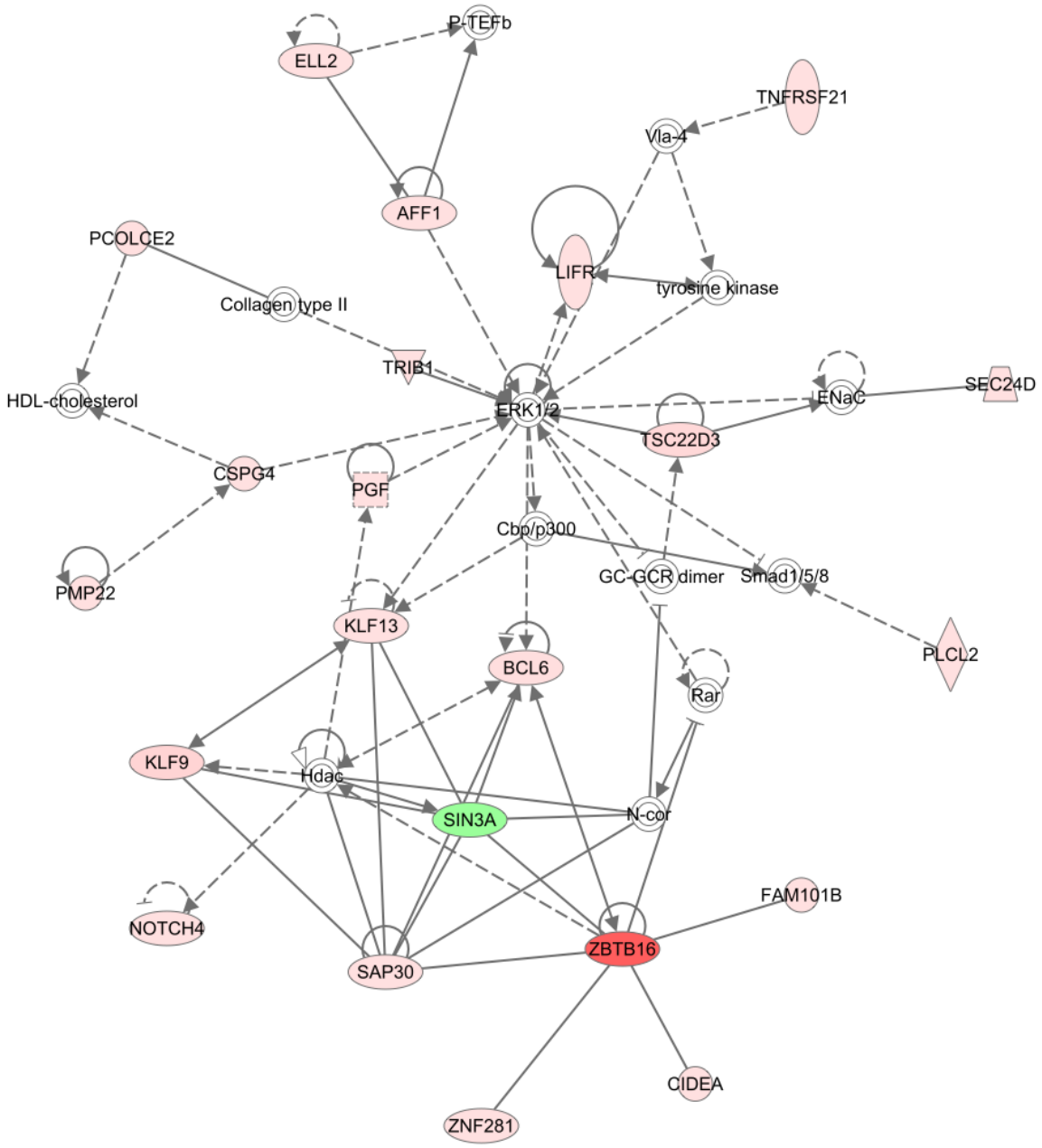

© 2000-2014 Ingenuity Systems, Inc. All rights reserved.

B

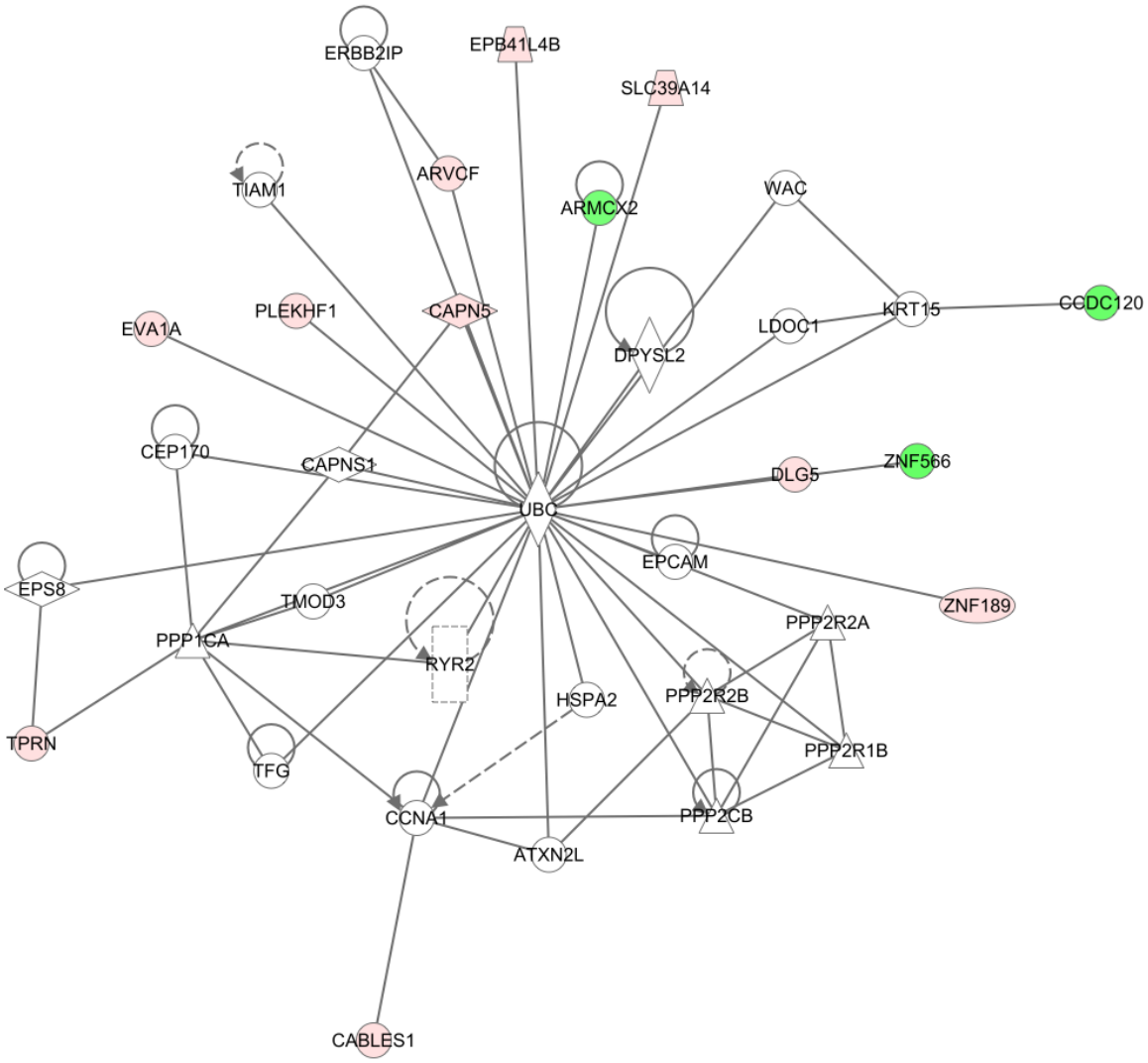

© 2000-2014 Ingenuity Systems, Inc. All rights reserved.

C

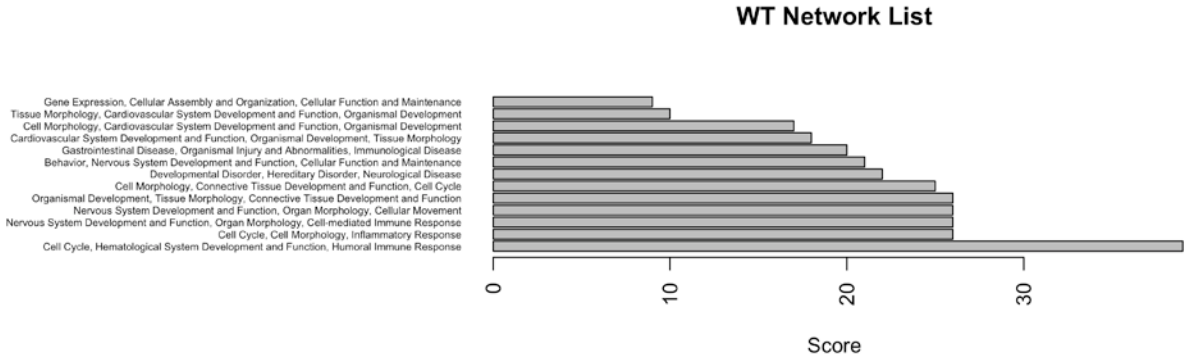

D

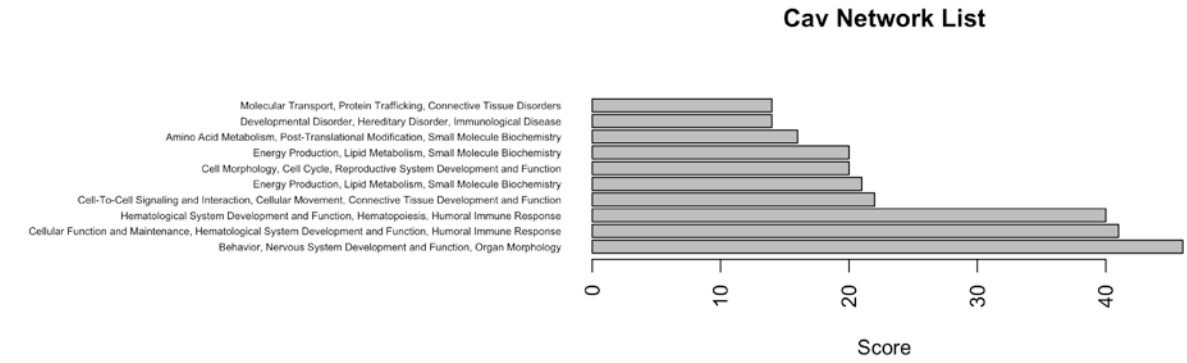

Figure 11. Dex regulated genes in C57 and Cav-1 KO CC-NPSCs comprise distinct cell cycle regulated networks.

IPA analysis using lists from Dex regulated genes in C57 (A, C) and Cav-1 KO (B,D) CC-NPSCs define distinct cell cycle networks shown. Upregulated genes are depicted in red and downregulated genes in green. The shading of red and green symbols indicates the extent of Dex upregulation or downregulation, respectively.

In contrast to C57 Dex regulated networks, Cav-1 KO CC-NPSCs demonstrated only one highly rated network involved in nervous system development (Fig. 11D). Although GR signaling pathways were part of nervous system development networks in both Dex treated C57 and Cav-1 KO CC-NPSCs, the genes in the two networks were different (Fig. 12A, 12B). In addition, the only cell cycle network (6^{th} highest) in Dex regulated Cav-1 KO CC-NPSCs was unrelated to the highest rated cell cycle network in Dex treated C57 CC-NPSCs (Figs. 11A, 11B).

A

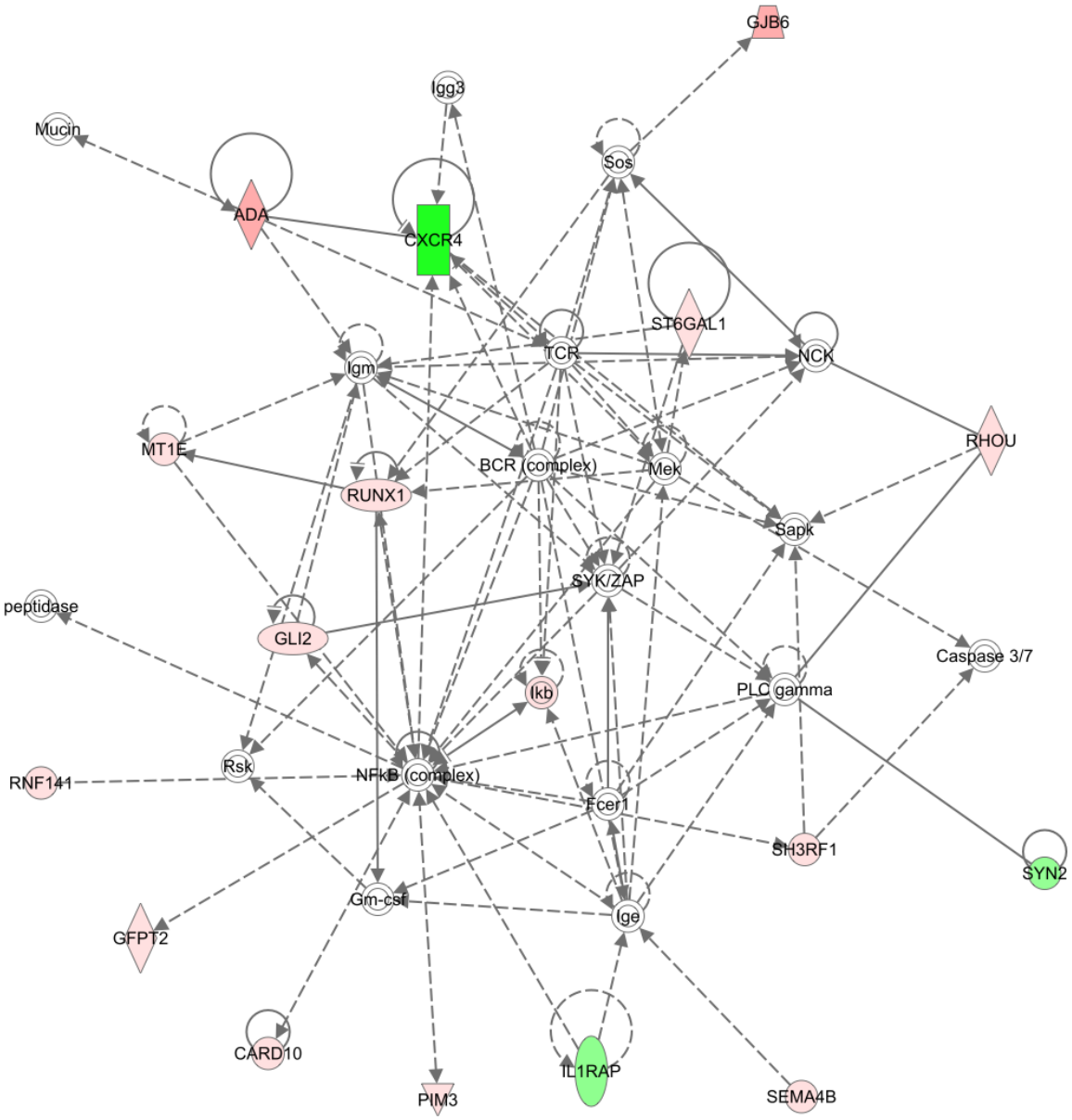

© 2000-2014 Ingenuity Systems, Inc. All rights reserved.

B

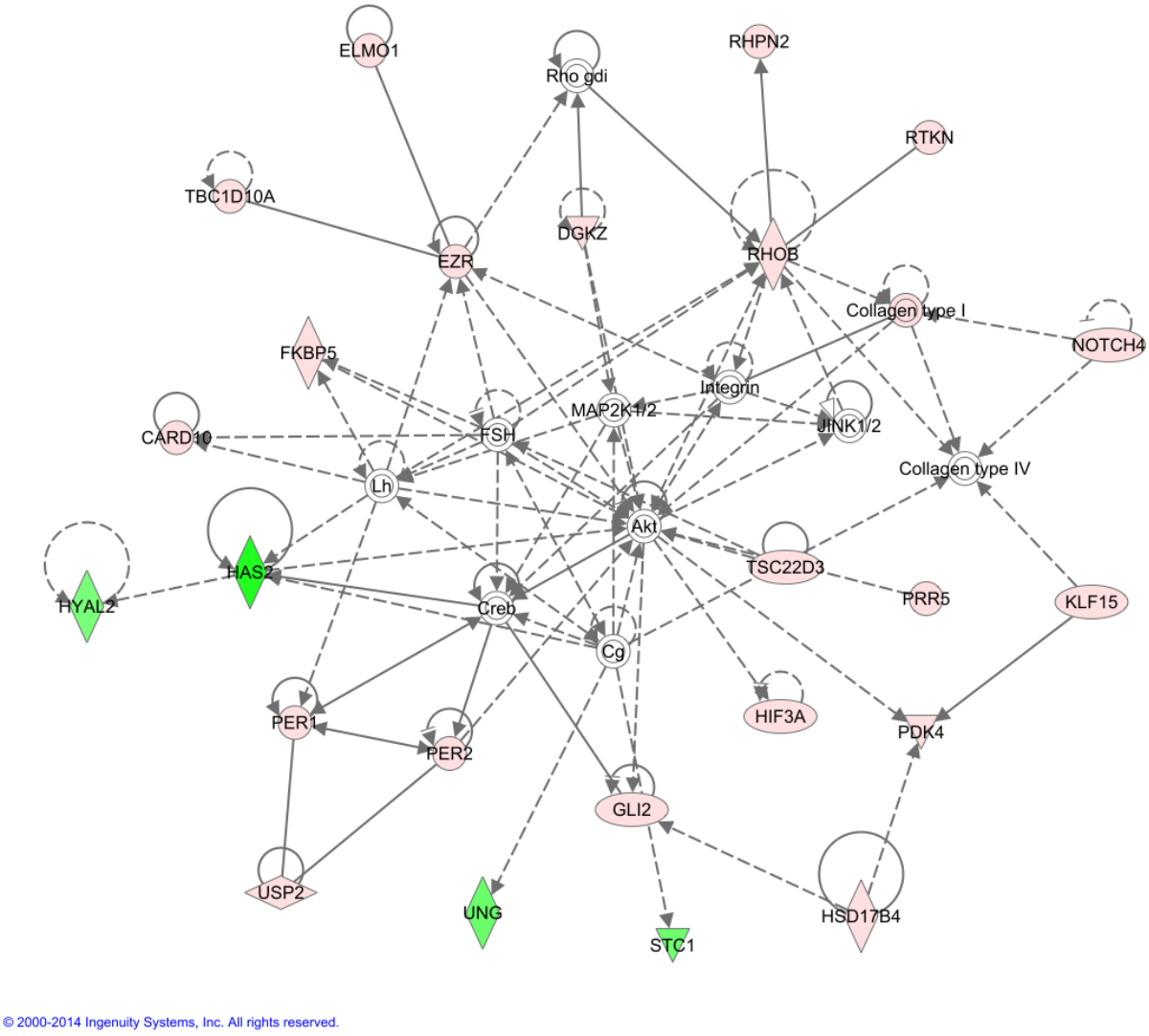

© 2000-2014 Ingenuity Systems, Inc. All rights reserved.

Figure 12. Dex regulated genes in C57 and Cav-1 KO CC-NPSCs comprise distinct nervous system development networks.

IPA analysis using lists from Dex regulated genes in C57 (A) and Cav-1 KO (B) CC-NPSCs define distinct nervous system development networks shown. Upregulated genes are depicted in red and downregulated genes in green. The shading of red and green symbols indicates the extent of Dex upregulation or downregulation, respectively.

The previous analysis used Dex regulated genes from C57 and Cav-1 KO CC-NPSCs, including those that were similarly responsive to hormone in the two genotypes. To examine differences in Dex responsiveness between the two genotypes, IPA analysis was performed using genes determined to be significantly different by ANOVA with regards to Dex response. This analysis showed that approximately half (i.e. 13) of the 25 highly rated networks formed by differentially Dex responsive genes were involved in some aspect of organ or tissue development (Figure 13C). In fact, the most highly rated networks function in nervous system development (Figure 12A, 12B), protein ubiquitylation (Figure 13C), and axon guidance or cellular/extracellular matrix interactions (Figure 13C). GC effects on neuronal migration and ubiquitin-proteasome mediated degradation have previously been observed in neural stem cells (36, 81) and may be influenced by Cav-1.

A

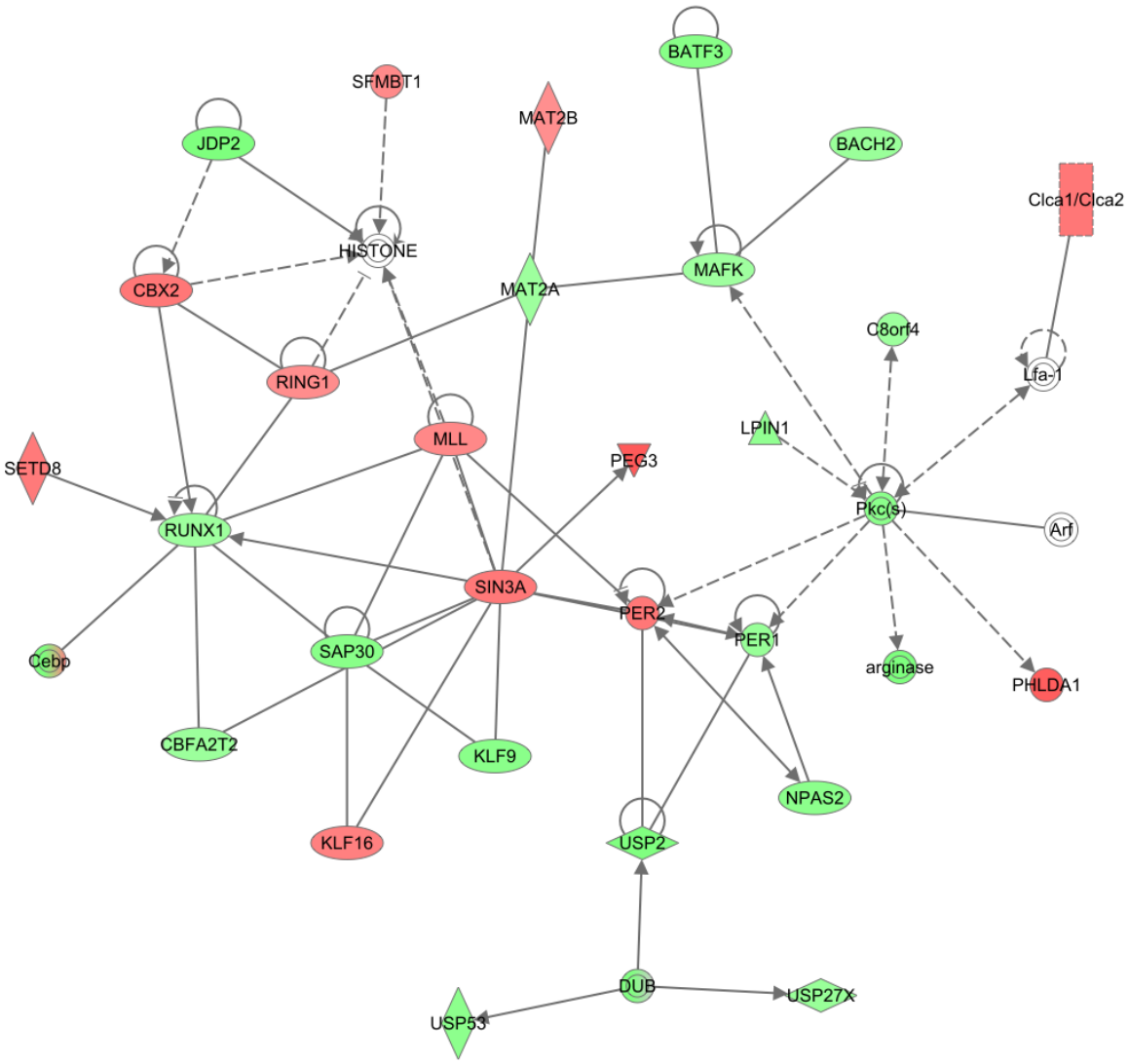

© 2000-2014 Ingenuity Systems, Inc. All rights reserved.

B

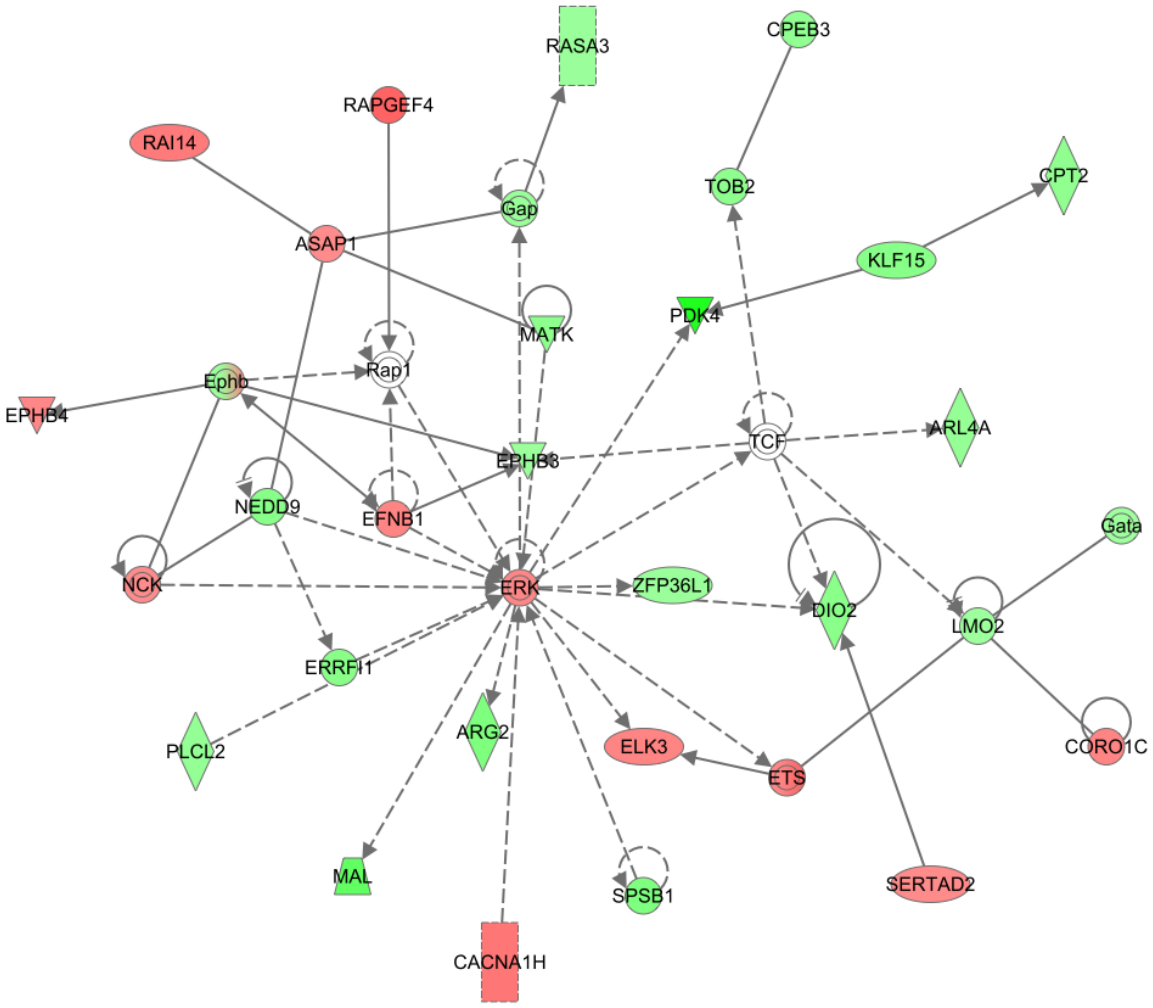

© 2000-2014 Ingenuity Systems, Inc. All rights reserved.

C

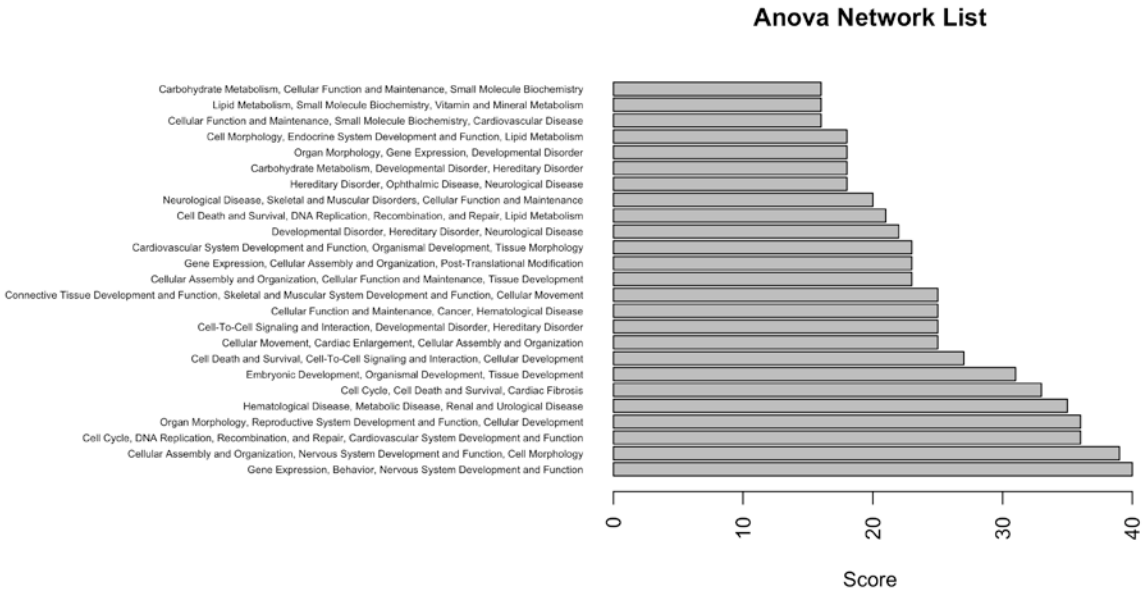

Figure 13. Genes differentially regulated by Dex in C57 versus Cav-1 KO CC-NPSCs comprise distinct nervous system development networks.

Shown are the top two distinct nervous system development networks defined by IPA analysis using lists from genes differentially regulated by Dex in C57 (A) versus Cav-1 KO (B) CC-NPSCs. Upregulated genes are depicted in red and downregulated genes in green. The shading of red and green symbols indicates the extent of Dex upregulation or downregulation, respectively. Panel C indicates the 25 most highly rated networks formed by genes differentially responsive to Dex.

To summarize, in addition to identification many novel primary GC responsive genes in CC-NPSCs, our microarray data implicated Cav-1 as a modulator of both rapid signaling and genomic action of GR.

2.4.2 Identification of Novel Dex Regulated Genes in CC-NPSCs.

To identify Dex regulated genes that are unique to neural stem cells, the NextBio® data mining tools (see Methods) were used to compare the GR regulated transcriptome in CC-NPSCs to others from cell and tissue sources as diverse as the 3134 mouse mammary adenocarcinoma cell line (71) and a mouse oligodendrocyte progenitor cell line (74) (Table 1). Specifically, this analysis included 14 separate studies; a union of differentially expressed genes from each of these studies generated 5000 GC regulated genes. A comparison of the GC regulated gene list in our NPSC cultures (Fig. 14A, Set 3) with a subset of these studies that used closely related cell types (i.e. rat neural (30) and oligodendrocyte progenitors (74); Fig 14A, Set 2) revealed 176 common genes (Fig. 14A). However, of the 5000 GC regulated genes from 14 data sets only 6 were uniquely GC regulated in our mouse NPSC cultures--*Gjb6, Gbx2, Card10, Plcl2, Smc5, Rnf157*. Three of these genes (*Gjb6, Gbx2, Plcl2*) were validated as Dex regulated in qRT-PCR analysis of independent samples (Figs. 14B-D). Therefore, the GR transcriptome in three-dimensional cultures of mouse NPSCs only included a limited number of unique target genes.

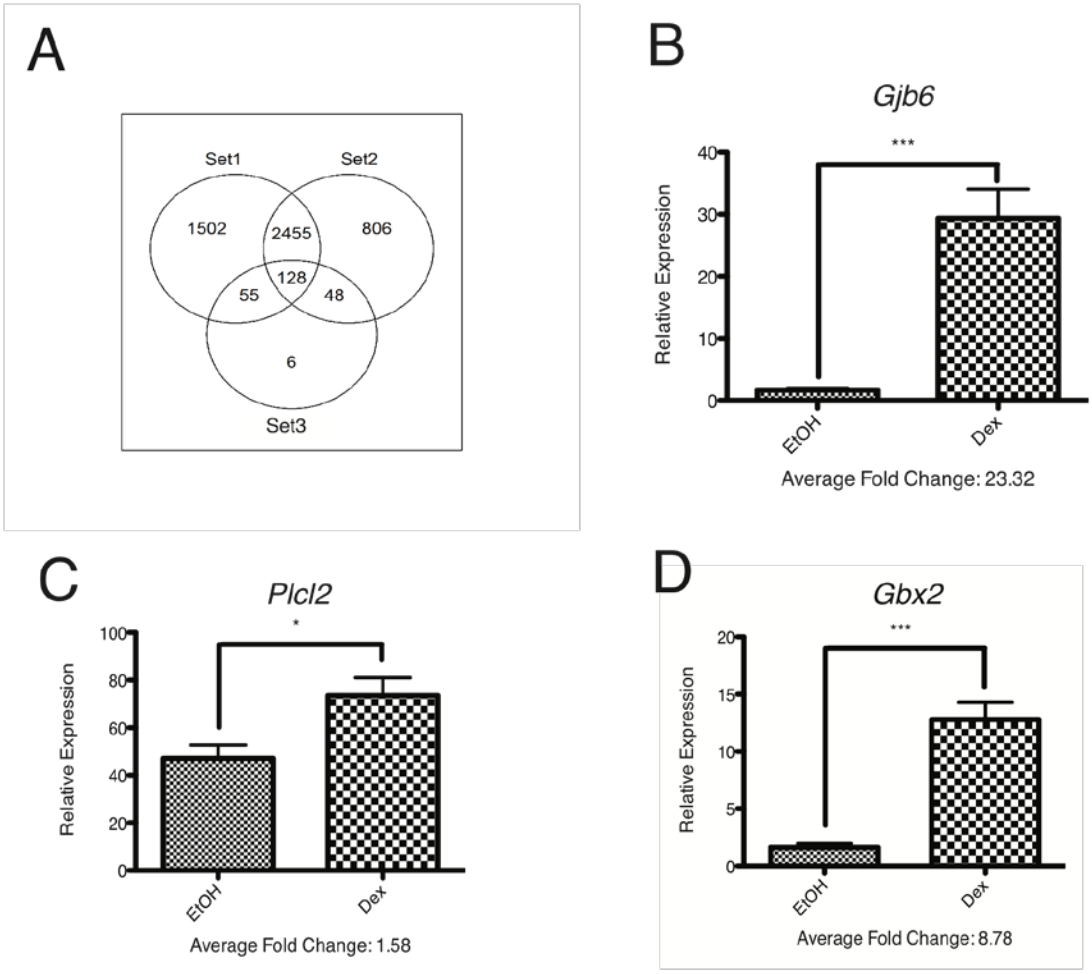

Figure 14. Next-Bio analysis reveals a subset of genes regulated by Dex in embryonic mouse CC-NPSC cultures.

A. Venn diagram comparing the GC-regulated gene lists in the 14 studies used to perform meta-analysis in NextBio. The genes contained in Set 1 are from study ID# 3-8, 12-14 (Table 1) and derived from cell types most distant from our mouse embryonic CC-NPSCs (Set 3). The genes contained in Set 2 are from study ID# 9-11 (Table 1) and derived from cell types closely related to our mouse embryonic CC-NPSCs (i.e. rat neural progenitors or mouse oligodendrocyte progenitor cells). B-D. C57 KO CC-NPSCs from tissues independent of those used in the microarray were treated for 4 h with 100 nM Dex and induction of *Gjb6* (B), *Plcl2* (C) and *Gbx2*

(D) mRNA analyzed using qRT-PCR. Error bars represent SEM, n=6. Student's t-test, * represents $p<0.05$, *** represents $p<0.001$.

One of the most highly induced genes uncovered in our microarray dataset was the cystic fibrosis transmembrane regulator (CFTR). CFTR is a chloride ion channel implicated in cystic fibrosis and is also expressed in neurons where it works with NKCC1 to regulate synaptic events (82). Using biological materials from samples independent of those used for the microarray analysis, the induction of CFTR in CC-NPSCs was validated (Figure 15A). To assess if a previous exposure to glucocorticoids, either the synthetic Dex or the natural ligand Corticosterone or Cort, resulted in long lasting effects on later expression of *Cftr*, we performed a "memory" experiment where cells were treated at P1 with GC, cultured under naïve conditions for an additional two weeks, and then re-treated for four hours (See §3.2, Figure 22) . Both Dex and Cort treatment results in reduced induction of *Cftr* at P3, indicating that a previous hormone exposure can influence later GC-regulated transcriptional activity.

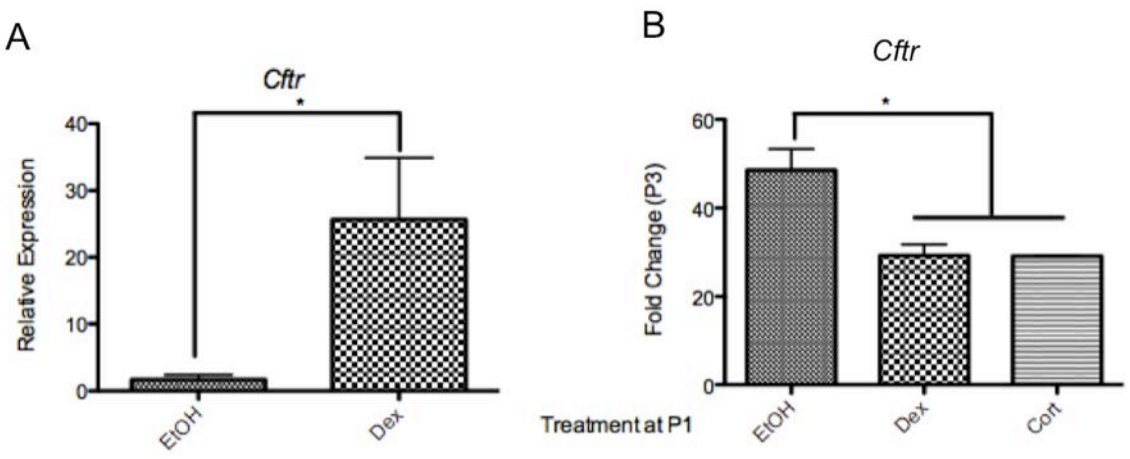

Figure 15. CFTR is a novel GR regulated gene in CC-NPSCs.

A. After four hours of Dex treatment, the mRNA expression of *Cftr* is substantially induced (n=6, Student's t-test, $p<0.05$). B. Pre-exposure of CC-NPSCs to Dex for one hour at P1 and subsequent analysis at P3 after treatment with Dex or cortisol (Cort) indicates that previous exposure to Dex influences later GR-mediated expression of *Cftr* (n=3, One-way ANOVA with Tukey's Post Test, * indicates $p<0.05$).

2.5 MECHANISMS FOR ALTERATIONS OF GR REGULATED GENE EXPRESSION IN CAV-1 KO CC-NPSCS

2.5.1 Cav-1 protein is not detectable in the nucleus of CC-NPSCs, nor does loss of Cav-1 impact mRNA or protein expression of GR

To determine a mechanism for Cav-1 effects on GR transcriptional activity, we first sought to determine if Cav-1 was found in the nucleus of CC-NPSCs. In ovarian carcinoma cell lines, Cav-1 regulates cell cycle regulatory gene expression through direct DNA binding (83). Cav-1 also affects transcription in lung epithelial Beas-2B cells by directly binding the transcription factor nuclear erythroid 2 p45-related factor 2 (Nrf2) (84). Our previous work (29) revealed an interaction between Cav-1 and GR in CC-NPSCs. However, Cav-1 was undetectable in nuclear fractions prepared from untreated or Dex-treated CC-NPSCs (Fig. 16). Dex-dependent nuclear translocation of GR occurred in both genotypes (Fig. 16).

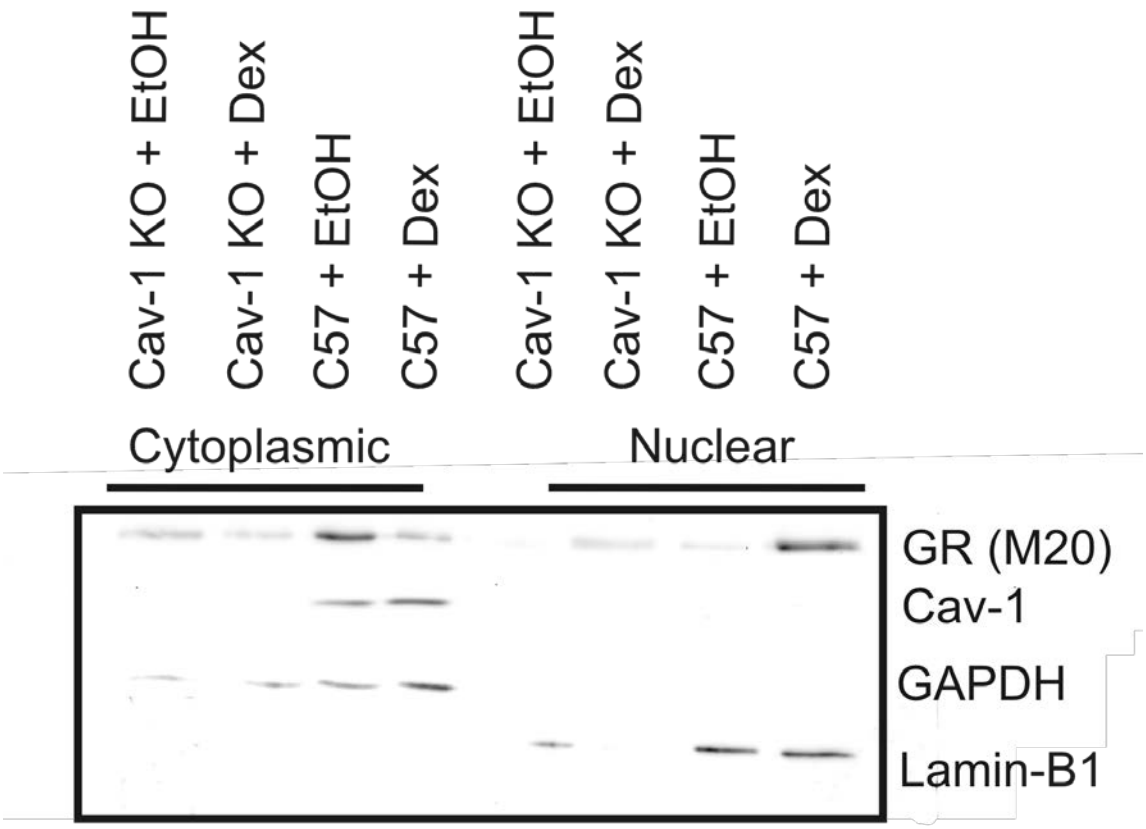

Figure 16. Fraction experiments indicate no detectable Cav-1 protein in the nucleus.

Cytoplasmic and nuclear fractions prepared from C57 and Cav-1 KO CC-NPSCs treated for 1 h with 100 nM Dex or EtOH vehicle were subjected to Western Blot analysis to detect GR, Cav-1 and markers for cytoplasmic (GAPDH) or nuclear (Lamin-B1) proteins. Cav-1 was not detected in nuclear fractions from C57 CC-NPSCs lysates and in either cytoplasmic or nuclear fractions from Cav-1 KO cells. Blot shown is representative of three independent experiments.

Furthermore, GR protein and mRNA levels were unaltered in Cav-1 KO CC-NPSCs (Figure 17). Therefore, Cav-1 may indirectly affect GR transcriptional response via regulation of a cytoplasmic signaling pathway that ultimately impacts GR bound at specific gene targets.

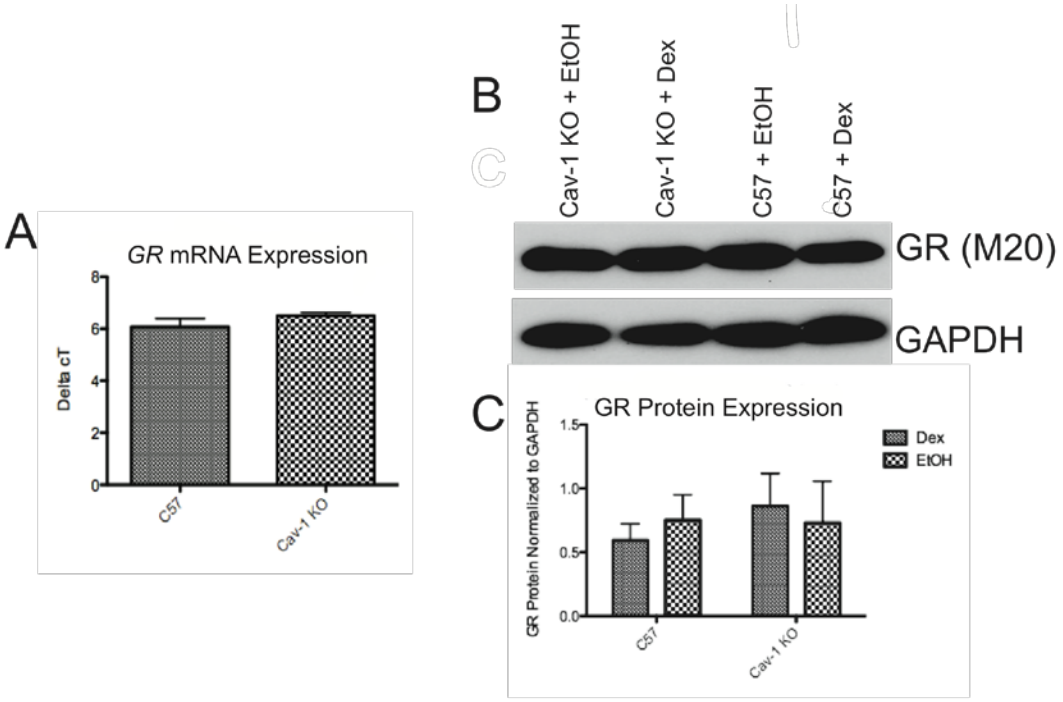

Figure 17. Loss of Cav-1 does not impact mRNA or protein expression of the GR in CC-NPSCs

A. qRT-PCR analysis indicated no difference in GR mRNA expression between C57 and Cav-1 KO cells (n=5). B-C Western Blot analysis also indicated no difference in GR protein (relative to GAPDH) expression between C57 and Cav-1 KO cells treated with 100 nM Dex or EtOH vehicle for 4 h (n=4) Error bars represent SEM.

2.5.2 Cav-1 Influences Site Specific GR Phosphorylation

Site-specific GR phosphorylation influences its transcriptional regulatory activity. In fact, different phosphorylation patterns within the amino-terminal activation function-1 domain can dictate which target genes will be bound by GR (17). Both MAPKs, targets of rapid GR signaling, and cyclin dependent kinase-2 (CDK2), phosphorylate GR and influence its transcriptional activity (18). Therefore, we tested the impact of Cav-1 deletion on MAPK and CDK2 dependent phosphorylation of GR at Serine 211 (S211) and Serine 226 (S226), respectively. As shown in Figure 18, phosphorylation at S211, a Dex responsive site, was undetectable in Cav-1 KO neurospheres. Since hormone-dependent phosphorylation at S211 is associated with transcriptionally active GR, the loss of phosphorylation at S211 may explain diminished Dex responsiveness of select genes in Cav-1 KO CC-NPSCs (e.g. Figure 10). GR phosphorylation at S226 is unaltered in Cav-1 KO CC-NPSCs. Therefore, Cav-1 does not alter global GR phosphorylation.

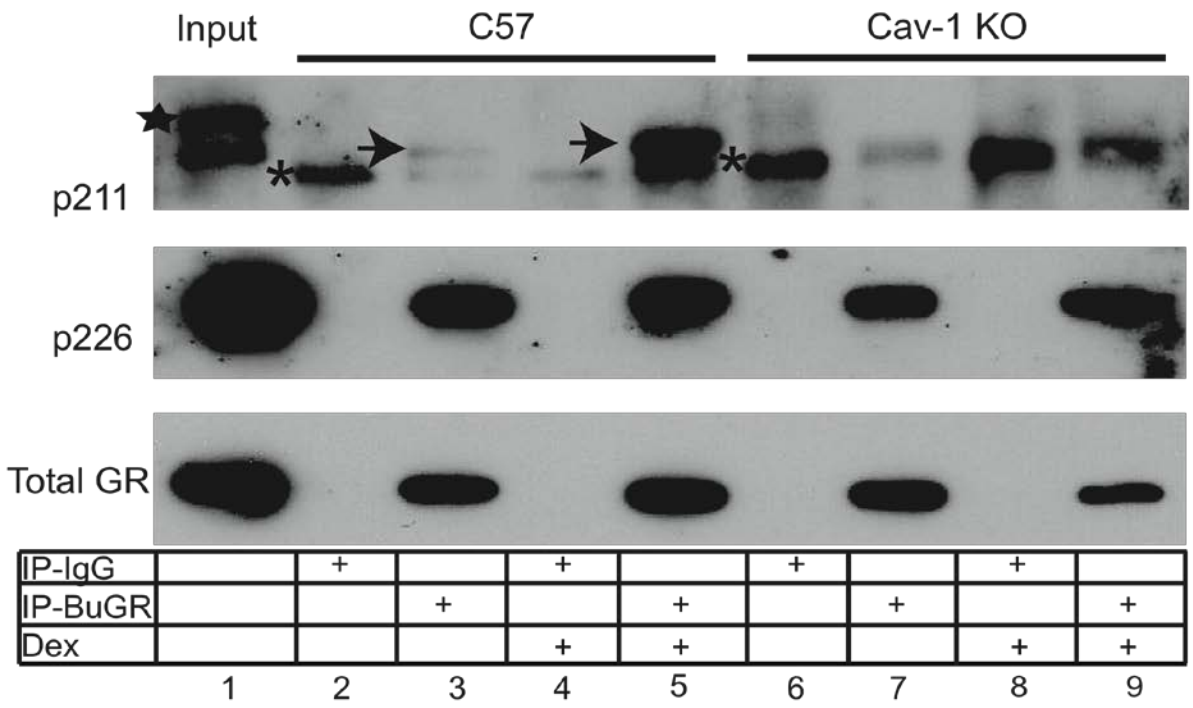

Figure 18. GR phosphorylation at S211, but not S226 is altered in Cav-1 KO CC-NPSCs.

Whole cell lysates from C57 and Cav-1 KO NPSCs treated for 1 h with 100 nM Dex or EtOH vehicle were subjected to immunoprecipitation with the BuGR-2 mouse monoclonal antibody against GR or non-immune mouse IgG and then subjected to Western blot analysis to detect total GR, phospho-S211 or phospho-S226 GR isoforms. Asterisk shows non-specific band detected in all lanes following pull-down with non-immune IgG. The identity of the higher molecular weight band in the input lane (star) is unknown but it is not detected in anti-GR antibody immunoprecipitates. The Dex inducible phospho-S211 isoform, detectable in C57 but not Cav-1 KO CC-NPSC lysates, is indicated by the arrow. GR phosphorylation at S226 is similar in C57 and Cav-1 KO lysates. Blot is representative of three biologically independent experiments.

2.5.3 Cav-1 Influences Recruitment of GR to Target Genes

We next determined if any of the genes differentially regulated in C57 and Cav-1 KO CC-NPSCs (Figure 10) were direct targets of GR and if recruitment of GR to gene regulatory regions was altered in Cav-1 KO cells. Directed chromatin immunoprecipitation (ChIP) assays were used to reveal GR recruitment to select target genes affected by Cav-1 KO, using previously reported GR binding sites in other cell lines (14, 15, 77, 78). As shown in Figure 19, three genes validated as differentially expressed in C57 versus Cav-1 KO CC-NPSCs have significantly decreased chromatin recruitment of GR in response to Dex treatment in Cav-1 KO CC-NPSCs (Figure 19A-C). Since GR phosphorylation at Ser211 is undetectable in Cav-1 KO cells (Figure 18) we did not expect to detect any recruitment of pSer211-GR to glucocorticoid regulated genes. Nonetheless, this we confirmed by ChIP assays with the pSer211-GR antibody as shown in Figure 19D, which also demonstrated diminished recruitment of pSer211-GR to the *Sgk-1* promoter in C57 CC-NPSCs. Therefore, reduced transcriptional responses to Dex in Cav-1 KO CC-NPSCs can be mediated by diminished recruitment of select GR phosphoisoforms to target gene regulatory sites.

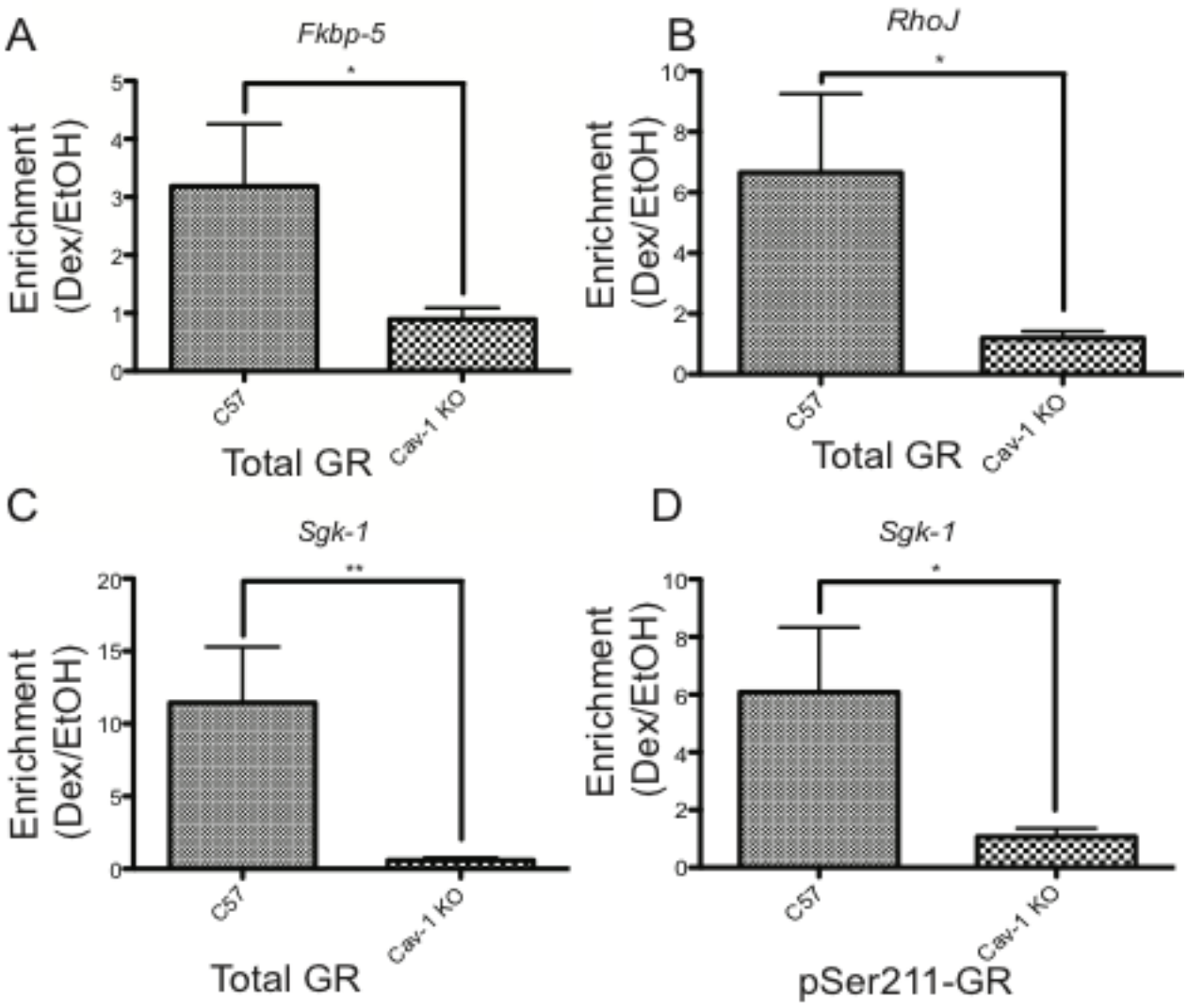

Figure 19. Chromatin immunoprecipitation experiments indicate altered recruitment of total and pSer-211 GR.

Chromatin Immunoprecipitation experiments using total GR (B-D) or phospho-S211 (E) antibodies indicates attenuated recruitment of GR to target genes in response to a 1.5 h treatment with 100 nM Dex. DNA was analyzed via qRT-PCR and final values shown are relative to total and IgG negative control before comparing enrichment in Dex vs. EtOH (n=3 biological replicates for C57 and n=5 for Cav-1 KO cells). Error bars represent SEM, Student's T-test, * represents $p<0.05$ and ** $p<0.01$.

2.6 DISCUSSION

The non-classical rapid activation of nuclear receptors residing at the plasma membrane mobilizes various cytoplasmic signaling pathways that can either directly alter cellular physiology (29, 56) or indirectly modulate transcriptional responses (58). Such crosstalk between rapid nuclear receptor signaling and classical genomic action can utilize nuclear receptors at target genes or independent transcription factors. In this report, we demonstrated that crosstalk between GR rapid and genomic pathways in embryonic NPSCs utilized Cav-1, a lipid raft protein. Cav-1 did not act as a classical coregulator of GR on genomic targets but rather altered the phosphorylation of GR on at least one site, S211. Phosphorylation of S211 in U2OS cells influences the GC transcriptional program (See §1.1) (17), and may likewise impact target genes regulated by GR in CC-NPSCs. In fact, alterations of the GR transcriptome in CC-NPSCs upon Cav-1 deletion define unique networks that potentially alter GC regulation of the cell cycle (See Model, Figure 20).

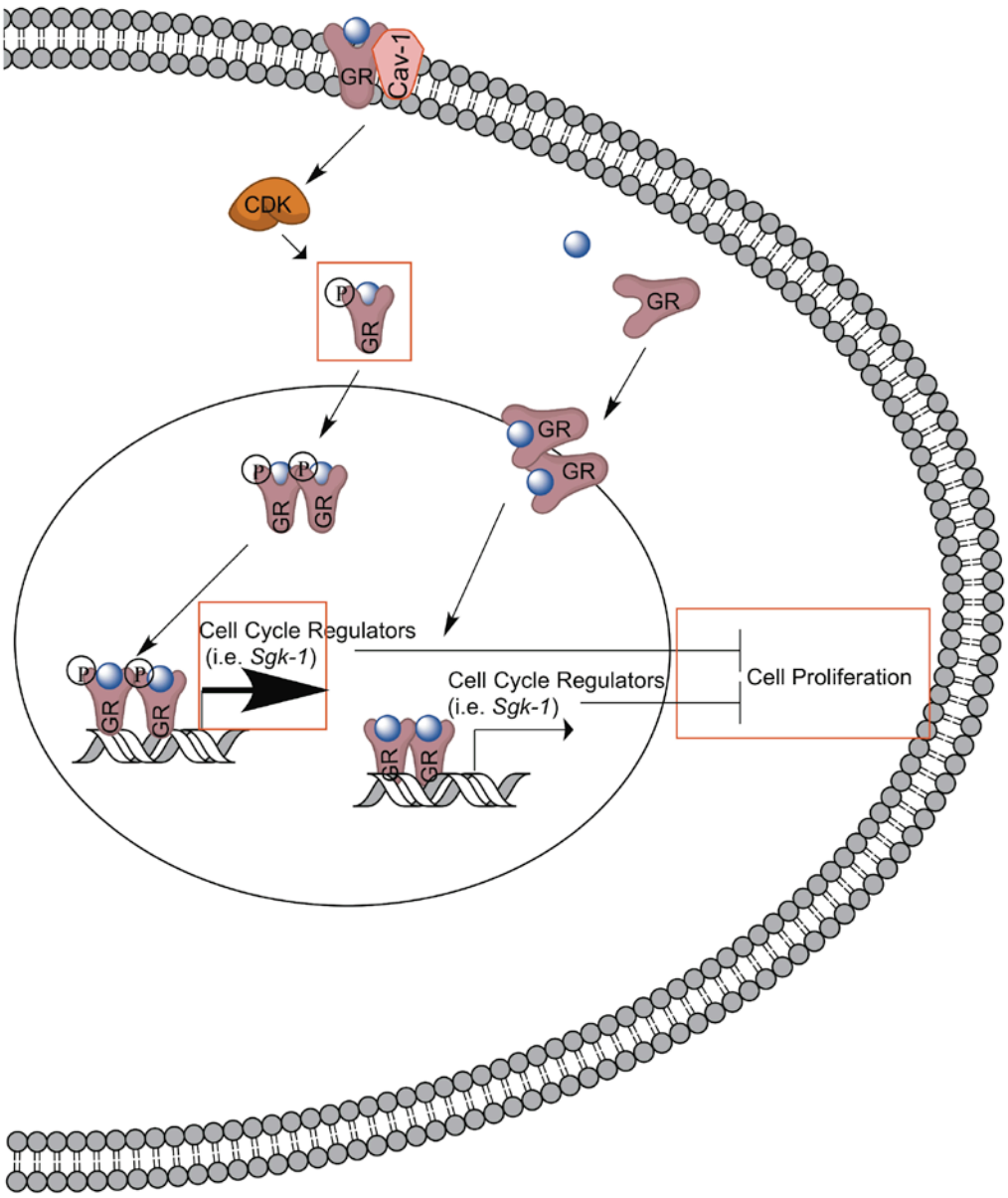

Figure 20. Model for Cav-1 mediated effects on genomic action of GR.

As shown on the right hand side of the figure, previous work demonstrated that GR binds to the promoter of *Sgk-1* (85), a GR target implicated in the anti-proliferative effects of GC in neural progenitor cells (68). New findings presented in this chapter are surrounded by red rectangles.

2.6.1 Loss of Cav-1 Results in Alterations in the GR Transcriptome in CC-NPSCs

The most prominent pathways defined by the GR transcriptome in C57 CC-NPSCs involved cell cycle progression and contain a number of genes that could contribute to the anti-proliferative effects of GCs (29, 36, 56). Notably, one validated GR target gene, *Sgk-1*, is required for the anti-proliferative effects of GC in embryonic mouse CC-NPSCs (this report) and a human hippocampal progenitor cell line (68) but did not reach significance as GC regulated in our microarray analysis or in analysis of hippocampal progenitors (72). The high stringency applied to microarray data sets, while reducing the number of false positives, may miss *bona fide* GR targets that play an important role in the biological effects of GCs. The inability of GR to induce *Sgk-1* expression in Cav-1 KO CC-NPSCs may underlie in part the loss of an antiproliferative response to Dex. However, it may be possible that the lack of anti-proliferative response in the Cav-1 KO may be due to fundamental differences in basal proliferation resulting in a state where the rate of cell cycling cannot be attenuate further. Importantly, a number of cell cycle regulated genes were also found to be differentially responsive to Dex in C57 versus Cav-1 KO CC-NPSCs so there are likely to be multiple GR targets that participate in the complex regulation of proliferation in CC-NPSCs, which are influenced by Cav-1. Since the GR transcriptome in C57 and Cav-1 KO embryonic CC-NPSC cultures also defines a number of pathways implicated in neuronal development, future studies may reveal a role for Cav-1 operating through either rapid signaling (29) or crosstalk with genomic GR pathways to influence antenatal effects of GCs on neurodevelopment.

Our study supports a role for Cav-1 in mediating genomic action of GR in addition to its role in rapid GR signaling. CC-NPSCs null for Cav-1 contain a subset of genes that are differentially regulated by GR in response to Dex. All of the genes validated exhibited no

differences in basal expression, except for *Pcolce2*, which demonstrated slight variability, but not enough to offset the difference in Dex induced expression. Of the subset that we validated, *Fkbp5* is a known target of GR involved in negative regulation of GR and the stress response. Improper regulation and expression of *Fkbp5* can contribute to neuropsychiatric diseases such as post-traumatic stress disorder (see §. 3.1.1). Alterations in regulation of *Fkbp5* may explain why adult Cav-1 KO animals tend to exhibit more anxious behaviors than their wild type counterparts (66). Additional studies in Cav-1 KO animals assessing cortisol reactivity and FKBP5 levels after exposure to a stressor may indicate changes in the HPA axis, which may underlie the anxious behaviors.

2.6.2 Identification of Novel GR Target Genes in CC-NPSCs

Gjb6, Gbx2 and *Plcl2* were novel validated GR target genes in CC-NPSC cultures but their role in regulating neural stem or progenitor cell function has yet to be determined. *Gjb6* encodes connexin 30, a gap junction protein expressed primarily in astrocytes but not until postnatal day 10 in mice (86). Therefore, Dex induction of *Gjb6* in our neurosphere cultures may be reflective of GR action in astrocyte progenitor cells. Future experiments utilizing specifically astrocyte progenitor cells either isolated by fluorescence activated cell sorting or identified using immunocytochemistry treated with Dex could indicate if *Gjb6* expression is specific to this population of cells. *Gbx2* is a homeobox transcriptional factor that has been shown to regulate various aspects of neural stem cell differentiation (87) and may contribute to reported effects of GCs on differentiation of distinct neuroprogenitors (38-40). Preliminary data indicates that the differentiation of oligodendrocyte progenitors may be altered in the Cav-1 KO CC-NPSCs. Data from others (31) and preliminary evidence from our lab indicates that Dex treatment in wild type

cells yields increased differentiation of oligodendrocytes with the largest effect seen in P3 CC-NPSCs. In the Cav-1 KO, it appears that the largest increase in the number of oligodendrocyte progenitors post Dex treatment occurs at P1. Since CC-NPSCs are able to recapitulate *in vivo* differentiation *in vitro*, the enhanced respond to Dex treatment at P1 in the Cav-1 KO versus P3 in C57 may indicate the existence of "sensitive" periods during development where cells are particularly susceptible to GC induced changes. In the Cav-1 KO, this GC-sensitive period may occur earlier possibly due to changes in gene expression. Future experiments addressing alterations in response to GC treatment *in vivo* in Cav-1 KO versus C57 animals may indicate further abnormalities in oligodendrocyte differentiation and maturation.

No role for phospholipase C-related protein (*Plcl2*) in neurodevelopment or GC action has been reported although *Plcl2* was identified in exome sequencing analysis as one of 40 genes with protein coding sequence variations in Schizophrenia patients (88). Notably, prenatal stress is thought to contribute to the development of schizophrenia (54). Our analysis revealed that one of the most highly regulated genes in our dataset was *Cftr*. *Cftr* is expressed throughout the human brain (89) and in embryonic but not adult rabbit brain (90). Further analysis of publically available DNA Hypersensitivity Assay datasets indicated an area of open chromatin around *Cftr* present only in E14.5 and E18.5 mouse brain tissue and not adult brain tissues (See Appendix 1, Figure 30). Previous work in a porcine model demonstrated that CFTR is functional within Schwann Cells. New born pigs null for *Cftr* demonstrate alterations in myelin sheath, reduced axonal density, and decreased nerve conduction velocity, therefore supporting a role for *Cftr* in the developing nervous system (91). We also observed that transcription of *Cftr* can be permanently altered in response to an earlier GC treatment, and without fully understanding the role of *Cftr* in cerebral cortex development, the full implications

of this altered regulation are unknown. Furthermore, microarray studies in oligodendrocyte progenitor cell lines indicate that in cells stimulated to differentiate in the presence of Dex, expression of *Cftr* is induced (74). Therefore, these data may indicate an role for *Cftr* in the developing brain, and another method by which GC treatment could alter later neuronal function.

2.6.3 Top Differentially Regulated Genes Between C57 and Cav-1 KO CC-NPSCs are Involved in Nervous System Development

Of the 25 highly rated networks identified by our analysis of genes differentially responsive to Dex in C57 versus Cav-1 KO CC-NPSCs, approximately half were related to organ or tissue development—the top two from our dataset involving nervous system development. Notably, one of these pathways involves protein ubiquitinylation. Multiple studies have revealed an impact of GCs on protein degradation of NPSCs. For example, GC treatment in rat embryonic neural stem cells results in decreased proliferation by enhancing ubiquitin-mediated degradation of the cell cycle regulator, Cyclin-D1 (36). In embryonic rat cells, Dex treatment increases expression of a deubiquitinating enzyme, Usp8/Ubpy that can indirectly cause increased degradation of the BRUCE/Apollo inhibitor of apoptosis protein. As a result of increased BRUCE degradation, there is a consequent decrease in cell proliferation (81). Interestingly, Cav-1 interacts with and regulates the polyubiquitinylation of active Rac1 (92). Rac1 is a member of the Rho-like GTPases and also involved in actin polymerization and protrusion and cell migration. Therefore, loss of Cav-1 may influence cell migration in NPSCs mediated by Rho-like GTPases.

The second most highly regulated pathway we uncovered during our network analysis involved axon guidance. Interestingly, *RhoJ,* and *Arl4D* were validated as genes differentially

regulated between C57 and Cav-1 KO and are both implicated in actin mediated cell migration (93, 94). Furthermore, *Cxcr4* was also validated as a differentially regulated gene and is implicated in dopaminergic cell migration (95). GC effects on neural stem cell migration are well documented (30). Therefore, GR signaling mediated by Cav-1 could have a critical impact on the biology and development of CC-NPSCs by regulating the degradation of cell cycle regulators or migration of differentiated cells derived from CC-NPSCs to their final position in the cortex. Radial migration assays indicated that Cav-1-KO CC-NPSCs are more pro-migratory than their C57 counterparts—a phenomenon that is enhanced upon treatment with Dex. Since *RhoJ* and *Arl4D* are pro-migratory and *Cxcr4* is anti-migratory, and all three do not reach the same levels as C57 of activation/repression in the Cav-1-KO, this indicates that there may be other genes or mechanisms that are dysregulated upon loss of Cav-1 to result in enhanced migration, and treatment with Dex results in a synergistic effect.

2.6.4 Changes in GR Transcriptome Linked to Alterations in Phosphorylation of GR at S211

Although Cav-1 was not found in the nucleus of CC-NPSCs, it influenced site-specific GR phosphorylation, which in turn could impact the GR transcriptome. Specifically, phosphorylation at S211, but not S226, was affected in Cav-1 KO CC-NPSCs. Therefore, the GC response of genes that require pSer211-GR to reach peak activation may be altered in Cav-1 KO CC-NPSCs. For example, pSer211-GR is recruited to promoters of genes such as *Gilz* and *Tat* to activate their transcription (17). Since GR phosphorylated at S211 is associated with activated gene transcription, alterations in pSer211-GR are consistent with the attenuated activation of select GR target genes in Cav-1 KO CC-NPSCs. Results from ChIP assays on select GR target genes

provide additional mechanistic insights regarding the role of Cav-1 in GC regulated transcription and show reduced recruitment of GR (and pSer211-GR) to select regulatory regions of genes differentially responsive to Dex in C57 versus Cav-1 KO CC-NPSCs. Since GR is recruited to multiple binding sites of its target genes, a more comprehensive analysis of the GR cistrome in C57 versus Cav-1 KO CC-NPSCs using ChIP-seq will be required to uncover other mechanistic features of site-specific Cav-1-dependent GR recruitment. Given that the majority of Dex regulated genes in CC-NPSCs were unaffected by Cav-1 KO, GR chromatin recruitment is not globally regulated by Cav-1. Finally, other future experiments directed towards identifying genes occupied by distinct GR phosphoisoforms (e.g. pSer211-GR) in CC-NPSCs could identify specific GC regulated gene networks that are influenced by crosstalk with cytoplasmic signaling pathways. In fact, alterations in GR phosphorylation in specific adult rat brain regions are generated in response to specific stresses and may impact select genes that modulate behavioral responses to stressful states (96).

Phosphorylation of GR at S211 and S226 is mediated by two different kinases—CDK2 at S211 and MAPK at S226. Others have suggested that Cav-1 is a tumor suppressor gene due to its role in mitogenic signaling (97). Ablation of Cav-1 in metastatic lung cancer cell lines results in proliferation arrest and decreased expression of cyclin-D1 and CDK4 (97). Therefore, Cav-1 loss may independently affect the expression or activity of cell cycle regulators or in conjunction with rapid GR signaling impact CDK2 and consequently genomic action of GR.

2.6.5 Summary

In summary, Cav-1 is a multi-functional regulator of GR action in NPSCs. Cav-1 influences both GR-dependent rapid changes in intercellular communication through gap junctions (29), which is required for establishment of cerebral cortical architecture (79) and the GR transcriptome, including genes responsible for regulating NPSC proliferation. The wide variety of GR gene networks affected by Cav-1 also suggests that this novel regulator of receptor action could impact the ultimate fate and laminar position of cells derived from embryonic cerebral cortical NPSCs exposed prematurely to GCs during fetal development.

3.0 GLUCOCORTICOID TREATMENT OF HYPOTHALAMIC NPSCS RESULTS IN SEXUALLY DIMORPHIC AND LONG LASTING CHANGES IN REGULATION OF GR TARGET GENES

3.1 INTRODUCTION

3.1.1 The Hypothalamus Links the Central Nervous and Endocrine Systems

During embryonic development, the hypothalamus (HT) derives from a region of the ventral diencephalon known as the hypothalamic sulcus that can be distinguished morphologically from embryonic day 9.5 in the mouse (98, 99). Proper patterning of the HT involves the contribution of several signaling pathways including sonic hedgehog and Wnt signaling (reviewed in (99)). Several transcription factors serve important roles in proper development of the HT. For example, without SIM1 and/or its dimerization partner ARNT2, mutant mice are lacking all neurons that comprise the paraventricular nucleus (99). SIM1 and ARNT2 also control the regulation of *Brn2*, another transcription factor with an essential role in the differentiation of corticotropin releasing hormone (CRH) neurons (99). SF1 is a member of the NR superfamily and knock-out studies indicate an essential role for SF1 in mediating survival, migration, and differentiation within the hypothalamus (99).

Although the HT serves as a link between the central nervous and endocrine systems, it compromises a very small percentage of the overall brain volume, slightly less than 2% (100). The mature hypothalamus is located beneath the thalamus and adjacent to the pituitary gland. The HT can be classified into three distinct regions: the periventricular, medial and lateral. Each of these three regions contain specific nuclei or regions such as the paraventricular nucleus and anterior hypothalamus each having specific functions and controlling a wide variety of processes including growth, metabolism and reproduction (99). Distributed throughout the HT are a variety of neurosecretory neurons. These include cells that secrete CRH, an important component of the hypothalamic-pituitary adrenal (HPA) axis, and cells that secrete thyrotropin-releasing hormone to regulate the production and release of thyroid hormone (reviewed in (99)). The secretion of CRH (and others) then stimulate the anterior pituitary to control hormone secretion (99).

One of the critical roles of the HT is in regulation of the HPA axis, a physiological process that contributes to regulation of the body's stress response (Figure 21). In response to stress or as a part of normal circadian rhythms, the hypothalamus secretes CRH. CRH then stimulates the transcription of pro-opiomelanocortin (POMC) within the pituitary gland, which then gives rise to adrenocorticotropic hormone or ACTH. ACTH travels through the blood stream to the adrenal cortex, a heavily vascularized gland residing above the kidneys. The adrenal gland is comprised of three areas, each of which gives rise to a different hormone in response to signals from the pituitary gland. In the case of the HPA axis, ACTH stimulation leads to the production of GCs from the region of the adrenal gland known as the zona fasciculate. These GCs act in a variety of manners through the GR in all cell types of body to aid in the body's response to a stressful situation. GCs are integral in shutting down the stress response at all levels. For example, GCs decrease the transcription of POMC, which then leads to

less production of ACTH. Furthermore, GCs also inhibit the production and secretion of CRH. At the level of the GR, GC stimulation causes increased transcription of *Fkbp5*, leading to increased levels of FK506 binding protein 51 (FKBP5), which binds to the GR to de-activate the receptor (100, 101).

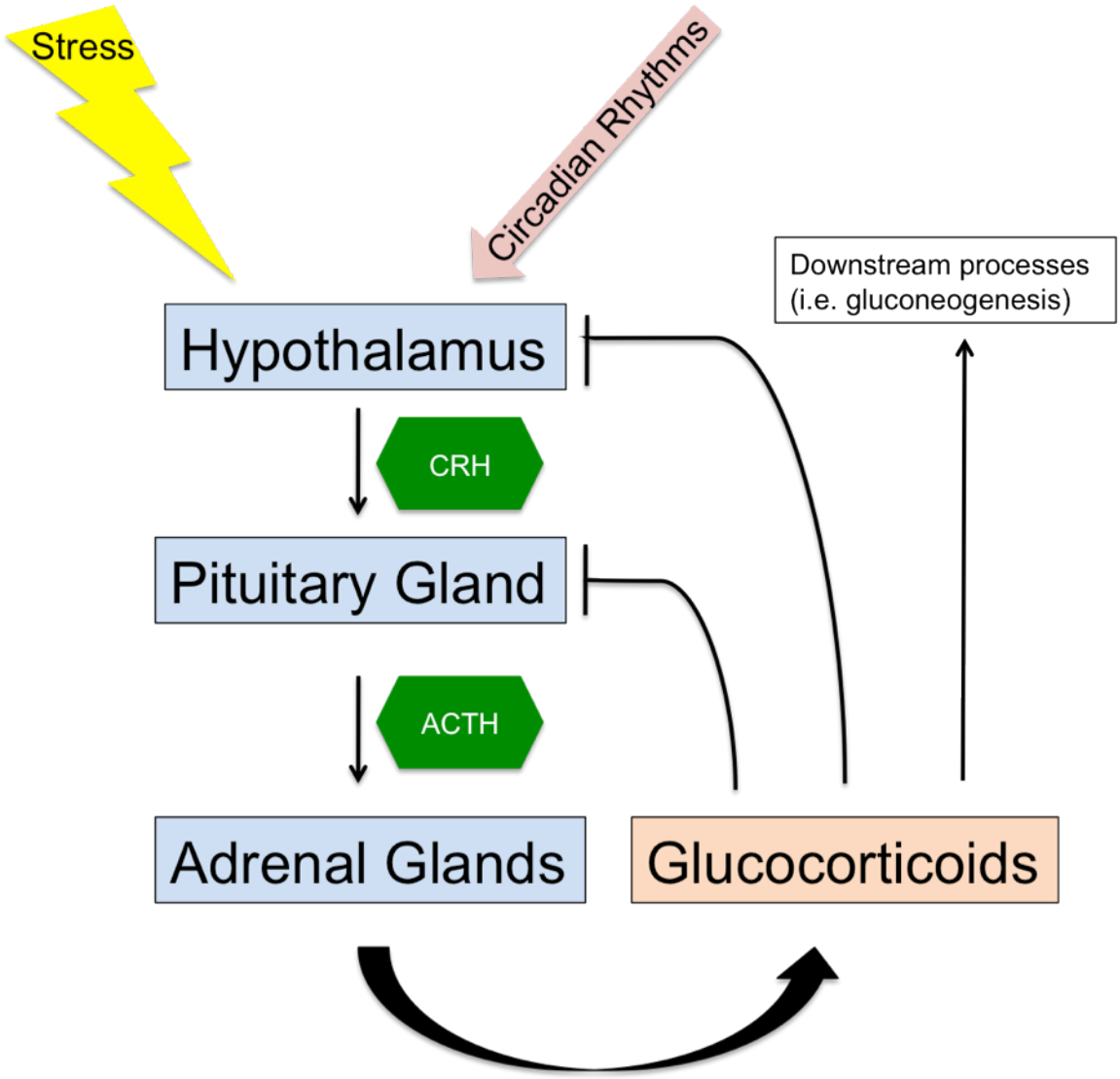

Figure 21. Schematic of HPA Axis.

Improper regulation of *Fkbp-5* or the HPA axis overall is implicated in a variety of neuropsychiatric disorders. Polymorphisms in *Fkbp5* are associated with an increased risk for recurrent depressive episodes (102) and also with increased risk for development of post-traumatic stress disorder (PTSD) (103). In the case of PTSD, polymorphisms result in enhanced induction of *Fkbp5* and impairment of negative feedback leading to over activation of the GR (101). In fact, recent work demonstrated a link between the *Fkbp5* polymorphism rs136078 and regulation of HPA axis reactivity (104). Furthermore, human patients with melancholic depression display an over activation of the HPA axis (105). In addition to depression, HPA axis dysfunction is also associated with diseases such as schizophrenia and PTSD (Reviewed in (98)).

3.1.2 Programming of the HT by GCs During the Fetal Period

Programming refers to the ability of non-genetic factors to cause permanent changes during the fetal period that eventually lead to stable changes in adult physiology (106). In fact, prenatal treatment with GCs such as Dex may alter the programming of the HT leading to alterations in adult functioning. Within the central nervous system, the HPA axis is considered to be vulnerable to programming, and as discussed above, dysregulation of the HPA axis is associated with a variety of neuropsychiatric conditions. Given the role of GCs in the HPA axis, it is not surprising that elevated levels of GCs during the fetal period are associated with predisposition to the development of neuropsychiatric conditions and altered stress reactivity (See §1.3 and (33)). In addition to changes in the HPA axis, there are also alterations in the hypothalamic-pitutary-gonadal and growth hormone axes. In female mice, antenatal Dex treatment resulted in delayed puberty and irregular estrus cycles, potentially due to inhibition of gonadotropin-releasing hormone neurons in the HT or up-regulated production of gonadotropin-inhibitory hormone

(107). In rats, prenatal treatment with Dex resulted in decreased expression of growth hormone releasing hormone in the HT and increased fat accumulation in the liver (108). Interestingly, growth hormone axis function was found to be impaired only in the adult female offspring, not in the males (108).

3.1.3 Sexually Dimorphic Action of Glucocorticoids

Within the central nervous system, there are structural and genomic differences that may contribute to altered prevalence of neurological disorders. For example, microarray analysis in the adult mouse HT indicates sexually dimorphic expression patterns (109). In humans, structural differences within the brain are prevalent in young adults, indicating that sex differences in the connectome of the brain begin early in life (110). With regards to neurodevelopmental disorders, women have affective disorders at a rate twice that of males. Autism spectrum disorders also tend to occur at much higher rates in males than females. Furthermore, the onset of disorders such as schizophrenia and depression tend to occur at the same time as adolescence—a time when major sex-specific changes are occurring in the brain (111). In major depressive disorder, not only is there a higher prevalence in women, but also the action of the HPA axis differs between men and women. For example, only men display altered ACTH pulsatility whereas women tend to have higher levels of cortisol secretion (reviewed in (112)).

In addition to sexually dimorphic prevalence of neurological disorders, there are other disorders displaying a male/female bias including rheumatoid arthritis, Cushing's disease, and kidney diseases (113). Interestingly, these diseases all involve inflammatory processes; therefore, gender and the action of GCs may converge to contribute to the development of these diseases. Using male versus female rat liver cells, microarray analysis indicated gender-specific actions of

GCs resulting in distinct regulation of target genes depending on the sex (113). Therefore, it may be possible that gender prevalence of disorders linked to aberrant HPA axis function may have a basis in prenatal programming of the HT by GCs. In fact, some have suggested that the sexually dimorphic basis for diseases such as schizophrenia are rooted in abnormal development of sexually dimorphic areas of the brain associated with mood or HPA axis function (112).

3.1.4 Long Lasting Consequences of GC Exposure

Treatment with GCs during the fetal period is associated with long lasting changes in the structure of the brain, behavior, and stress reactivity (see §1.3). Several studies have assessed if a previous GC treatment can impact future GR mediated gene expression. For example, in rat hippocampal progenitor cells, Dex treatment results in specific demethylation of sites within the *Fkbp-5* gene. This demethylation persists at twenty days after treatment indicating a permanent change such that the cells have a "memory" of hormone exposure (103). Notably, this differentially methylated site within *Fkbp-5* in humans harbors not only three GREs, but contains a polymorphism associated with increased risk for the development of PTSD (103). Furthermore, synthetic GC exposure during the fetal period is associated with transgenerational changes in gene expression. To assess transgenerational changes in gene expression, rats were treated prenatally with Dex or vehicle (F0), reared, and then bred to create the F1 and F2 generations. Importantly, only the F0 generation was exposed to Dex, but genetic differences in both the F1 and F2 generation were identified. For example, within the liver of the F1 animals, increased expression of *Igf2* and *H19*, two imprinted genes, were observed, but *Igf2* expression decreased in the F2 generation. Alterations in methylation of *Igf2* were only noted in the F1 generation while *H19* gene methylation was only affected in the F2. Notably, within only the F2 generation,

expression of imprinted genes depended on which parent was exposed to Dex. For example, if the father was exposed to Dex prenatally, in the F2 generation there was increased expression of *H19* and other maternally expressed genes. Therefore, GC exposure can have long lasting impacts on gene expression and imprinting for multiple generations (114). However, these results must take into consideration that the pregnant females were injected with Dex or vehicle every day for a week. Within clinical practice, three or more courses of synthetic GCs in the prenatal period are associated within increased fetal death (25). Therefore, 7 doses of GCs may not adequately model human outcomes. These studies are particularly notable as during mammalian brain development, there are major changes in DNA methylation. For example, DNA methylation occurs at both CG and non-CG regions; although methylation in non-CG regions is initially low, it increases over developmental time (human childhood to adolescence) and predominates in mature neurons (115). Since Dex treatment can alter methylation status of genes such as *Fkbp-5* (103), global changes in methylation due to GC exposure may lead to changes in gene expression and possible increased risk of disease.

3.1.5 Rationale and Summary

In spite of the crucial role for the HT in regulating a wide variety physiological processes, we are only now beginning to understand the molecular program underlying differentiation and maturation of the HT. Furthermore, as the number of individuals suffering from stress-related disorders increases, we are beginning to recognize the presence of sexually dimorphic responses to stress possibly due to sex specific differences in the development of the HT (100). Given the sexually dimorphic actions of GCs and their implications in programming the developing HT, we sought to determine the GR regulated transcriptome and male or female specific HT-NPSCs.

Previous work from others has demonstrated that NPSCs from the hypothalamus can be grown in culture as neurospheres and differentiated to form specific subtypes of neurons (116). RNA-Seq analysis of HT-NPSCs treated with Dex revealed the presence of distinct sex specific profiles of GR regulated gene expression. Candidates from the RNA-Seq analysis were further analyzed to ascertain if a previous GC exposure resulted in alterations of future GR transcriptional activity. We found sexually dimorphic long lasting effects on expression of *Fkbp-5* and permanent alterations in GR regulation of *H19* expression. Finally, preliminary data of HT-NPSCs previously exposed to Dex demonstrate an altered proliferative response, possibly due to changes in *H19* and miR-675 regulation. Taken together, this study indicates that treatment with Dex results in long lasting, sexually dimorphic changes in HT-NPSC biology that may contribute to overall programming and function of the HT.

3.2 MATERIALS AND METHODS

Mouse NPSC cultures: NPSCs were derived from E14.5 hypothalami of wild-type C57Bl/6 mice grown as three-dimensional neurosphere cultures. Following harvest, cells were genotyped to ascertain presence of SRY to determine sex. Cells were passaged every seven days and experiments were performed at P3.

RNA-Seq Library Preparation and Analysis: HT-NPSCs were treated with 100 nM Dex or Ethanol (vehicle) for a period of four hours. Cells were harvested in Trizol and RNAs isolated using the Machery-Nagel Nucelospin RNA II Kit. RNA-Seq library was generated according to manufacturer's instructions using the TruSeq Stranded Total RNA Kit (Illumina, RS-122-2201). The library was then submitted to Tufts Genomics Core for next generation sequencing. Following sequencing, the reads were assessed for quality using a FastQC tool. The reads were then mapped to the mm9 version of the mouse genome using tophat2 and the technical replicates merged. Cuffdiff was run with the default parameters on these samples to find the differentially expressed genes in FPKM values, then further refined to only contain genes induced by Dex by greater than 1.5 fold. The bam files were submitted to GEO (accession # GSE55113).

Dex Programming Experiments: P1 neurospheres were cultured for 6 days after passaging (3 days after replenishment with fresh epidermal growth factor and fibroblast growth factor-1) and treated for a period of 24 hours with 100nM Dex (Sigma Chemicals, St. Louis, MO) or vehicle (EtOH). Following treatment, cells were passaged using standard conditions and grown for an additional two weeks. P3 neurospheres were then re-treated with Dex for 4 hours (for protein/RNA studies) or 24 hours for BrdU incorporation analysis at 6 days post passaging and harvested (Figure 22).

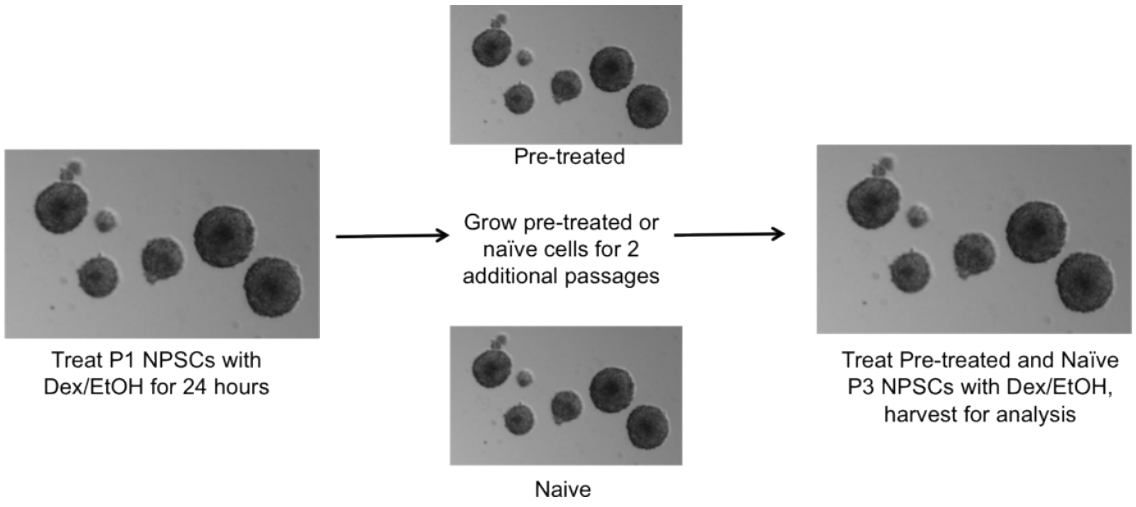

Figure 22. Schematic of *in vitro* programming experiments.

Quantitative Real Time-PCR (qRT-PCR): P3 previously Dex/EtOH treated neurospheres were re-treated with Dex or ethanol for 4 h and were harvested in Trizol and processed for RNA isolation using the Machery-Nagel Nucelospin RNA II Kit. For samples that were to be analyzed for miR-675, a standard precipitation method was used to isolated RNA to preserve the small RNA species. cDNA synthesis was performed using iScript Select cDNA Synthesis Kit (Bio Rad #170-8897). qRT-PCR reactions were performed on a BioRad CFx qRT-PCR machine using iTaq Universal SYBR Green Supermix (Bio Rad #172-5121) and primers with efficiencies calculated to be greater than 80%.

NPSC BrdU Assays: Passage 3 neurospheres were treated with 100nM Dex (Sigma Chemicals, St. Louis, MO) or vehicle (Ethanol) for 24 hours. During the last 4 hours of Dex treatment, 10uM Bromodeoxyuridine (BrdU) (Sigma Chemicals, B-9285) was added. Neurospheres were then dissociated into single cells and attached to poly-D-lysine treated coverslips prior to fixation with 4% paraformaldehyde. Fixed cells were processed for immunocytochemistry using standard methods. A rat anti-BrdU antibody (Abcam, ab6326) was used at 1:500 and Anti-Rat Alexa Flour 488 (Invitrogen, A21208) at 1:1000. Images were captured using a Nikon Eclipse E400 Microscope and Photometrics Cool Snap E52 camera.

3.3 RESULTS

3.3.1 Sexually Dimorphic Action of the GR in HT-NPSCs

To determine if Dex treatment of HT-NPSCs results in patterns of sexually dimorphic gene expression, we performed RNA-Seq analyses. Analysis of protein coding genes that were regulated by at least 1.5 fold revealed 224 genes regulated in common and almost twice as many female specific genes than male specific genes (Figure 23B). This result is consistent with the distribution of male/female specific genes reported in the liver by (113). The female specific genes also tend to be repressed in response to Dex treatment (Figure 23C). Interestingly, one of the most highly regulated genes in both datasets was *Cftr* (see §2.4.2). We also observed the male specific regulation of *Gjb6* (see §2.4.2 and §2.6). Within the female data set we observed repression of *Rxrg*, a gene associated with despair and depressive behaviors and changed in serotonin signaling in mice (117). Other notable targets and their functions are represented in Table 4.

A

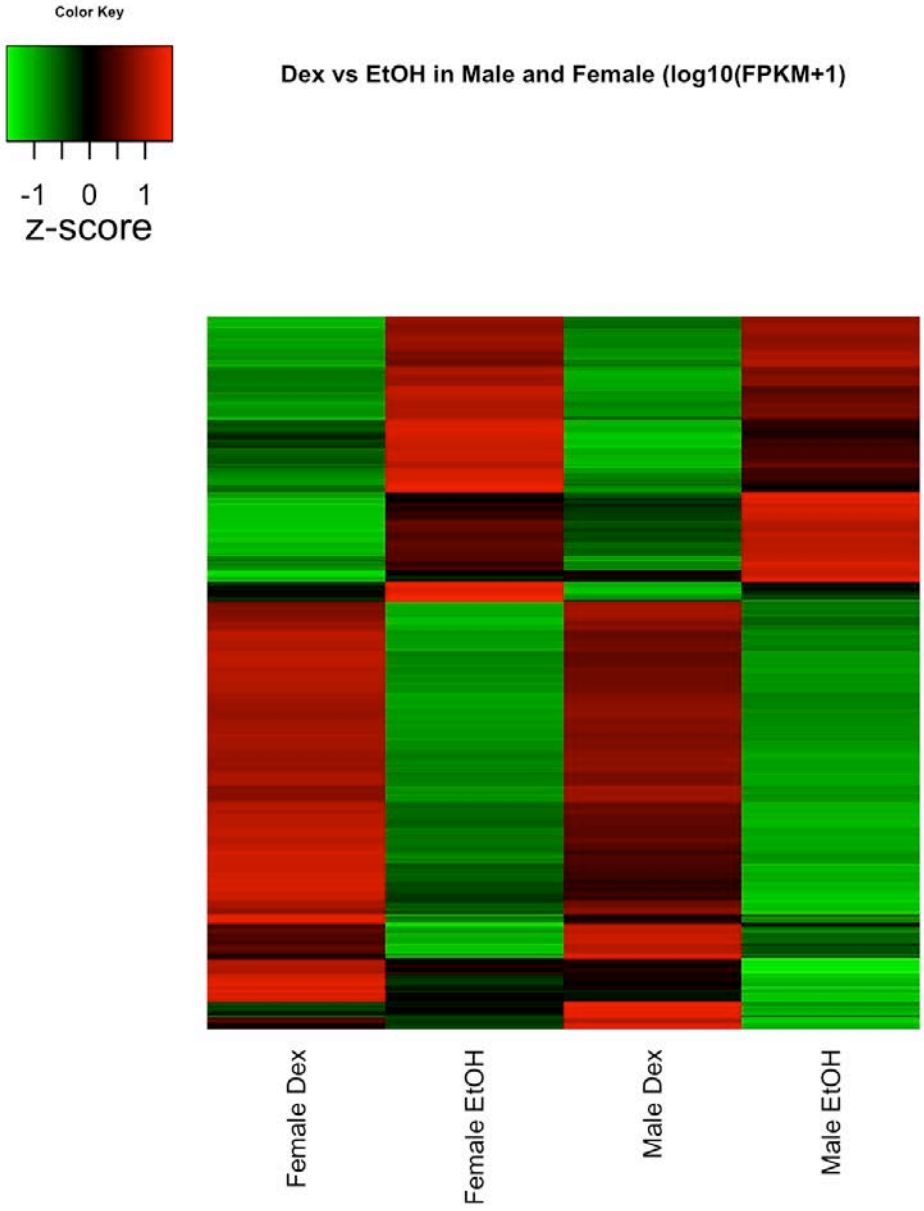
Color Key
-1 0 1
z-score
Dex vs EtOH in Male and Female (log10(FPKM+1)
Female Dex
Female EtOH
Male Dex
Male EtOH

B

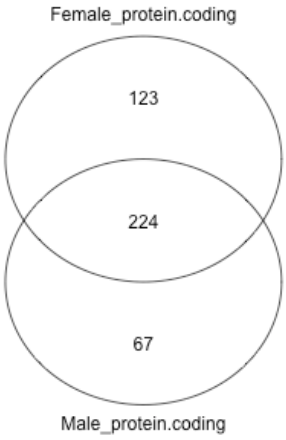
Female_protein.coding
123
224
67
Male_protein.coding

C

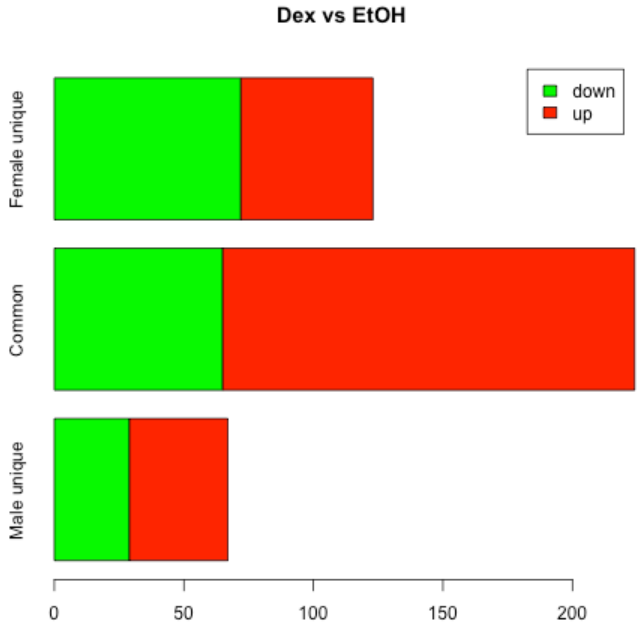
Dex vs EtOH
down
up
Female unique
Common
Male unique
0
50
100
150
200

Figure 23. Dex treatment of HT-NPSCs results in sexually dimorphic patterns of gene expression.

A. Heat map representing gene expression in response to 4 hour Dex treatment. B-C Refinement of expression data indicates a subset of genes regulated by GR in both sexes, and distinct subsets of male and female specific genes.

Table 4. Select candidates revealed in RNA-Seq analysis of HT-NPSCs

Gene Name	Induced/Repressed	Male/Female	Function
Fkbp-5	Induced	Both	Negative regulator of GR
Rxrg	Repressed	Female Only	Associated with despair and hedonistic behaviors in mice
H19	Induced	Both	Long non-coding RNA, encodes miR-675, roles in proliferation and differentiation
Ada	Induced	Both, higher in females	CDK2 Regulator, role in cell cycle
Cftr	Induced	Both, higher in males	Ion channel, implicated in cystic fibrosis
Gjb6	Induced	Male Only	Gap junction protein, involved in blood brain barrier regulation

Following initial analysis of the protein coding RNA-Seq dataset, the list of male and female specific genes was loaded into IPA. In both the male and female datasets, the number one network was comprised of cell cycle regulatory genes (Figure 24). Interestingly, the constituents of each of these cell cycle networks is different between the two sexes (Figure 24). Therefore, Dex regulated alterations in proliferation between the two sexes likely occur through distinct mechanisms.

A

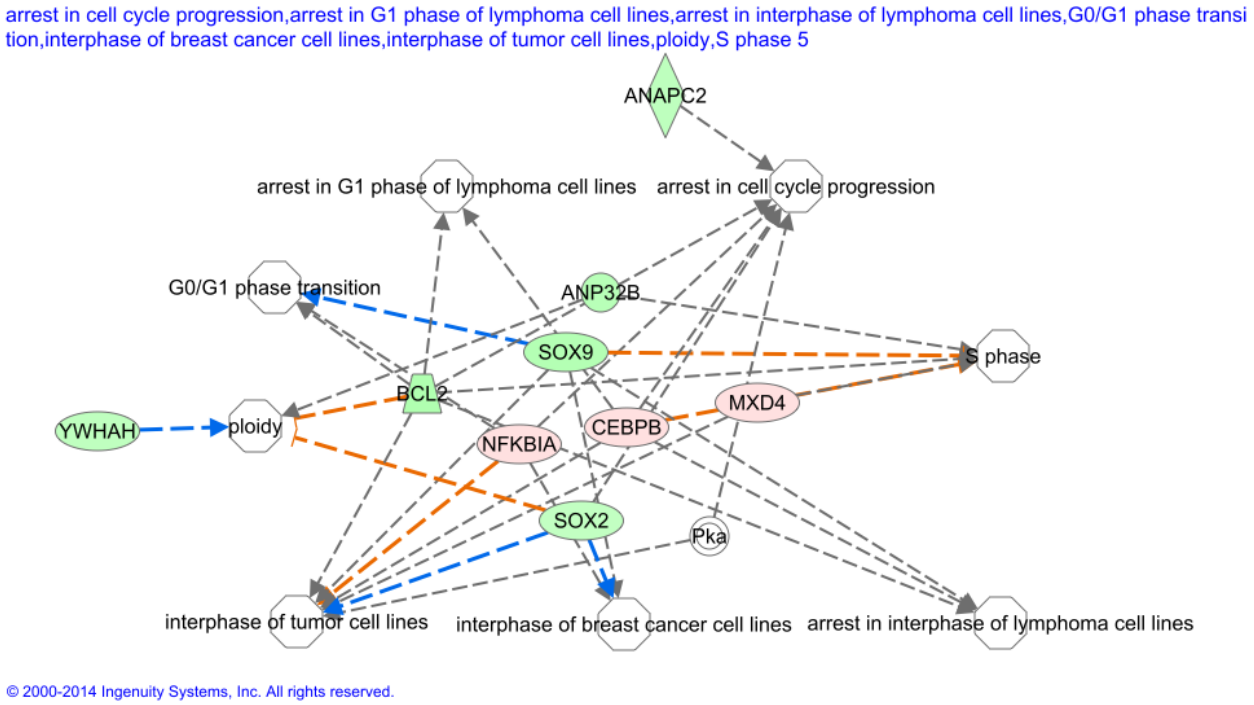

B

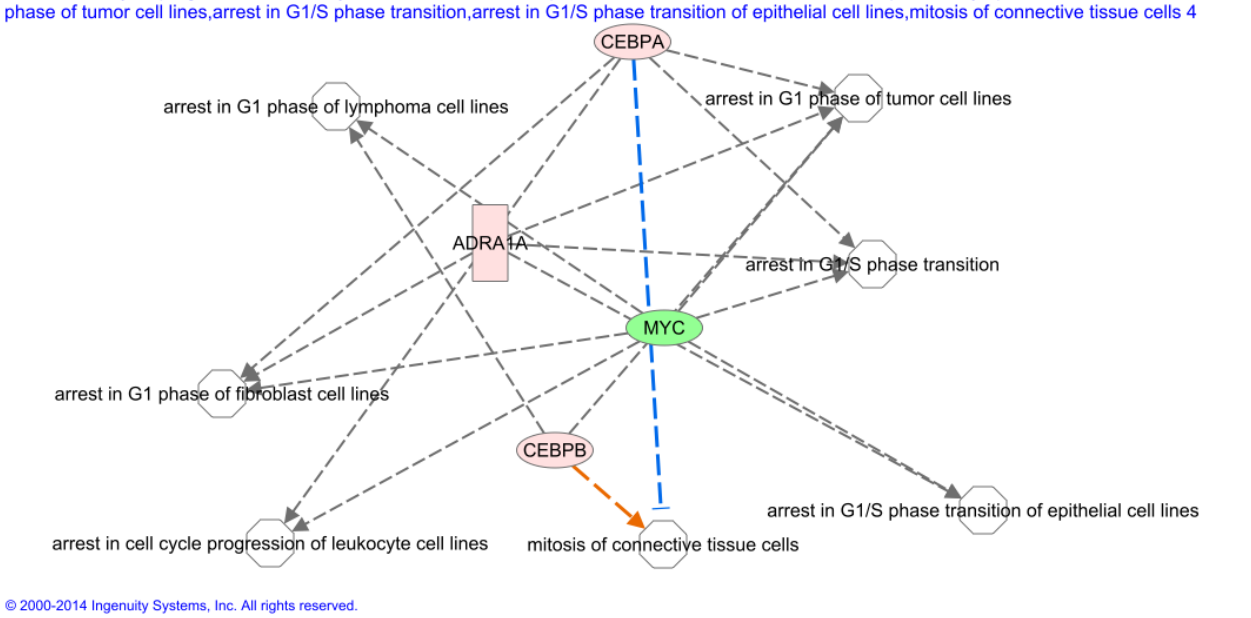

Figure 24. Cell cycle regulatory networks are highly enriched in both male and female datasets, but vary in their constituents.

IPA analysis using lists from Dex regulated genes in female (A) and male (B) HT-NPSCs define the distinct cell cycle networks shown. Upregulated genes are depicted in red and downregulated genes in green. The shading of red and green symbols indicates the extent of Dex upregulation or downregulation, respectively.

Based on the top candidates identified from the RNA-Seq analysis (Table 4) we then tested if any of these genes demonstrated long term alterations in GR gene regulation. Given the role of *Fkbp-5* in regulating GR and implications for *Fkbp-5* polymorphisms in HPA axis dysfunction, we first sought to determine if future regulation of *Fkbp-5* by GR is altered by a previous exposure to Dex. In male cells, pre-treatment with Dex (see methods section), has no effect on P3 expression of *Fkbp-5* (Figure 25A). However, in female cells, a previous exposure to Dex results in attenuated activation of *Fkbp-5* in response to Dex (Figure 25A). Interestingly, term-born human females, but not males, treated prenatally with synthetic GCs go on to have altered stress responsiveness and secrete higher levels of cortisol in response to stress (33). Therefore, alterations in GC-mediated expression of *Fkbp-5* in the HT may contribute to this altered stress reactivity later in life. Although the induction of *Fkbp-5* by Dex is only altered in the females, it is interesting to note that both sexes display alterations in baseline expression of *Fkbp-5* (Figure 25B).

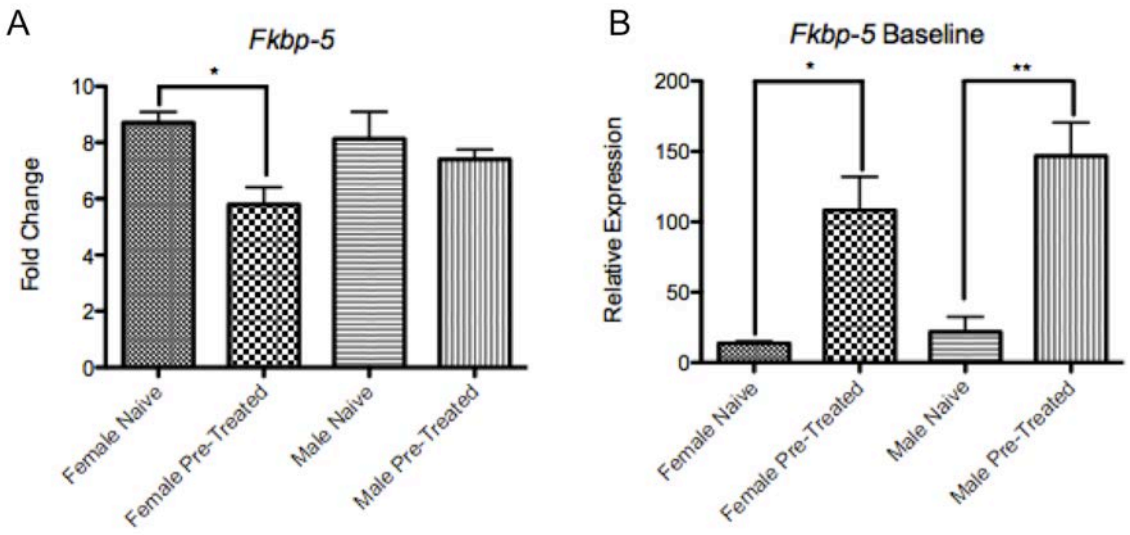

Figure 25. *Fkbp-5* is subject to sexually dimorphic long lasting changes in GC-regulated expression.

A. Cells either naïve or previously exposed to Dex for 24 hours (Pre-Treated) were treated with 100nM Dex at P3, and expression of *Fkbp-5* analyzed. Pre-treatment of male cells had no effect of Dex treatment whereas female cells demonstrate less induction of *Fkbp-5* when compared to controls. B. Baseline values of *Fkbp-5* relative to GAPDH are altered in both male and female cells previously exposed to Dex. n=3 biological replicates per sex, One-way ANOVA with Tukey's Post-Test, * represents $p<0.05$, ** represents $p<0.01$.

3.3.2 Long Lasting Alterations in GC-Regulated Activity in HT-NPSCs

One of the Dex-regulated genes identified in our RNA-Seq analysis was the long intergenic non-coding RNA, *H19*. *H19* is a maternally imprinted gene that is highly expressed during embryonic development and harbors two highly conserved miRNAs, miR-675-3p and miR-675-5P. These miRNAs are implicated in both regulation of stem cells proliferation and also skeletal muscle differentiation (46, 118). Given the interesting biology of *H19* and the role of miR-675 in regulating stem cell proliferation, we next sought to determine if *H19* expression was altered in

response to an early treatment with Dex. In both male and female cells that were not treated at P1, a Dex treatment at P3 results in a 2-fold increase in *H19* mRNA expression (Figure 26A). Surprisingly, in cells pre-treated with Dex at P1, upon re-treatment with Dex at P3, H19 is no longer induced, but repressed by 0.5 fold (Figure 26A). Although we see the same phenomenon in both male and female cells, analysis of baseline expression of *H19* revealed that only female cells revealed alterations in basal expression of *H19* (Figure 26B).

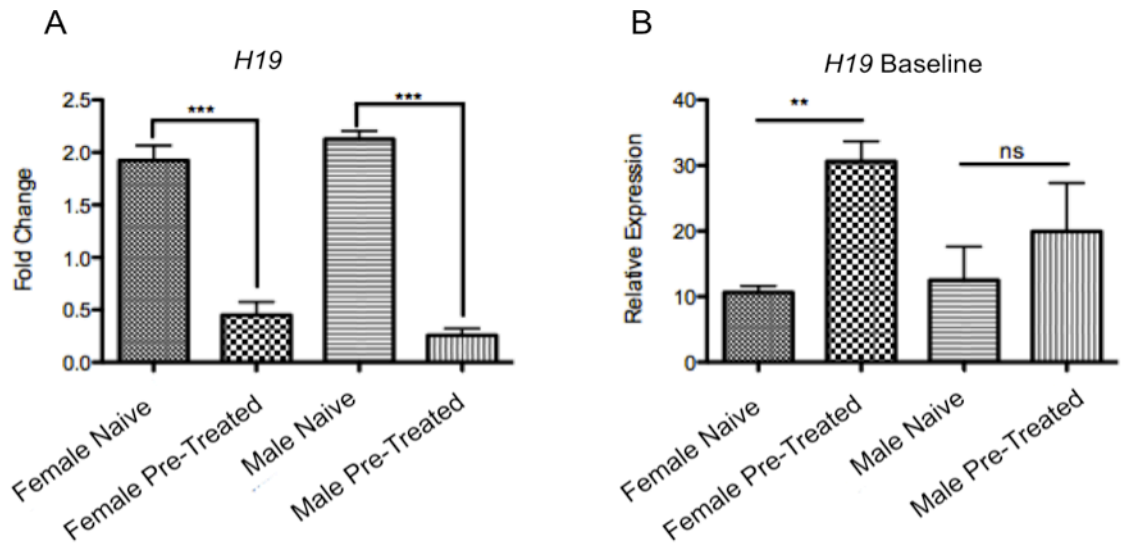

Figure 26. Pre-treatment with Dex leads to long lasting alterations in GR mediated regulation of H19.

A. Cells either naïve or previously exposed to Dex for 24 hours (Pre-Treated) were treated with 100nM Dex at P3, and expression of *H19* analyzed. Cells of both sexes demonstrate that pre-treated with Dex results in GC mediated transcriptional repression instead of activation. B. Baseline values of *H19* relative to GAPDH are altered in only female cells previously exposed to Dex. n=3 biological replicates per sex, One-way ANOVA with Tukey's Post-Test, ** represents $p<0.01$ and *** represents $p<0.001$.

Since H19 is induced in HT-NPSCs, we next determined if there was any GR-regulated induction of miR-675. Preliminary data from our RNA-Seq analysis indicates an increased number of reads in the region of H19 that contains miR-675, and that they may be induced in response to Dex (Figure 27).

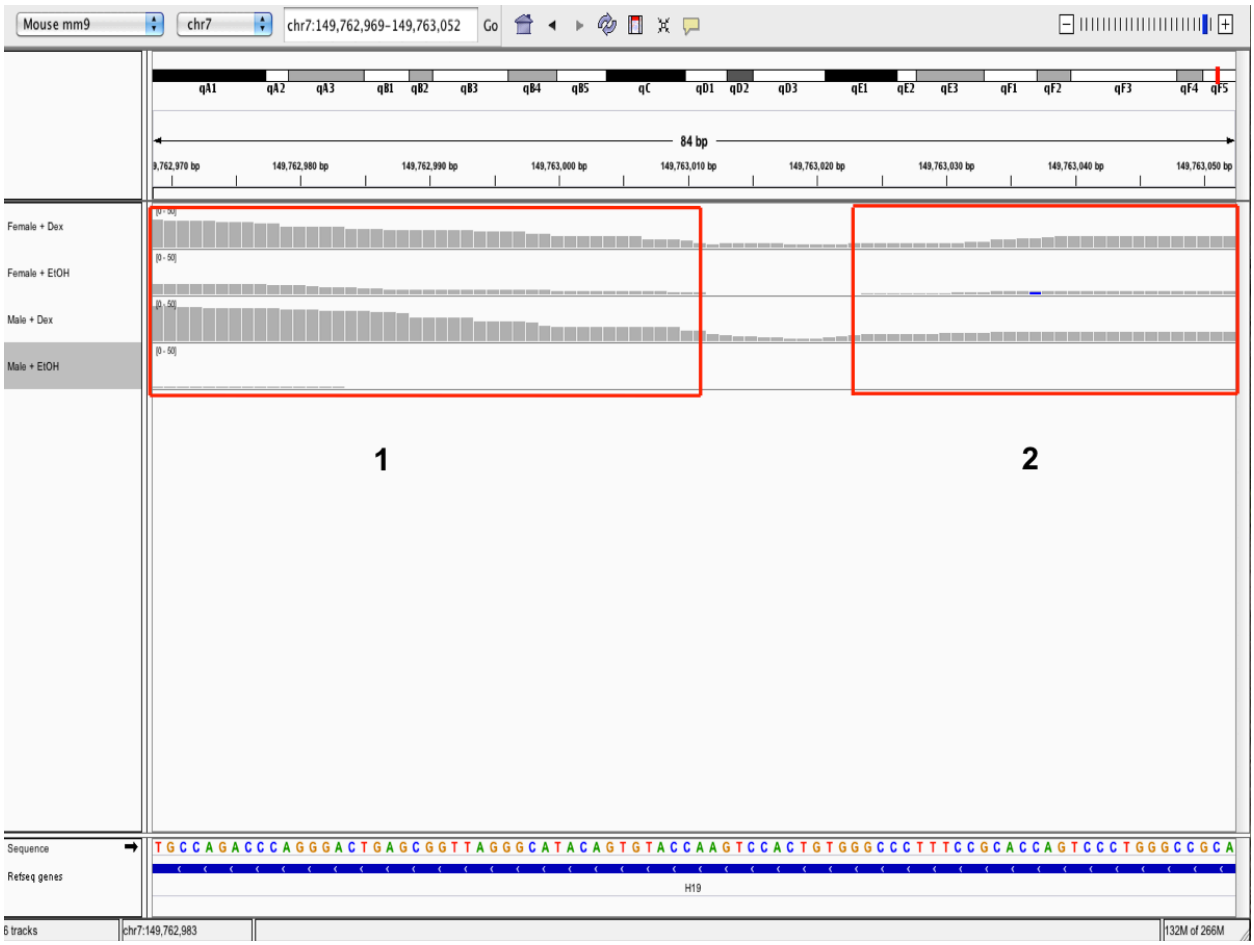

Figure 27. miR-675 may be Dex regulated in HT-NPSCs.

Read data from representative male/female samples from each treatment group were loaded into Integrative Genome Viewer (IGV). As shown by the grey boxes, there are increased reads at both miR-675-3P (Region 1) and miR-675-5P (Region 2) in both male and female cells treated with Dex.

miR-675 is harbored within exon 1 of *H19* and gives rise to two distinct miRNAs, miR-675-3P and miR-675-5P. Although collectively miR-675 and *H19* are associated with tumor suppression, each individual miRNA can have a stronger anti-proliferative effect depending on the cell line. For example, miR-675-5P decreases proliferation in embryonic stem cells whereas in mouse embryonic fibroblast cells, the 3P form has a greater antiproliferative effect (46). Since preliminary data indicate that both forms of miR-675 may be upregulated in HT-NPSCs in response to a 4 hour Dex treatment, we next determined if BrdU incorporation and therefore proliferation were altered in HT-NPSCs previously exposed to Dex. The anti-proliferative effects of Dex are well documented (29, 36, 56), but it is not known if a previous exposure to Dex can impact future proliferation. Preliminary data indicate that in cells that were previously treated with Dex, there is a much greater anti-proliferative response to a P3 Dex treatment (Figure 28). Although a decrease in proliferation is noted among all samples, only cells previously treated with Dex demonstrate a statistically significant response. Interestingly, in only the female cells, previous exposure to Dex results in a significant increase in BrdU labeling under baseline conditions (Figure 28). This result is particularly interesting since female, but not male cells, have elevated baseline levels of *H19* in response to a previous treatment with Dex (Figure 26).

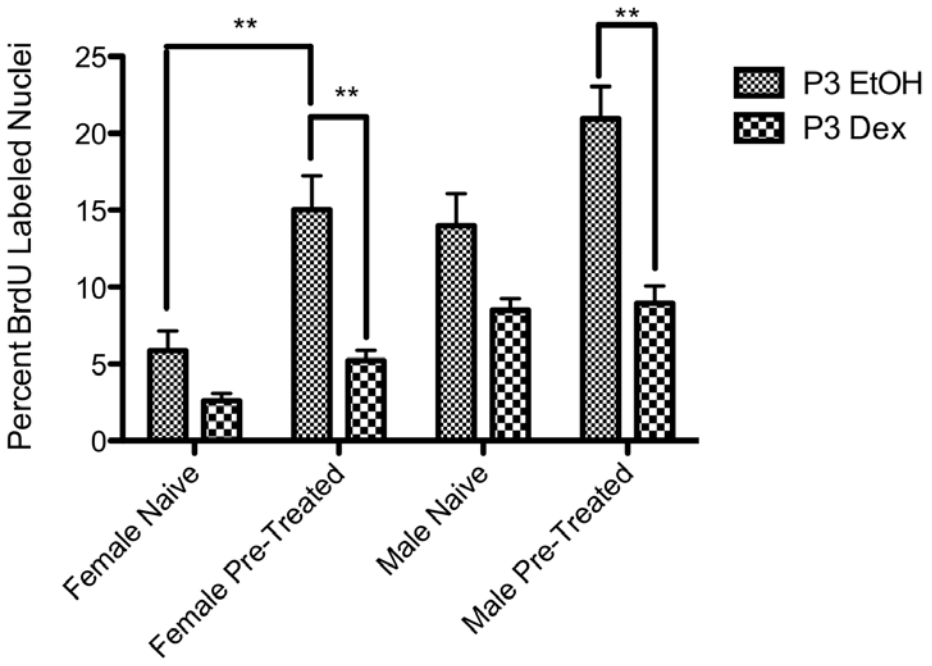

Figure 28. Pretreatment with Dex results in enhanced anti-proliferative effect at P3

Female or male HT-NPSCs were treated with Dex or vehicle (Ethanol; EtOH) for 24 h and pulsed with BrdU during the four hours of treatment. Immunocytochemistry was performed to detect BrdU positive nuclei. Shown are three independent coverslips per sex counted to ascertain the percentage of cells that passed through S-phase (i.e. BrdU positive nuclei). Error bars represent SEM, n=1 biological replicate per sex. One-way ANOVA with Tukey's post test, $p<0.01$.

To determine if alterations in Dex responsiveness at P3 in cells previously exposed to GCs were the result of changes in GR expression, we next sought to determine if a pre-treatment with Dex resulted in changes in GR mRNA or protein levels. Previous exposure of HT-NPSCs to Dex resulted in no change in the mRNA expression of GR at P3 (Figure 29). Preliminary analysis of GR protein also indicated no change in GR expression in P3 HT-NPSCs previously exposed to Dex (Data not shown). Therefore, alterations in regulation of *Fkbp-5* and *H19* may be due to alterations in function/recruitment of the receptor or epigenetic changes (see discussion §3.4).

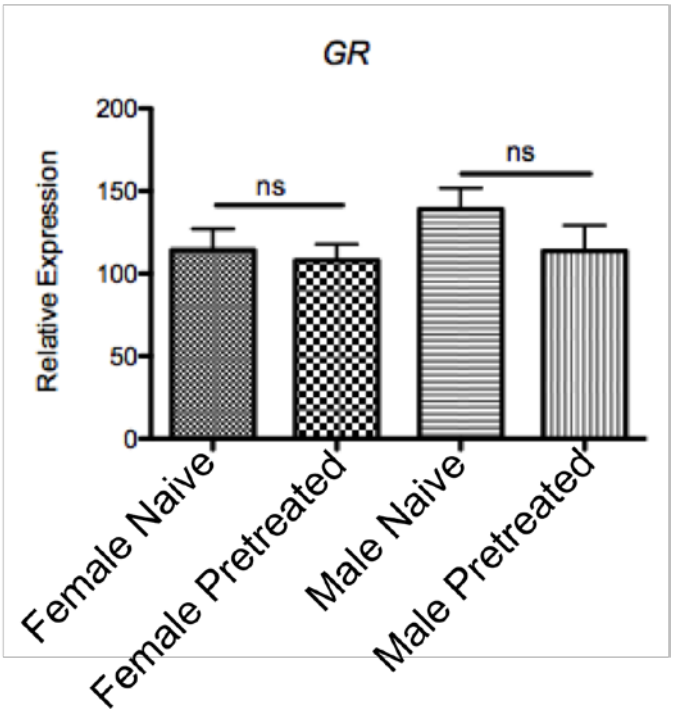

Figure 29. Pre-treatment with Dex results in no change in GR mRNA expression at P3.

A. Cells either naïve or previously exposed to Dex for 24 hours (Pre-Treated) were treated with 100nM EtOH vehicle at P3, and expression of *GR* relative to GAPDH analyzed. No difference in baseline expression of *GR* mRNA was detected in either sex. n=3 biological replicates per sex.

3.4 DISCUSSION

Neuropsychiatric disorders related to dysfunction of the HPA axis cost Americans a significant amount of money, with the economic burden of depression alone reaching an estimated cost of $83.1 billion in 2000 (119). Therefore, understanding their neurodevelopmental basis may prevent these disorders or lead to more effective treatment options, improving quality of life and decreasing overall economic burden. The influence of GC programming on the HT, and specifically sexually dimorphic effects of GCs may further yield additional insights into the basis for these diseases. In this chapter, we used HT-NPSCs to identify sexually dimorphic GR target genes, and then assessed the long-term impact of GC treatment on gene expression. We identified that Dex-induced expression of *Fkbp-5* is attenuated only in female cells. Furthermore, the long intergenic non-coding RNA, *H19,* is no longer Dex-induced in HT-NPSCs previously exposed to Dex but transcriptionally repressed. Given the role of miR-675 in regulation embryonic stem cell proliferation, changes in *H19* and consequently miR-675 may explain the alterations in proliferation seen in HT-NPSCs previously exposed to Dex. Therefore, exposure of HT-NPSCs to Dex treatment can lead to sexually dimorphic persistent changes in gene expression that impact NPSC function.

3.4.1 GC Treatment Results in Sexually Dimorphic Gene Expression

Our RNA-Seq analysis revealed the presence of distinct GR regulated genes for each sex, and a set of 224 genes that were regulated in both sexes. As shown in Table 4, some of these co-regulated genes like *Cftr* are expressed to different extents in male versus female cells demonstrating that sexually dimorphic actions of GR are not limited to expressed/not expressed.

Notably, there are approximately twice as many female specific genes as male specific genes—which is consistent with studies performed in the liver (113). However, there were significantly more genes in each class identified within the liver (i.e. 4293 female specific genes in the liver vs. 123 in the hypothalamus), which may be indicative of fundamental differences between the liver and hypothalamus. Further analysis of our RNA-Seq data set using IPA demonstrated that in both male and female HT-NPSCs, the most highly regulated network formed by each involved the cell cycle. However, the cell cycle regulatory genes for each of the male/female cells varied extensively. Therefore, the regulation of cell cycle relies on sexually dimorphic pathways, and may contribute to differences in HPA axis development/function.

3.4.2 Long Lasting Changes in GC Regulated Genes

FKBP5 is an important regulator of the GR, involved in a negative feedback loop to resolve GR activation. Increased activity of GR and/or polymorphisms in *Fkbp5* impacting its function can lead to dysfunction of the HPA axis. In HT-NPSCs, we observe long lasting changes in GR regulated expression of *Fkbp5* in female cells only. In female HT-NPSCs previously exposed to Dex, future *Fkbp5* transcriptional induction by Dex is attenuated. Less induction of *Fkbp5* may then lead to an inability to resolve the stress response. In fact, in a study of term born children, female infants exposed to GCs during the fetal period exhibited much higher levels of salivary cortisol in response to a stressful situation (33). Therefore, the elevated levels of cortisol specifically in the female children may be the result of a sex specific effects on regulation of *Fkbp5* within the hypothalamus. There may also be altered regulation of *Fkbp5* in other tissues, and future experiments could ascertain if this sex specific programming exists exclusively within the HT.

Fkbp5 contains a polymorphism associated with PTSD located in a differentially methylated region within a trio of GREs residing in intron 7. Notably, data mining of publically available DNAse hypersensitivity studies indicates a region of open chromatin within intron 7 of *Fkbp5* that exists only within the adult mouse brain (See Appendix, Figure 31). Changes in the chromatin status during embryonic development may disturb the presence and location of these hypersensitive sites, therefore changing the transcriptional activity of that gene. For example, treatment of hippocampal progenitor cells with Dex results in demethylation within intron 7 of *Fkbp5*. The decreased in methylation at intron 7 results in less induction of *Fkbp5* by GR—similar to the memory effect we see in HT-NPSCs (103). Taken together, alterations in chromatin status triggered by treatment with Dex lead to sex-specific aberrant regulation of *Fkbp5*. This altered regulation of *Fkbp5* within the HT may contribute to the development of abnormalities in HPA axis regulation. Bisulfite sequencing of intron 7 of *Fkbp5* in male/female specific HT-NPSCs pre-treated with Dex will indicate if changes in methylation are sexually dimorphic. Additional genomic experiments such as DNase hypersensitivity assays and RNA-Seq experiments in pre-treated HT-NPSCs will yield important insight into the mechanisms behind long lasting changes in gene expression and other susceptible genes.

We also observed changes in the basal mRNA expression of *Fkbp5*, although we have yet to assess protein levels of FKBP5. In both male and female cells, pre-exposure to Dex resulted in elevated baseline levels of *Fkbp5*. Since FKBP5 directly binds to GR in the cytoplasm of cells to maintain its inactive conformation by decreasing ligand binding and impeding translocation to the nucleus, alterations in its baseline levels may impede the ability of GR to activate. Additional experiments examining the activation of the receptor and its ability to translocate to the nucleus in HT-NPSCs previously exposed to Dex would indicate if overall GR activation is impaired in

cells previously exposed to hormone. Since GR resistance (i.e. the inability of GR to respond to high levels of cortisol) is another hallmark of mood disorders (120), changes in the activation of the receptor due to early programming of HT-NPSCs may also be a contributing factor to altered HPA axis.

Previous work indicated that the expression of *H19* was undetectable in the fetal mouse brain (46). Since we see an induction of *H19* in response to Dex treatment within HT-NPSCs, and the HT comprises a very small portion of the brain overall, this may indicate that *H19* is specifically expressed only within the HT. Therefore, *H19* or miR-675 may serve a very specific function within the developing HT. Future experiments using *in situ* hybridization to assess the expression of *H19* will yield insight into both the extent of expression within the developing brain and also the time points at which it is expressed. miR-675 is implicated in a wide variety of cellular processes such as proliferation and differentiation all of which are important to proper hypothalamic development. Preliminary data from our RNA-Seq study indicates that miR-675 may also be Dex regulated in HT-NPSCs. However, additional experiments such as northern blotting or qRT-PCR are necessary to confirm that the reads seen in the region of H19 where miR-675 is located are true reads.

In both male and female cells, *H19* is induced by Dex approximately 2 fold. Provocatively, a pre-exposure to Dex results in transcriptional *repression* instead of activation. Since *H19* harbors miR-675, expression of the miRNAs and their functionality may also be altered. In HT-NPSCs previously exposed to Dex, we observed changes in BrdU incorporation. In both male and female cells, we see an enhanced proliferative response to Dex treatment. Preliminary data indicate that female untreated cells demonstrate ~2% decrease and untreated cells a 5% decrease compared to a ~10% decreases in labeling seen in both sexes pre-treated

with Dex. In female cells alone, we see an increase in basal levels of *H19* and BrdU labeling. These results are counterintuitive because we would predict that if miR-675 is mediating these proliferative effects, the increased expression of *H19* at basal levels in the female HT-NPSCs would lead to decreased basal proliferation. Furthermore, if *H19* is less induced in response to Dex, we would predict that there would be less of a proliferative response not an enhanced response. This may be explained because miR-675-3P and miR-675-5P, although both are associated with anti-proliferative response, have different affects depending on the cell type. For example in embryonic stem cells, miR-675-5P is the primary driver of the anti-proliferative response (46). Furthermore, GR is known to regulate a wide variety of cell cycle regulators such as Cyclin-D1 (36) and the control of proliferation is likely to involve a wide variety of different components. As shown by IPA analysis, in HT-NPSCs, male versus female cells each have their own distinct networks of genes involved in cell cycle regulation. Since each sex has different GR regulated genes that contribute to its regulation of cell proliferation, this may explain why we only detect changes in basal levels of proliferation female HT-NPSCs.

3.4.3 Summary

In summary, GC treatment of HT-NPSCs generates sexually dimorphic patterns of gene expression, and long-term consequences on gene expression and NPSC function. RNA-Seq analysis indicated the existence of female and male specific classes of genes. Further analysis of *Fkbp5* indicated that in female HT-NPSCs, previous exposure to Dex result in alterations in later expression of *Fkbp5*. Therefore, changes in *Fkbp5* may contribute to future alterations in GR signaling and HPA axis response in the future. Regulation *H19* also demonstrated long-lasting changes in GC-mediated gene expression in HT-NPSCs previously exposed to Dex. Alterations

in *H19* and its cognate miRNA, miR-675 may contribute to changes in proliferation seen in pre-treated HT-NPSCs. These changes in gene regulation may be due to alterations in chromatin status within these genes. Taken together, treatment with Dex causes a wide variety of changes in HT-NPSCs that may contribute to future abnormalities in the HPA axis.

4.0 DISCUSSION

4.1 SUMMARY OF FINDINGS

The use of GCs in decreasing mortality in premature babies is undisputed, but the neurological side effects are increasingly apparent (4, 32-34). Although the exact causes of these deficits are still not clear, this work revealed additional insights into how GCs could impact the developing brain through detailed mechanistic studies of GR signaling within CC-NPSCs and an examination of sex specific effects on programming of HT-NPSCs. In CC-NPSCs, we uncovered a new role for Cav-1 in mediating the genomic effects of GR. In the Cav-1 KO we also observed a lack of anti-proliferative response to Dex treatment, which may be due to changes in expression of *Sgk1* in the Cav-1 KO CC-NPSCs. In addition to *Sgk-1*, loss of Cav-1 also resulted in the altered regulation of approximately 100 other GR-regulated genes. Alterations in GR-regulated gene expression may be due to changes in the phosphorylation of GR and its recruitment to target genes. In HT-NPSCs, we identified sexually dimorphic classes of GR regulated genes. Since the HPA axis and prevalence of diseases related to the HPA axis is sexually dimorphic (see §3.1.3), these distinct classes of GC regulate genes may underlie overall differences in the development and function of the HPA axis. We also identified a subset of genes that are susceptible to long lasting programming effects of GCs in HT-NPSCs. Previous

exposure to Dex resulted in persistent changes in the regulation of GR target genes such as *Fkbp5* and *H19*. The implications for these findings are discussed below.

4.2 CAV-1 MEDIATED CROSSTALK BETWEEN RAPID AND GENOMIC GR SIGNALING

Although both rapid and genomic GR signaling exists in NPSCs, it is not clear what the individual contribution of each is for negative neurodevelopmental outcomes of antenatal GCs. In §2, we identified a role for Cav-1 in mediating crosstalk between genomic and rapid GR. Given the importance of Cav-1, this may indicate a new pharmacologic target for manipulating the levels of genomic or rapid GR signaling. For example, let's consider a hypothetical scenario: Cav-1 KO animals exposed to Dex and delivered prematurely via C-section are no different than their wild-type counterparts in terms of their ability to breathe. This result would potentially indicate that Cav-1 dependent GC signaling may not be essential for the pulmonary benefits and be more of a factor in neurodevelopment consequences or programming effects. Therefore, if this hypothetical scenario were true, it may be beneficial to pharmacologically target Cav-1 using a compound such as incadronate (121) to keep the beneficial pulmonary benefits of synthetic GC use in the fetal period while mitigating negative effects on neurodevelopment. Since Cav-1 KO animals are viable and have functioning caveolae, this may be a low risk way to minimize negative side effects of synthetic GC use. Conversely, if in our hypothetical scenario the Cav-1 KO animals treated prenatally with Dex and delivered prematurely died shortly after birth from respiratory distress syndrome indicating that Cav-1 mediated GC signaling is essential for maintaining the pulmonary benefit, specifically targeting Cav-1 would not be beneficial.

However, further analysis of the ~100 genes identified in this study may indicate molecular candidates critical for the pulmonary benefit that could then be pharmacologically targeted. Therefore, further study of Cav-1 KO animals and their response to prenatal Dex, in conjunction with additional study of the gene targets presented in this study may indicate more specific pharmacological intervention.

4.3 SEXUALLY DIMORPHIC GC RESPONSES IN THE HT

In HT-NPSCs, unique sexually dimorphic profiles were revealed in response to Dex treatment, some of which were susceptible to sex-specific programming effects. Given the altered prevalence of disorders relating to HPA axis regulation in males versus females (See §3.1.3), differences in the development of the HT may be a contributing factor. This result complements current discussions within the medical community related to sex-specific recommendations in dosing for adults. In fact, women are 50-75% more likely to have an adverse reaction to a drug response due to greater sensitivities to medicine possibly linked to differences in metabolism, clearance, and absorption (122). This is especially important given that in a 2012 study, term born ***females*** exposed to GCs in the fetal period had elevated levels of cortisol in response to a stressful situation (33). Therefore, sex of the fetus needs to be of greater concern before treating with antenatal steroids, and in future studies assessing differences in brain structure or behavior in response to a pre-natal exposure to GCs.

4.4 REACHING AN IMPROVED THERAPY: WHAT CAN THIS WORK TELL US ABOUT ANTENATAL USAGE OF DEXAMETHASONE V. BETAMETHASONE?

Within clinical practice, antenatal GCs are prescribed either as two courses of Beta given 24 hours apart, or four doses of Dex given 12 hours apart (27). Although upon initial glance the two GCs appear functionally equivalent, differing only in the isomeric positioning of one methyl group, the functionality of these two hormones varies significantly and current studies reveal no consistently "better" GC for antenatal use (Reviewed in (27)). For example, in mice, Beta induced greater lung maturation with less growth restriction than Dex. However, these studies are all performed *in vivo* and examined physiological changes like lung maturation or fetal heart rate, and not the underlying molecular mechanisms for these affects. In order to reach improve therapies, we need a better understanding of the molecular basis for these effects. As shown in Chapter 3, Dex treatment of HT-NPSCs can cause long lasting programming of certain genes. Is this a Dex specific phenomenon? Similar experiments using Beta, or other GCs may indicate if some are more likely than others to cause long lasting changes in GR regulated genes. Furthermore, as discussed in §4.3 fundamental differences between males and females lead to different response to pharmacological interventions. Preliminary work from our lab indicates that induction of genes such as *Cftr*, *Fkbp5*, and *Gjb6*, vary both in their response to GC and differences between the sexes. In male CC-NPSCs, all three genes are induced to a greater extent when treated with an equivalent dose of Beta instead of Dex. In contrast, female CC-NPSCs, actually have a reduced response when treatment with Beta instead of Dex (Anthony Rudine, Personal Communication). In term born children treated during the fetal period with GCs, the authors noted no difference in cortisol reactivity if the child was treated with Dex or Beta (33). However, in spite of reporting sexually dimorphic changes in cortisol secretion, the authors did

not separate the Dex/Beta treated groups by sex prior to analysis. Therefore, it may be possible that treating with different GCs may change overall programming of NPSCs.

Strikingly, although Beta and Dex have similar affinities for the GR and similar genomic potencies, Dex has a 5-fold greater potency for the rapid action of GR than Beta in rat thymocytes (26). As discussed previously (§4.2), different GR signaling modalities may exert discrete influences on neurodevelopment and/or pulmonary benefits. Therefore, if rapid signaling was gives rise to more severe neurodevelopmental abnormalities, but the genomic action of GR is needed for pulmonary benefits, the use of Beta instead of Dex is indicated. Furthermore, there are other clinically relevant GCs, each of which has different genomic and rapid potencies. For example, Prednylidene has a 13-fold greater rapid potency than Beta and 2.5-fold greater rapid potency than Dex compared to 7-fold less potent than both for genomic effects (26). Therefore, use of Prednylidene may be indicated if rapid and not genomic activation of GR is required. However, further studies on the *in vivo* potencies and potencies in different cell types are also needed, as the numbers mentioned refer to one particular cell type and they may not be exactly applicable to NPSCs.

Furthermore, the programming effect seen in HT-NPSCs may be the result of a genomic or rapid GR signaling, or both. Exposing NPSCs to GCs with different genomic or rapid potencies may yield insight into which GCs cause a larger programming effect. Since loss of Cav-1 ablation changes the Dex regulated transcriptome, treating Cav-1 KO NPSCs with Beta or other GCs may result in GR mediated regulation of a different subset of genes. Comparing the Beta vs. Dex regulated profiles in the Cav-1 KO NPSCs, will yield additional insights into the functional genomic consequences of using one GC versus the other.

4.5 CONCLUDING REMARKS

Each chapter of this thesis examined very distinct roles for GR in neurodevelopment. However, each of the new insights presented in Chapters 2 and 3 into GR action in NPSCs leads to complementary questions. For example, does the role of Cav-1 in mediating crosstalk between the rapid and genomic actions vary depending on the region of the brain in question or the sex? If a similar microarray was performed in Cav-1 KO HT-NPSCs, would we see similar altered regulation of the same target genes identified in CC-NPSCs? In HT-NPSCs, we see lasting changes in Dex-mediated gene transcription—would we see these changes in Cav-1 KO NPSCs? Phosphorylation of the GR, particularly at S211, was shown to be important in CC-NPSCs. Does phosphorylation of GR vary at this site or others in different sexes or in response to treatment with different GCs? Are different phosphorylation sites more or less important in different regions of the brain? What about sex specific gene regulation? Will the profile we see in the HT be applicable to all regions of the brain? Finally, what do these each of these questions mean in terms of antenatal GC action *in vivo*? Taken together, this thesis revealed novel insights into GR signaling in CC-NPSCs and sexually dimorphic and persistent changes in hypothalamic gene expression. This new knowledge may lead to improved antenatal GC therapies that maximize therapeutic benefit while minimizing neurodevelopmental complications.

APPENDIX A

SUPPLEMENTAL IGV FIGURES

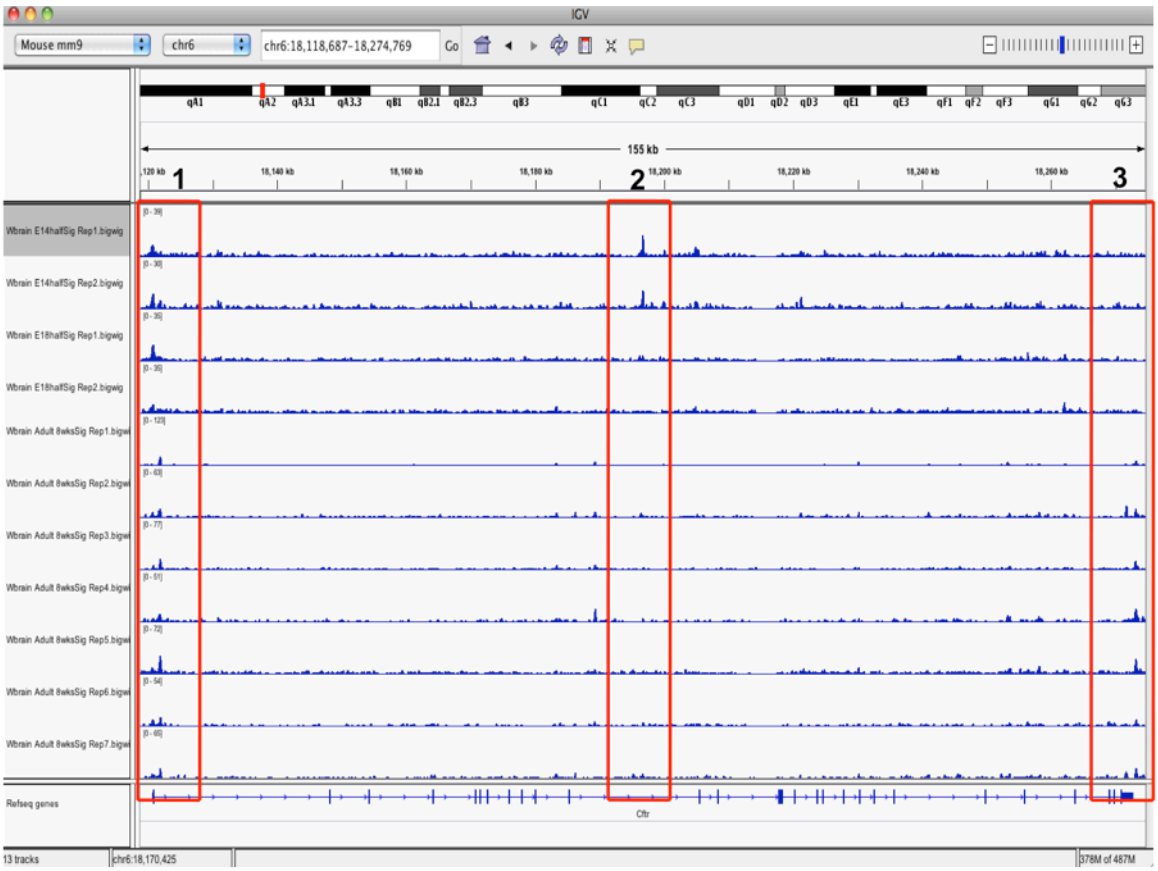

Figure 30. DNAse hypersensitivity assays in E14.5, E18.5 and adult mouse brain indicate developmentally dynamic changes in chromatin status within *Cftr*.

Each of the red boxes highlights DNAse sensitive regions within *Cftr*. Region 1 is sensitive to treatment at all time points. Region 2 however is only in an open conformation at E14.5, and not E18.5 or in the 8 week old adult. However, in Region 3, the hypersensitive site only exists in the adult animal, not at E14.5 or E18.5 Shown are 2 biological replicates from E14.5 and E18.5 and 7 8 week old adult C57/BL6 animals. Data accessible using GEO # GSM1014151.

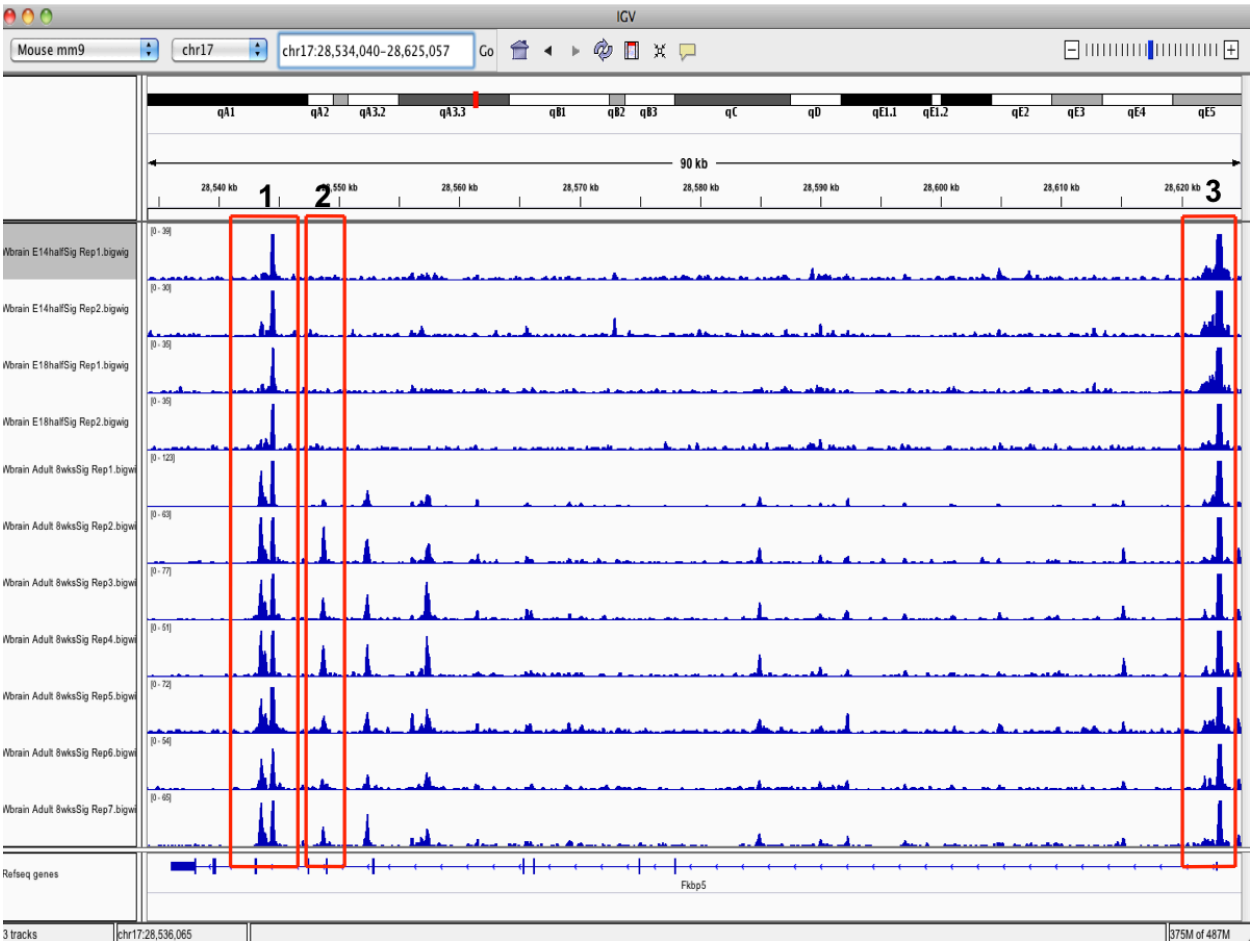

Figure 31. DNAse hypersensitivity assays in E14.5, E18.5 and adult mouse brain indicate that the region within intron 7 of *Fkbp-5* is only open in the adult brain.

Each of the red boxes highlights DNAse sensitive regions within *Fkbp-5*. Regions 1 and 3 are sensitive to treatment at all time points. Region 2, which is located within intron 7, however is only in a hypersensitive state in the adult animal, not at E14.5 or E18.5. Shown are 2 biological replicates from E14.5 and E18.5 and 7 8 week old adult C57/BL6 animals. Data accessible using GEO # GSM1014151.

BIBLIOGRAPHY

1. **Chapman, K., M. Holmes, and J. Seckl.** 2013. 11beta-hydroxysteroid dehydrogenases: intracellular gate-keepers of tissue glucocorticoid action. Physiol Rev **93:**1139-1206.
2. **Malaeb, S. N., and B. S. Stonestreet.** 2014. Steroids and Injury to the Developing Brain: Net Harm or Net Benefit? Clin Perinatol **41:**191-208.
3. **Baker, M. E., J. W. Funder, and S. R. Kattoula.** 2013. Evolution of hormone selectivity in glucocorticoid and mineralocorticoid receptors. J Steroid Biochem Mol Biol **137:**57-70.
4. **Damsted, S. K., A. P. Born, O. B. Paulson, and P. Uldall.** 2011. Exogenous glucocorticoids and adverse cerebral effects in children. Eur J Paediatr Neurol **15:**465-477.
5. **Oitzl, M. S., D. L. Champagne, R. van der Veen, and E. R. de Kloet.** 2010. Brain development under stress: hypotheses of glucocorticoid actions revisited. Neurosci Biobehav Rev **34:**853-866.
6. **Matthews, S. G.** 2000. Antenatal glucocorticoids and programming of the developing CNS. Pediatr Res **47:**291-300.
7. **George, A. A., R. L. Schiltz, and G. L. Hager.** 2009. Dynamic access of the glucocorticoid receptor to response elements in chromatin. Int J Biochem Cell Biol **41:**214-224.
8. **Rhen, T., and J. A. Cidlowski.** 2005. Antiinflammatory action of glucocorticoids--new mechanisms for old drugs. N Engl J Med **353:**1711-1723.
9. **Kadmiel, M., and J. A. Cidlowski.** 2013. Glucocorticoid receptor signaling in health and disease. Trends Pharmacol Sci **34:**518-530.
10. **Bagamasbad, P., and R. J. Denver.** 2011. Mechanisms and significance of nuclear receptor auto- and cross-regulation. Gen Comp Endocrinol **170:**3-17.
11. **Germain, P., B. Staels, C. Dacquet, M. Spedding, and V. Laudet.** 2006. Overview of nomenclature of nuclear receptors. Pharmacol Rev **58:**685-704.
12. **Oakley, R. H., and J. A. Cidlowski.** 2013. The biology of the glucocorticoid receptor: new signaling mechanisms in health and disease. J Allergy Clin Immunol **132:**1033-1044.
13. **Meijsing, S. H., M. A. Pufall, A. Y. So, D. L. Bates, L. Chen, and K. R. Yamamoto.** 2009. DNA binding site sequence directs glucocorticoid receptor structure and activity. Science **324:**407-410.
14. **John, S., P. J. Sabo, R. E. Thurman, M. H. Sung, S. C. Biddie, T. A. Johnson, G. L. Hager, and J. A. Stamatoyannopoulos.** 2011. Chromatin accessibility pre-determines glucocorticoid receptor binding patterns. Nat Genet **43:**264-268.

15. **Yu, C. Y., O. Mayba, J. V. Lee, J. Tran, C. Harris, T. P. Speed, and J. C. Wang.** 2010. Genome-wide analysis of glucocorticoid receptor binding regions in adipocytes reveal gene network involved in triglyceride homeostasis. PLoS One **5:**e15188.
16. **Arambasic, J., G. Poznanovic, S. Ivanovic-Matic, D. Bogojevic, M. Mihailovic, A. Uskokovic, and I. Grigorov.** 2010. Association of the glucocorticoid receptor with STAT3, C/EBPbeta, and the hormone-responsive element within the rat haptoglobin gene promoter during the acute phase response. IUBMB Life **62:**227-236.
17. **Blind, R. D., and M. J. Garabedian.** 2008. Differential recruitment of glucocorticoid receptor phospho-isoforms to glucocorticoid-induced genes. J Steroid Biochem Mol Biol **109:**150-157.
18. **Galliher-Beckley, A. J., J. G. Williams, J. B. Collins, and J. A. Cidlowski.** 2008. Glycogen synthase kinase 3beta-mediated serine phosphorylation of the human glucocorticoid receptor redirects gene expression profiles. Mol Cell Biol **28:**7309-7322.
19. **Simic, I., M. Adzic, N. Maric, D. Savic, J. Djordjevic, M. Mihaljevic, M. Mitic, Z. Pavlovic, I. Soldatovic, M. Krstic-Demonacos, M. Jasovic-Gasic, and M. Radojcic.** 2013. A preliminary evaluation of leukocyte phospho-glucocorticoid receptor as a potential biomarker of depressogenic vulnerability in healthy adults. Psychiatry Res **209:**658-664.
20. **Lambert, W. M., C. F. Xu, T. A. Neubert, M. V. Chao, M. J. Garabedian, and F. D. Jeanneteau.** 2013. Brain-derived neurotrophic factor signaling rewrites the glucocorticoid transcriptome via glucocorticoid receptor phosphorylation. Mol Cell Biol **33:**3700-3714.
21. **Vinukonda, G., K. Dummula, S. Malik, F. Hu, C. I. Thompson, A. Csiszar, Z. Ungvari, and P. Ballabh.** 2010. Effect of prenatal glucocorticoids on cerebral vasculature of the developing brain. Stroke **41:**1766-1773.
22. **Habermehl, D., J. R. Parkitna, S. Kaden, B. Brugger, F. Wieland, H. J. Grone, and G. Schutz.** 2011. Glucocorticoid activity during lung maturation is essential in mesenchymal and less in alveolar epithelial cells. Mol Endocrinol **25:**1280-1288.
23. **Graham, E. M., A. M. Atz, K. E. McHugh, R. J. Butts, N. L. Baker, R. E. Stroud, S. T. Reeves, S. M. Bradley, F. X. McGowan, Jr., and F. G. Spinale.** 2014. Preoperative steroid treatment does not improve markers of inflammation after cardiac surgery in neonates: Results from a randomized trial. J Thorac Cardiovasc Surg **147:**902-908.
24. **Miller, W. L., and S. F. Witchel.** 2013. Prenatal treatment of congenital adrenal hyperplasia: risks outweigh benefits. Am J Obstet Gynecol **208:**354-359.
25. **Merrill, J. D., and R. A. Ballard.** 2000. Clinical use of antenatal corticosteroids: benefits and risks. Pediatr Rev **1:**E91-98.
26. **Buttgereit, F., M. D. Brand, and G. R. Burmester.** 1999. Equivalent doses and relative drug potencies for non-genomic glucocorticoid effects: a novel glucocorticoid hierarchy. Biochem Pharmacol **58:**363-368.
27. **Wapner, R., and A. H. Jobe.** 2011. Controversy: antenatal steroids. Clin Perinatol **38:**529-545.
28. **Davis, E. P., C. A. Sandman, C. Buss, D. A. Wing, and K. Head.** 2013. Fetal glucocorticoid exposure is associated with preadolescent brain development. Biol Psychiatry **74:**647-655.
29. **Samarasinghe, R. A., R. Di Maio, D. Volonte, F. Galbiati, M. Lewis, G. Romero, and D. B. DeFranco.** 2011. Nongenomic glucocorticoid receptor action regulates gap

junction intercellular communication and neural progenitor cell proliferation. Proc Natl Acad Sci U S A **108:**16657-16662.

30. **Fukumoto, K., T. Morita, T. Mayanagi, D. Tanokashira, T. Yoshida, A. Sakai, and K. Sobue.** 2009. Detrimental effects of glucocorticoids on neuronal migration during brain development. Mol Psychiatry **14:**1119-1131.
31. **Chetty, S., A. R. Friedman, K. Taravosh-Lahn, E. D. Kirby, C. Mirescu, F. Guo, D. Krupik, A. Nicholas, A. C. Geraghty, A. Krishnamurthy, M. K. Tsai, D. Covarrubias, A. T. Wong, D. D. Francis, R. M. Sapolsky, T. D. Palmer, D. Pleasure, and D. Kaufer.** 2014. Stress and glucocorticoids promote oligodendrogenesis in the adult hippocampus. Mol Psychiatry.
32. **Davis, E. P., C. A. Sandman, C. Buss, D. A. Wing, and K. Head.** 2013. Fetal Glucocorticoid Exposure Is Associated with Preadolescent Brain Development. Biol Psychiatry.
33. **Alexander, N., F. Rosenlocher, T. Stalder, J. Linke, W. Distler, J. Morgner, and C. Kirschbaum.** 2012. Impact of antenatal synthetic glucocorticoid exposure on endocrine stress reactivity in term-born children. J Clin Endocrinol Metab **97:**3538-3544.
34. **Cheong, J. L., A. C. Burnett, K. J. Lee, G. Roberts, D. K. Thompson, S. J. Wood, A. Connelly, P. J. Anderson, and L. W. Doyle.** 2014. Association between Postnatal Dexamethasone for Treatment of Bronchopulmonary Dysplasia and Brain Volumes at Adolescence in Infants Born Very Preterm. J Pediatr **164:**737-743 e731.
35. **Murphy, B. P., T. E. Inder, P. S. Huppi, S. Warfield, G. P. Zientara, R. Kikinis, F. A. Jolesz, and J. J. Volpe.** 2001. Impaired cerebral cortical gray matter growth after treatment with dexamethasone for neonatal chronic lung disease. Pediatrics **107:**217-221.
36. **Sundberg, M., S. Savola, A. Hienola, L. Korhonen, and D. Lindholm.** 2006. Glucocorticoid hormones decrease proliferation of embryonic neural stem cells through ubiquitin-mediated degradation of cyclin D1. J Neurosci **26:**5402-5410.
37. **Noguchi, K. K., K. C. Walls, D. F. Wozniak, J. W. Olney, K. A. Roth, and N. B. Farber.** 2008. Acute neonatal glucocorticoid exposure produces selective and rapid cerebellar neural progenitor cell apoptotic death. Cell Death Differ **15:**1582-1592.
38. **Moors, M., R. Bose, K. Johansson-Haque, K. Edoff, S. Okret, and S. Ceccatelli.** 2012. Dickkopf 1 mediates glucocorticoid-induced changes in human neural progenitor cell proliferation and differentiation. Toxicol Sci **125:**488-495.
39. **Sabolek, M., A. Herborg, J. Schwarz, and A. Storch.** 2006. Dexamethasone blocks astroglial differentiation from neural precursor cells. Neuroreport **17:**1719-1723.
40. **Wagner, K., S. Couillard-Despres, B. Lehner, G. Brockhoff, F. J. Rivera, A. Blume, I. Neumann, and L. Aigner.** 2009. Prolactin induces MAPK signaling in neural progenitors without alleviating glucocorticoid-induced inhibition of in vitro neurogenesis. Cell Physiol Biochem **24:**397-406.
41. **Tsiarli, M. A., A. Paula Monaghan, and D. B. Defranco.** 2013. Differential subcellular localization of the glucocorticoid receptor in distinct neural stem and progenitor populations of the mouse telencephalon in vivo. Brain Res **1523:**10-27.
42. **Reynolds, B. A., and S. Weiss.** 1996. Clonal and population analyses demonstrate that an EGF-responsive mammalian embryonic CNS precursor is a stem cell. Dev Biol **175:**1-13.
43. **Rajan, P., and R. D. McKay.** 1998. Multiple routes to astrocytic differentiation in the CNS. J Neurosci **18:**3620-3629.

44. **Qian, X., Q. Shen, S. K. Goderie, W. He, A. Capela, A. A. Davis, and S. Temple.** 2000. Timing of CNS cell generation: a programmed sequence of neuron and glial cell production from isolated murine cortical stem cells. Neuron **28:**69-80.
45. **Shen, Q., Y. Wang, J. T. Dimos, C. A. Fasano, T. N. Phoenix, I. R. Lemischka, N. B. Ivanova, S. Stifani, E. E. Morrisey, and S. Temple.** 2006. The timing of cortical neurogenesis is encoded within lineages of individual progenitor cells. Nat Neurosci **9:**743-751.
46. **Keniry, A., D. Oxley, P. Monnier, M. Kyba, L. Dandolo, G. Smits, and W. Reik.** 2012. The H19 lincRNA is a developmental reservoir of miR-675 that suppresses growth and Igf1r. Nat Cell Biol **14:**659-665.
47. **Kriegstein, A., and A. Alvarez-Buylla.** 2009. The glial nature of embryonic and adult neural stem cells. Annu Rev Neurosci **32:**149-184.
48. **Malatesta, P., I. Appolloni, and F. Calzolari.** 2008. Radial glia and neural stem cells. Cell Tissue Res **331:**165-178.
49. **Corbin, J. G., N. Gaiano, S. L. Juliano, S. Poluch, E. Stancik, and T. F. Haydar.** 2008. Regulation of neural progenitor cell development in the nervous system. J Neurochem **106:**2272-2287.
50. **Allen, N. J., and B. A. Barres.** 2009. Neuroscience: Glia - more than just brain glue. Nature **457:**675-677.
51. **Rajkowska, G., and J. J. Miguel-Hidalgo.** 2007. Gliogenesis and glial pathology in depression. CNS Neurol Disord Drug Targets **6:**219-233.
52. **Rubenstein, J. L.** 2011. Annual Research Review: Development of the cerebral cortex: implications for neurodevelopmental disorders. J Child Psychol Psychiatry **52:**339-355.
53. **Arnsten, A. F., and K. Rubia.** 2012. Neurobiological circuits regulating attention, cognitive control, motivation, and emotion: disruptions in neurodevelopmental psychiatric disorders. J Am Acad Child Adolesc Psychiatry **51:**356-367.
54. **Schmitt, A., B. Malchow, A. Hasan, and P. Falkai.** 2014. The impact of environmental factors in severe psychiatric disorders. Front Neurosci **8:**19.
55. **Heitzer, M. D., I. M. Wolf, E. R. Sanchez, S. F. Witchel, and D. B. DeFranco.** 2007. Glucocorticoid receptor physiology. Rev Endocr Metab Disord **8:**321-330.
56. **Matthews, L., A. Berry, V. Ohanian, J. Ohanian, H. Garside, and D. Ray.** 2008. Caveolin mediates rapid glucocorticoid effects and couples glucocorticoid action to the antiproliferative program. Mol Endocrinol **22:**1320-1330.
57. **Hammes, S. R., and E. R. Levin.** 2011. Minireview: Recent advances in extranuclear steroid receptor actions. Endocrinology **152:**4489-4495.
58. **Wong, W. P., J. P. Tiano, S. Liu, S. C. Hewitt, C. Le May, S. Dalle, J. A. Katzenellenbogen, B. S. Katzenellenbogen, K. S. Korach, and F. Mauvais-Jarvis.** 2010. Extranuclear estrogen receptor-alpha stimulates NeuroD1 binding to the insulin promoter and favors insulin synthesis. Proc Natl Acad Sci U S A **107:**13057-13062.
59. **Sen, A., H. Prizant, and S. R. Hammes.** 2011. Understanding extranuclear (nongenomic) androgen signaling: what a frog oocyte can tell us about human biology. Steroids **76:**822-828.
60. **Razani, B., and M. P. Lisanti.** 2001. Caveolin-deficient mice: insights into caveolar function human disease. J Clin Invest **108:**1553-1561.

61. **Park, J. H., and H. J. Han.** 2009. Caveolin-1 plays important role in EGF-induced migration and proliferation of mouse embryonic stem cells: involvement of PI3K/Akt and ERK. Am J Physiol Cell Physiol **297:**C935-944.
62. **Jasmin, J. F., M. Yang, L. Iacovitti, and M. P. Lisanti.** 2009. Genetic ablation of caveolin-1 increases neural stem cell proliferation in the subventricular zone (SVZ) of the adult mouse brain. Cell Cycle **8:**3978-3983.
63. **Le Lay, S., and T. V. Kurzchalia.** 2005. Getting rid of caveolins: phenotypes of caveolin-deficient animals. Biochim Biophys Acta **1746:**322-333.
64. **Li, Y., W. M. Lau, K. F. So, Y. Tong, and J. Shen.** 2011. Caveolin-1 promote astroglial differentiation of neural stem/progenitor cells through modulating Notch1/NICD and Hes1 expressions. Biochem Biophys Res Commun **407:**517-524.
65. **Li, Y., J. Luo, W. M. Lau, G. Zheng, S. Fu, T. T. Wang, H. P. Zeng, K. F. So, S. K. Chung, Y. Tong, K. Liu, and J. Shen.** 2011. Caveolin-1 plays a crucial role in inhibiting neuronal differentiation of neural stem/progenitor cells via VEGF signaling-dependent pathway. PLoS One **6:**e22901.
66. **Gioiosa, L., C. Raggi, L. Ricceri, J. F. Jasmin, P. G. Frank, F. Capozza, M. P. Lisanti, E. Alleva, M. Sargiacomo, and G. Laviola.** 2008. Altered emotionality, spatial memory and cholinergic function in caveolin-1 knock-out mice. Behav Brain Res **188:**255-262.
67. **Trushina, E., J. Du Charme, J. Parisi, and C. T. McMurray.** 2006. Neurological abnormalities in caveolin-1 knock out mice. Behav Brain Res **172:**24-32.
68. **Anacker, C., A. Cattaneo, K. Musaelyan, P. A. Zunszain, M. Horowitz, R. Molteni, A. Luoni, F. Calabrese, K. Tansey, M. Gennarelli, S. Thuret, J. Price, R. Uher, M. A. Riva, and C. M. Pariante.** 2013. Role for the kinase SGK1 in stress, depression, and glucocorticoid effects on hippocampal neurogenesis. Proc Natl Acad Sci U S A **110:**8708-8713.
69. **Bolstad, B. M., R. A. Irizarry, M. Astrand, and T. P. Speed.** 2003. A comparison of normalization methods for high density oligonucleotide array data based on variance and bias. Bioinformatics **19:**185-193.
70. **Simon, R., A. Lam, M. C. Li, M. Ngan, S. Menenzes, and Y. Zhao.** 2007. Analysis of gene expression data using BRB-ArrayTools. Cancer Inform **3:**11-17.
71. **John, S., T. A. Johnson, M. H. Sung, S. C. Biddie, S. Trump, C. A. Koch-Paiz, S. R. Davis, R. Walker, P. S. Meltzer, and G. L. Hager.** 2009. Kinetic complexity of the global response to glucocorticoid receptor action. Endocrinology **150:**1766-1774.
72. **Anacker, C., A. Cattaneo, A. Luoni, K. Musaelyan, P. A. Zunszain, E. Milanesi, J. Rybka, A. Berry, F. Cirulli, S. Thuret, J. Price, M. A. Riva, M. Gennarelli, and C. M. Pariante.** 2013. Glucocorticoid-related molecular signaling pathways regulating hippocampal neurogenesis. Neuropsychopharmacology **38:**872-883.
73. **Kuo, T., M. J. Lew, O. Mayba, C. A. Harris, T. P. Speed, and J. C. Wang.** 2012. Genome-wide analysis of glucocorticoid receptor-binding sites in myotubes identifies gene networks modulating insulin signaling. Proc Natl Acad Sci U S A **109:**11160-11165.
74. **Gobert, R. P., L. Joubert, M. L. Curchod, C. Salvat, I. Foucault, C. Jorand-Lebrun, M. Lamarine, H. Peixoto, C. Vignaud, C. Fremaux, T. Jomotte, B. Francon, C. Alliod, L. Bernasconi, H. Abderrahim, D. Perrin, A. Bombrun, F. Zanoguera, C. Rommel, and R. Hooft van Huijsduijnen.** 2009. Convergent functional genomics of

oligodendrocyte differentiation identifies multiple autoinhibitory signaling circuits. Mol Cell Biol **29:**1538-1553.

75. **Pantoja, C., J. T. Huff, and K. R. Yamamoto.** 2008. Glucocorticoid signaling defines a novel commitment state during adipogenesis in vitro. Mol Biol Cell **19:**4032-4041.
76. **So, A. Y., S. B. Cooper, B. J. Feldman, M. Manuchehri, and K. R. Yamamoto.** 2008. Conservation analysis predicts in vivo occupancy of glucocorticoid receptor-binding sequences at glucocorticoid-induced genes. Proc Natl Acad Sci U S A **105:**5745-5749.
77. **Steger, D. J., G. R. Grant, M. Schupp, T. Tomaru, M. I. Lefterova, J. Schug, E. Manduchi, C. J. Stoeckert, Jr., and M. A. Lazar.** 2010. Propagation of adipogenic signals through an epigenomic transition state. Genes Dev **24:**1035-1044.
78. **Siersbaek, R., R. Nielsen, S. John, M. H. Sung, S. Baek, A. Loft, G. L. Hager, and S. Mandrup.** 2011. Extensive chromatin remodelling and establishment of transcription factor 'hotspots' during early adipogenesis. Embo J **30:**1459-1472.
79. **Malmersjo, S., P. Rebellato, E. Smedler, H. Planert, S. Kanatani, I. Liste, E. Nanou, H. Sunner, S. Abdelhady, S. Zhang, M. Andang, A. El Manira, G. Silberberg, E. Arenas, and P. Uhlen.** 2013. Neural progenitors organize in small-world networks to promote cell proliferation. Proc Natl Acad Sci U S A **110:**E1524-1532.
80. **Mercier, I., M. C. Casimiro, J. Zhou, C. Wang, C. Plymire, K. G. Bryant, K. M. Daumer, F. Sotgia, G. Bonuccelli, A. K. Witkiewicz, J. Lin, T. H. Tran, J. Milliman, P. G. Frank, J. F. Jasmin, H. Rui, R. G. Pestell, and M. P. Lisanti.** 2009. Genetic ablation of caveolin-1 drives estrogen-hypersensitivity and the development of DCIS-like mammary lesions. Am J Pathol **174:**1172-1190.
81. **Sippel, M., R. Rajala, L. Korhonen, B. Bornhauser, A. L. Sokka, M. Naito, and D. Lindholm.** 2009. Dexamethasone regulates expression of BRUCE/Apollon and the proliferation of neural progenitor cells. FEBS Lett **583:**2213-2217.
82. **Ostroumov, A., M. Simonetti, and A. Nistri.** 2011. Cystic fibrosis transmembrane conductance regulator modulates synaptic chloride homeostasis in motoneurons of the rat spinal cord during neonatal development. Dev Neurobiol **71:**253-268.
83. **Sanna, E., S. Miotti, M. Mazzi, G. De Santis, S. Canevari, and A. Tomassetti.** 2007. Binding of nuclear caveolin-1 to promoter elements of growth-associated genes in ovarian carcinoma cells. Exp Cell Res **313:**1307-1317.
84. **Li, W., H. Liu, J. S. Zhou, J. F. Cao, X. B. Zhou, A. M. Choi, Z. H. Chen, and H. H. Shen.** 2012. Caveolin-1 Inhibits Expression of Antioxidant Enzymes through Direct Interaction with Nuclear Erythroid 2 p45-related Factor-2 (Nrf2). J Biol Chem **287:**20922-20930.
85. **Itani, O. A., K. Z. Liu, K. L. Cornish, J. R. Campbell, and C. P. Thomas.** 2002. Glucocorticoids stimulate human sgk1 gene expression by activation of a GRE in its 5'-flanking region. Am J Physiol Endocrinol Metab **283:**E971-979.
86. **Ezan, P., P. Andre, S. Cisternino, B. Saubamea, A. C. Boulay, S. Doutremer, M. A. Thomas, N. Quenech'du, C. Giaume, and M. Cohen-Salmon.** 2012. Deletion of astroglial connexins weakens the blood-brain barrier. J Cereb Blood Flow Metab **32:**1457-1467.
87. **Chen, L., M. Chatterjee, and J. Y. Li.** 2010. The mouse homeobox gene Gbx2 is required for the development of cholinergic interneurons in the striatum. J Neurosci **30:**14824-14834.

88. **Xu, B., J. L. Roos, P. Dexheimer, B. Boone, B. Plummer, S. Levy, J. A. Gogos, and M. Karayiorgou.** 2011. Exome sequencing supports a de novo mutational paradigm for schizophrenia. Nat Genet **43:**864-868.
89. **Guo, Y., M. Su, M. A. McNutt, and J. Gu.** 2009. Expression and distribution of cystic fibrosis transmembrane conductance regulator in neurons of the human brain. J Histochem Cytochem **57:**1113-1120.
90. **McGrath, S. A., A. Basu, and P. L. Zeitlin.** 1993. Cystic fibrosis gene and protein expression during fetal lung development. Am J Respir Cell Mol Biol **8:**201-208.
91. **Reznikov, L. R., Q. Dong, J. H. Chen, T. O. Moninger, J. M. Park, Y. Zhang, J. Du, M. S. Hildebrand, R. J. Smith, C. O. Randak, D. A. Stoltz, and M. J. Welsh.** 2013. CFTR-deficient pigs display peripheral nervous system defects at birth. Proc Natl Acad Sci U S A **110:**3083-3088.
92. **Nethe, M., E. C. Anthony, M. Fernandez-Borja, R. Dee, D. Geerts, P. J. Hensbergen, A. M. Deelder, G. Schmidt, and P. L. Hordijk.** 2010. Focal-adhesion targeting links caveolin-1 to a Rac1-degradation pathway. J Cell Sci **123:**1948-1958.
93. **Li, C. C., T. C. Chiang, T. S. Wu, G. Pacheco-Rodriguez, J. Moss, and F. J. Lee.** 2007. ARL4D recruits cytohesin-2/ARNO to modulate actin remodeling. Mol Biol Cell **18:**4420-4437.
94. **Ho, H., A. Soto Hopkin, R. Kapadia, P. Vasudeva, J. Schilling, and A. K. Ganesan.** 2013. RhoJ modulates melanoma invasion by altering actin cytoskeletal dynamics. Pigment Cell Melanoma Res **26:**218-225.
95. **Bodea, G. O., J. H. Spille, P. Abe, A. S. Andersson, A. Acker-Palmer, R. Stumm, U. Kubitscheck, and S. Blaess.** 2014. Reelin and CXCL12 regulate distinct migratory behaviors during the development of the dopaminergic system. Development **141:**661-673.
96. **Adzic, M., J. Djordjevic, A. Djordjevic, A. Niciforovic, C. Demonacos, M. Radojcic, and M. Krstic-Demonacos.** 2009. Acute or chronic stress induce cell compartment-specific phosphorylation of glucocorticoid receptor and alter its transcriptional activity in Wistar rat brain. J Endocrinol **202:**87-97.
97. **Pancotti, F., L. Roncuzzi, M. Maggiolini, and A. Gasperi-Campani.** 2012. Caveolin-1 silencing arrests the proliferation of metastatic lung cancer cells through the inhibition of STAT3 signaling. Cell Signal **24:**1390-1397.
98. **Baumeister, D., S. L. Lightman, and C. M. Pariante.** 2014. The Interface of Stress and the HPA Axis in Behavioural Phenotypes of Mental Illness. Curr Top Behav Neurosci.
99. **Szarek, E., P. S. Cheah, J. Schwartz, and P. Thomas.** 2010. Molecular genetics of the developing neuroendocrine hypothalamus. Mol Cell Endocrinol **323:**115-123.
100. **Panagiotakopoulos, L., and G. N. Neigh.** 2014. Development of the HPA axis: Where and when do sex differences manifest? Front Neuroendocrinol.
101. **Binder, E. B.** 2009. The role of FKBP5, a co-chaperone of the glucocorticoid receptor in the pathogenesis and therapy of affective and anxiety disorders. Psychoneuroendocrinology **34 Suppl 1:**S186-195.
102. **Binder, E. B., D. Salyakina, P. Lichtner, G. M. Wochnik, M. Ising, B. Putz, S. Papiol, S. Seaman, S. Lucae, M. A. Kohli, T. Nickel, H. E. Kunzel, B. Fuchs, M. Majer, A. Pfennig, N. Kern, J. Brunner, S. Modell, T. Baghai, T. Deiml, P. Zill, B. Bondy, R. Rupprecht, T. Messer, O. Kohnlein, H. Dabitz, T. Bruckl, N. Muller, H. Pfister, R. Lieb, J. C. Mueller, E. Lohmussaar, T. M. Strom, T. Bettecken, T.**

Meitinger, M. Uhr, T. Rein, F. Holsboer, and B. Muller-Myhsok. 2004. Polymorphisms in FKBP5 are associated with increased recurrence of depressive episodes and rapid response to antidepressant treatment. Nat Genet **36:**1319-1325.

103. **Klengel, T., D. Mehta, C. Anacker, M. Rex-Haffner, J. C. Pruessner, C. M. Pariante, T. W. Pace, K. B. Mercer, H. S. Mayberg, B. Bradley, C. B. Nemeroff, F. Holsboer, C. M. Heim, K. J. Ressler, T. Rein, and E. B. Binder.** 2013. Allele-specific FKBP5 DNA demethylation mediates gene-childhood trauma interactions. Nat Neurosci **16:**33-41.
104. **Fujii, T., H. Hori, M. Ota, K. Hattori, T. Teraishi, D. Sasayama, N. Yamamoto, T. Higuchi, and H. Kunugi.** 2014. Effect of the common functional FKBP5 variant (rs1360780) on the hypothalamic-pituitary-adrenal axis and peripheral blood gene expression. Psychoneuroendocrinology **42:**89-97.
105. **Lamers, F., N. Vogelzangs, K. R. Merikangas, P. de Jonge, A. T. Beekman, and B. W. Penninx.** 2013. Evidence for a differential role of HPA-axis function, inflammation and metabolic syndrome in melancholic versus atypical depression. Mol Psychiatry **18:**692-699.
106. **Welberg, L. A., and J. R. Seckl.** 2001. Prenatal stress, glucocorticoids and the programming of the brain. J Neuroendocrinol **13:**113-128.
107. **Soga, T., S. L. Dalpatadu, D. W. Wong, and I. S. Parhar.** 2012. Neonatal dexamethasone exposure down-regulates GnRH expression through the GnIH pathway in female mice. Neuroscience **218:**56-64.
108. **Carbone, D. L., D. G. Zuloaga, R. Hiroi, C. D. Foradori, M. E. Legare, and R. J. Handa.** 2012. Prenatal dexamethasone exposure potentiates diet-induced hepatosteatosis and decreases plasma IGF-I in a sex-specific fashion. Endocrinology **153:**295-306.
109. **Xu, X., J. K. Coats, C. F. Yang, A. Wang, O. M. Ahmed, M. Alvarado, T. Izumi, and N. M. Shah.** 2012. Modular genetic control of sexually dimorphic behaviors. Cell **148:**596-607.
110. **Ingalhalikar, M., A. Smith, D. Parker, T. D. Satterthwaite, M. A. Elliott, K. Ruparel, H. Hakonarson, R. E. Gur, R. C. Gur, and R. Verma.** 2014. Sex differences in the structural connectome of the human brain. Proc Natl Acad Sci U S A **111:**823-828.
111. **Bale, T. L., T. Z. Baram, A. S. Brown, J. M. Goldstein, T. R. Insel, M. M. McCarthy, C. B. Nemeroff, T. M. Reyes, R. B. Simerly, E. S. Susser, and E. J. Nestler.** 2010. Early life programming and neurodevelopmental disorders. Biol Psychiatry **68:**314-319.
112. **Goldstein, J. M., R. J. Handa, and S. A. Tobet.** 2014. Disruption of fetal hormonal programming (prenatal stress) implicates shared risk for sex differences in depression and cardiovascular disease. Front Neuroendocrinol **35:**140-158.
113. **Duma, D., J. B. Collins, J. W. Chou, and J. A. Cidlowski.** 2010. Sexually dimorphic actions of glucocorticoids provide a link to inflammatory diseases with gender differences in prevalence. Sci Signal **3:**ra74.
114. **Drake, A. J., L. Liu, D. Kerrigan, R. R. Meehan, and J. R. Seckl.** 2011. Multigenerational programming in the glucocorticoid programmed rat is associated with generation-specific and parent of origin effects. Epigenetics **6:**1334-1343.
115. **Lister, R., E. A. Mukamel, J. R. Nery, M. Urich, C. A. Puddifoot, N. D. Johnson, J. Lucero, Y. Huang, A. J. Dwork, M. D. Schultz, M. Yu, J. Tonti-Filippini, H. Heyn, S. Hu, J. C. Wu, A. Rao, M. Esteller, C. He, F. G. Haghighi, T. J. Sejnowski, M. M.**

Behrens, and J. R. Ecker. 2013. Global epigenomic reconfiguration during mammalian brain development. Science **341:**1237905.

116. **Salvi, R., Y. Arsenijevic, M. Giacomini, J. P. Rey, M. J. Voirol, R. C. Gaillard, P. Y. Risold, and F. Pralong.** 2009. The fetal hypothalamus has the potential to generate cells with a gonadotropin releasing hormone (GnRH) phenotype. PLoS One **4:**e4392.
117. **Krzyzosiak, A., M. Szyszka-Niagolov, M. Wietrzych, S. Gobaille, S. Muramatsu, and W. Krezel.** 2010. Retinoid x receptor gamma control of affective behaviors involves dopaminergic signaling in mice. Neuron **66:**908-920.
118. **Dey, B. K., K. Pfeifer, and A. Dutta.** 2014. The H19 long noncoding RNA gives rise to microRNAs miR-675-3p and miR-675-5p to promote skeletal muscle differentiation and regeneration. Genes Dev **28:**491-501.
119. **Greenberg, P. E., R. C. Kessler, H. G. Birnbaum, S. A. Leong, S. W. Lowe, P. A. Berglund, and P. K. Corey-Lisle.** 2003. The economic burden of depression in the United States: how did it change between 1990 and 2000? J Clin Psychiatry **64:**1465-1475.
120. **Maddox, S. A., G. E. Schafe, and K. J. Ressler.** 2013. Exploring epigenetic regulation of fear memory and biomarkers associated with post-traumatic stress disorder. Front Psychiatry **4:**62.
121. **Iguchi, K., S. Matsunaga, T. Nakano, S. Usui, and K. Hirano.** 2006. Inhibition of caveolin-1 expression by incadronate in PC-3 prostate cells. Anticancer Res **26:**2977-2981.
122. **Whitley, H., and W. Lindsey.** 2009. Sex-based differences in drug activity. Am Fam Physician **80:**1254-1258.